Surface Functionalization of Polymer Substrates through Radiation-Induced Graft Polymerization: Conventional and Controlled Polymerization Techniques

DISSERTATION

Submitted for the Degree of Doctor of Philosophy
Division of Molecular Science
Gunma University
2018

by

Jordan F. Madrid
(B.Sc., M.Sc.)

THESIS DECLARATION

I, **Jordan F. Madrid**, certify that:

This thesis does not contain material which has been accepted for the award of any other doctorate degree or diploma in my name, in any university or other tertiary institution.

No part of this work will, in the future, be used in a submission in my name, for any other doctorate degree or diploma in any university or other tertiary institution.

This thesis does not contain any material previously published or written by another person, except where due reference has been made in the text.

The work(s) are not in any way a violation or infringement of any copyright, trademark, patent, or other rights whatsoever of any person.

This thesis contains published work and/or work prepared for publication, some of which has been co-authored.

Signature:

Date:

ABSTRACT

The formation of functional hybrid polymeric materials by attaching graft polymer chains with desirable and advantageous tailored properties to the surface of a base polymer with desirable bulk character is an attractive application of graft polymerization. The grafting process allows us to modify, tune and alter the characteristics of base polymers and to control their wettability, biocompatibility, adsorption capacity and behavior, conductivity, antimicrobial property, and reactivity. The resulting graft copolymer creates significant opportunities to develop new hybrid platforms for a number of applications.

In this work, graft copolymers were prepared from natural and synthetic base polymers through the radiation-induced graft polymerization in solution and emulsion phases. We report the synthesis of adsorbents based from lignocellulosic polymers (water hyacinth fibers and abaca-based nonwoven fabric) and the development of method for imparting hydrophobic property to microcrystalline cellulose. The radiation-induced method that we employed results in the synthesis of base polymers with covalently bonded poly(glycidyl methacrylate) graft polymers that serve as anchors for the ligand which is responsible for the enhanced adsorption character. The synthesized grafted adsorbents exhibited improved adsorption capacity and kinetics than the base polymers and in some cases even better than commercially available ion exchange resins. The “grafting from” approach that stemmed from radiation-induced initiation offers the possibility to functionalize the surface of these base materials with graft polymer chains that possess contrasting properties (hydrophobic/hydrophilic). The developed modification platform enables the fabrication of radiation grafted cellulose that is compatible with hydrophobic matrices.

We also investigated the graft polymerization of a polymer through a technique that combines the merits of radiation-induced synthesis and reversible addition-fragmentation chain transfer (RAFT) process in emulsion phase. We demonstrated the facile combination of these techniques in simple reaction that ultimately results in the fabrication of copolymer with immobilized epoxide groups on the surface. The preparation of graft copolymers through a method that combines the advantages and merits of radiation-induced grafting in water-based emulsion, an

environment friendly green method, and controlled radical polymerization via RAFT-mediation is described, for the first time, in the second major part of this thesis. Both electron beam- and γ-radiation initiation processes were used in the synthesis. While conventional graft polymerization in emulsion phase yielded graft copolymers with low degree of grafting values (< 7.5% at 10% (wt/wt) glycidyl methacrylate concentration), addition of RAFT agent to the graft polymerization system allowed the synthesis of polyethylene/polypropylene-g-poly(glycidyl methacrylate) (PE/PP-g-PGMA) with more tunable degree of grafting (8% $\leq$ Dg $\leq$ 94%) by controlling the grafting parameters. Relatively good control (PDI ~ 1.2 for selected grafting conditions) during polymerization was attained. The number average molecular weight of free homopolymers increased as a function of monomer conversion. NMR analyses of the free homopolymers indicate the presence of dithiobenzoate group from 4-cyano-4-((phenylcarbonothioyl)thio)pentanoic acid RAFT agent on the polymer chain. These evidences have been considered as a proof of RAFT mechanism.

Furthermore, the reactivity and adsorption behavior of the graft copolymer produced from the combination of radiation-induced grafting in emulsion phase and RAFT-mediation was evaluated. The PGMA graft chains from the PE/PP-g-PGMA that was prepared in emulsion phase through radiation-induced RAFT-mediated graft polymerization showed higher reactivity towards amination reaction at 40 °C compared to the conventionally prepared graft copolymer. Similar to the previously prepared adsorbent, the epoxide rings of PGMA served as a precursor group that were eventually converted to diglycol amic acid ligands. The diglycol amic acid modified PE/PP-g-PGMA prepared with RAFT mediation exhibited better Eu and Sm adsorption performance than the diglycol amic acid adsorbent prepared using conventional grafting. The diglycol amic acid modified PE/PP-g-PGMA exhibited selectivity for Eu over Cu and Fe in acidic solutions. The introduction of RAFT polymerization in the DA-modified adsorbent preparation process enhanced the reactivity and performance in terms of Eu and Sm adsorption.

TABLE OF CONTENTS

LIST OF FIGURES

LIST OF TABLES

LIST OF ABBREVIATIONS

^{1}H NMR	proton nuclear magnetic resonance
APNWF	abaca/polyester nonwoven fabric
APNWF-g-PGMA	abaca/polyester nonwoven fabric-graft-poly(glycidyl methacrylate)
ATR-FTIR	attenuated total reflection Fourier transformed infrared spectroscopy
BV	bed volumes
CPPA	4-cyano-4-((phenylcarbonothioyl)thio) pentanoic acid
CRP	controlled radical polymerization
CTA	chain transfer agent
D	distribution coefficient
DA	diglycol amic acid
DCM	dichloromethane
Dg	degree of grafting
DGA	diglycolic anhydride
DMF	dimethylformamide
DMSO	dimethylsulfoxide
DSC	differential scanning calorimetry
DTG	derivative thermogravimetry
EB	electron beam
EDA	ethylenediamine
EDX	energy dispersive X-ray spectroscopy
FTIR	Fourier transformed infrared spectroscopy
GMA	glycidyl methacrylate
GPC	gel permeation chromatography

ICP-OES	inductively coupled plasma optical emission spectrometer
IPA	isopropanol
MCC	microcrystalline cellulose
MCC-g-PGMA	microcrystalline cellulose-graft-poly(glycidyl methacrylate)
M_n	number average molecular weight
NWF	nonwoven fabric
PDI	polydispersity index
PE	polyethylene
PE/PP	polyethylene/polypropylene
PE/PP-g-PGMA	polyethylene/polypropylene-graft-poly(glycidyl methacrylate)
PGMA	poly(glycidyl methacrylate)
PNRI	Philippine Nuclear Research Institute
PP	polypropylene
RAFT	reversible addition-fragmentation chain transfer
REE	rare earth element
RIGP	radiation-induced graft polymerization
SEM	scanning electron microscopy
T_g	glass transition temperature
TG	thermogravimetry
TGA	thermogravimetric analysis
THF	tetrahydrofuran
WHF	water hyacinth fibers
WHF-g-PGMA	water hyacinth fibers-graft-poly(glycidyl methacrylate)
XPS	X-ray photoelectron spectroscopy
XRD	X-ray diffraction

ACKNOWLEDGEMENT

First and foremost, I would like to express my sincere gratitude to my advisors Dr. Takeshi Yamanobe, Dr. Lucille Abad, and Dr. Noriaki Seko for their advices, guidance and support during the conduct of the researches discussed in this thesis, especially to Yamanobe sensei and Seko san for accepting me to work in their laboratories. They unhesitatingly provided me with all the resources and assistance required for the successful execution of this research. Doumo arigatou gozaimasu.

I gratefully acknowledge (1) Japan Society for the Promotion of Science (JSPS) for the RONPAKU Ph.D. Fellowship award that gave me the opportunity to get my doctor degree here in Japan and (2) Philippine Council for Industry, Energy and Emerging Technology Research and Development (PCIEERD-DOST) for some financial assistance during the conduct of this work.

My utmost appreciation goes to the members of the Research Project Environmental Polymer (Noriaki Seko, Yuji Ueki, Seichi Saiki, Natsuki Hayashi, Haruyo Amada, Hiroyuki Hoshina, Jinhua Chen, Noboru Kasai, Makikatsu Takahashi, Takashi Hamada, Masaaki Omiichi, Shoko Taguchi, Yoko Shimoyama, Tomomi Higuchi) for their support and assistance in the conduct of experiments and also for making my life here in Japan a very comfortable and enjoyable one.

My deepest gratitude to the current and former members of the PNRI Chemistry Research Group for the serious and not so serious discussions, and the excellent company on and off work.

Most importantly and above all, to Mama, Papa, Ate, Kuya Tutong, Bashong, Ivy, LJ, Jabeth, Kuya Raul, Ate Beth and the soon to be member of our family, my former girlfriend and future wife, Lanilyn. Everything is about you guys, my treasured and most cherished family. This thesis is for you all!

/JFM

INTRODUCTION

Graft polymerization is a well-established and widely accepted method for customizing polymer properties. The immense interest given by polymer scientists in the development of graft copolymers can be credited to the unique characteristics observed from this type of macromolecule. A graft copolymer may combine some of the characteristic properties of both polymers while random copolymers usually exhibit properties that are intermediate between those of the two basic homopolymers; hence graft copolymers have a similar role in polymer science, as do alloys in metallurgy. Another reason for the increasing interest in developing these materials is based on the potential applications in various fields such as separation and purification [1], adsorption of dyes, precious and heavy metals [2 – 6], energy conversion and energy storage [7], solid phase catalyst for biodiesel production [8] and biomedical applications [9 – 10].

Numerous methods have been suggested for the preparation of graft copolymers. In general, these methods confer graft side chains on the base polymer backbone by robust covalent bonding [11]. Three basically different grafting approaches are known: the “grafting to” approach which couples the reactive end group of a pre-formed polymer to a functional group on the polymer backbone; the “grafting from” approach that allows the growth of the graft polymer chain from active initiating sites on the polymer backbone; and the “grafting through” approach which is the copolymerization of a macro monomer with a low molecular weight co-monomer [12].

In practice, the “grafting from” approach is the most commonly utilized method for grafting. This approach requires formation of active sites (free radicals or charged intermediates) that will serve as initiation points on the main trunk polymer backbone. Graft polymerization may be initiated by chemical reactions, plasma, UV-light and ionizing radiation. In recent years, an increasing number of papers have been published on ionizing radiation-induced graft polymerization of natural and synthetic polymers [1 – 10], mostly because of the fact that the methods using ionizing radiation are often easier to handle than most conventional chemical techniques. Moreover, radiation-induced grafting methods are very general, owing to the

unselective absorption of radiation in matter. Radiation-induced graft polymerization (RIGP) has the advantages of (a) facile preparation, (b) final material free from toxic chemical initiators, (c) availability of various radiation sources, (d) ambient conditions required for RIGP, (e) possibility of surface- and bulk-grafting, and (f) ability to combine polymers with incompatible properties. The proper combination of monomer, polymer substrate, radiation source and RIGP technique allowed the synthesis of functional polymers for new applications and better performance than conventional polymer materials [1, 3].

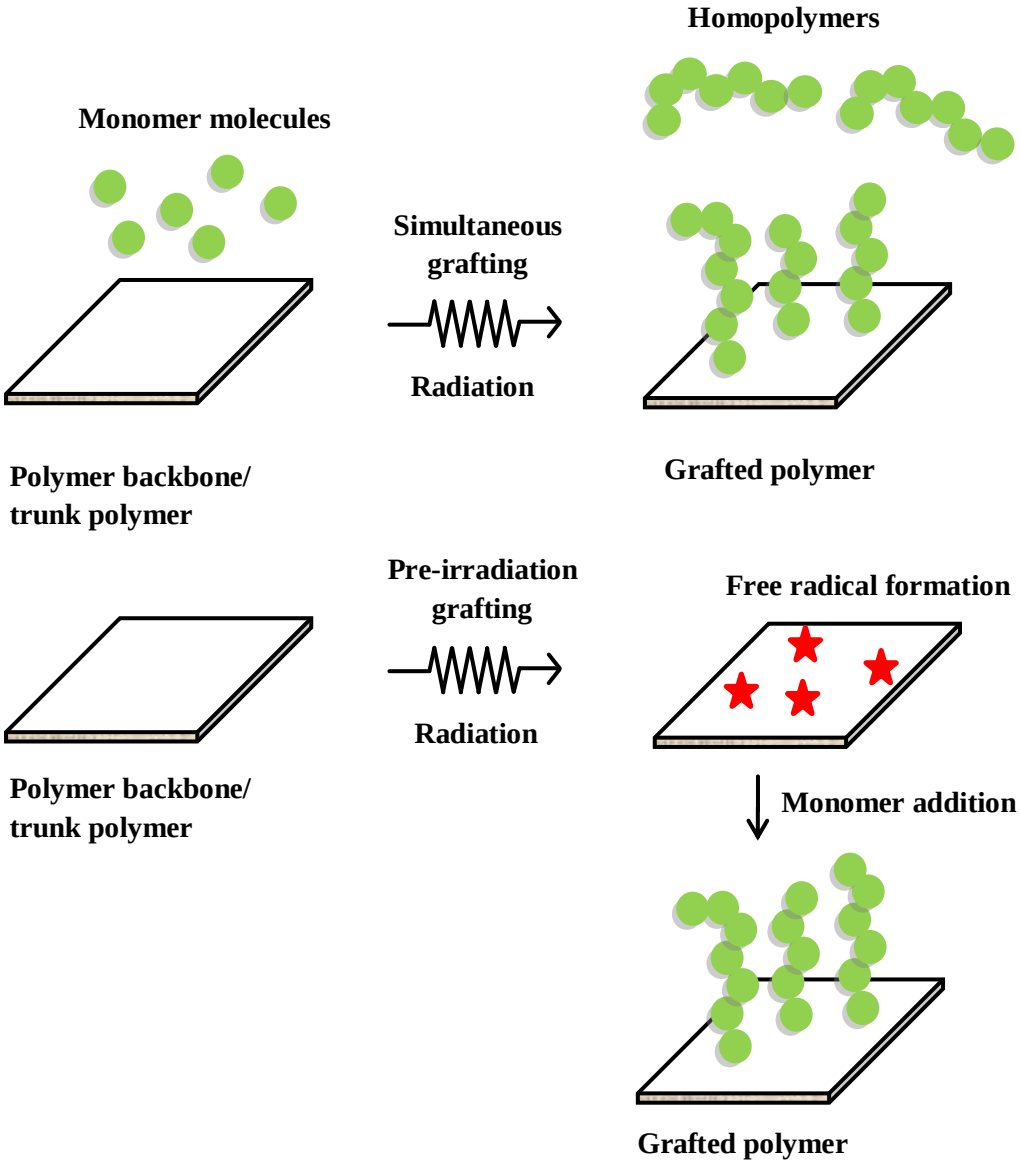

Figure 1 Simultaneous and pre-irradiation grafting

Two main techniques are generally used in performing RIGP: (1) simultaneous (mutual) irradiation grafting and (2) pre-irradiation grafting techniques. These techniques are illustrated in Figure 1. In the simultaneous irradiation technique, the trunk polymer is immersed in the monomer solution and the mixture is irradiated. An inevitable side reaction for the simultaneous method is the formation of too much free homopolymers because the monomer is also subjected to radiation. This homopolymerization can be suppressed by adding homopolymerization inhibitors in the monomer solution. In the pre-irradiation technique, the trunk polymer is irradiated (*in vacuo* or inert conditions) to produce free radicals and subsequently, is thoroughly mixed with pure monomer or monomer mixture under regulated reaction conditions. Because the monomer molecules are not irradiated, pre-irradiation methods produce very minimal to zero homopolymers.

A detailed report for the effects of grafting reaction parameters (e.g. absorbed dose, dose rate, type of monomer, monomer concentration, type of trunk polymer, type of solvent, reaction temperature, and reaction time) on the amount of grafted polymer chain, normally expressed as degree of grafting (*Dg*), was provided by Nasef and Hegazy (2004) [13]. Among the reaction parameters, the solvent plays a critical part in the diffusion of the monomer molecules to the free radical sites and in the initiation, propagation and termination of the grafted polymer chains. Therefore, the type of solvent used in the grafting reaction has a significant effect on the *Dg*, degree of graft penetration and homogeneity [14]. In a solvent-mediated grafting, the monomer and trunk polymer are mixed in an appropriate solvent to facilitate monomer diffusion and to improve swelling of the base polymer. This technique has been commonly used in various RIGP methods. However, the type of solvent has to cautiously chosen to prevent early termination of the grafted polymer chains. Polar solvents (e.g. alcohols and dimethylsulfoxide) and non-polar solvents (e.g. toluene, chloroform) are commonly used in monomer dilution for RIGP. However, it is also possible to use water instead of organic solvents to perform grafting, through the emulsion-mediated grafting method. In emulsion-mediated grafting, the monomer mixture is prepared by homogenizing the monomer in water in the presence of a surfactant. The minimal use of organic solvents contributes to the green chemistry of the process [4]. Also, water provides an almost ideal solvent medium because unlike many organic solvents, it is highly resistant to attack by free radicals so that chain

transfer to the solvent can be kept to a minimum [15]. Moreover, grafting in emulsion phase provides advantages in terms of decrease in both irradiation dose and monomer concentration requirements, thus it is cheaper and economically feasible [4, 16].

Most RIGP processes proceed via free-radical mechanism. Irreversible termination of propagating polymer chains and chain transfer reactions are features intrinsic to the process of free radical polymerization. Both irreversible termination of propagating polymers and chain transfer reactions result in a loss of control over chain length and chain structure together with broadening of the molecular weight distribution [17 – 19]. These drawbacks have led to the research area of controlled free-radical polymerization (CRP), a group of polymerization techniques which applies chain transfer agents (CTA) in conventional free radical polymerization. It has been established that CTA has profound effects in free radical polymerization processes. Chain transfer processes can be utilized to control the polymer architecture and to reduce polydispersity [20]. Developments in the field of chain transfer polymerizations include the use of conventional transfer agents [21], catalytic transfer agents based on cobalt complexes [22], degenerative transfer [23], and chain transfer by reversible addition-fragmentation (RAFT) [18, 24 – 29].

Among the CRP techniques, chain transfer by reversible addition-fragmentation (RAFT) is one of the most adaptable techniques for providing pseudo-living characteristics to free radical polymerization [17, 30, 31]. RAFT polymerization shows high potential because it possesses significant advantages such as suitability to wide range of monomer (e.g. acrylates, methacrylates, and styrenic monomers), applicability under a wide array of polymerization conditions (e.g. wide range of solvents, ambient temperature, photo- or γ-initiation) and processes (e.g. solution or emulsion). RAFT-mediated graft polymerization at ambient conditions by means of γ-radiation has been successfully conducted for different types of monomers [32]. In this technique, thiocarbonyl organic compounds such as trithiocarbonates and dithioesters are used as chain transfer agents. During RAFT mediated γ-radiation initiated grafting, propagation of both grafted polymer chains (covalently linked to the surface), and free/ungrafted polymer chains (in the solution) are regulated by the same RAFT agent simultaneously. Hence, the molecular weights and molecular weight distributions of grafted and ungrafted/free polymer chains should be very similar when the grafting proceeds from the trunk polymer surface [31].

Free radical polymerization is commonly employed in the industrial production of a wide range of synthetic materials, with approximately 50% of these conventional free radical polymerization processes currently being performed in emulsions. In order to achieve industry acceptance, RAFT-mediated polymerization and other CRP methods must be viable in emulsion, particularly in water-based emulsion system [17]. Besides being an environment friendly solvent, the use of water-based emulsions offers additional advantages in terms of easy processing of the product material. Although emulsion-mediated RIGP using the "grafting from" approach has been performed using several combinations of monomers and base polymers [2 – 4, 6, 16], so far there is no study on the effects of CTA, particularly RAFT agents, on the emulsion-mediated RIGP using electron beam or γ-radiation for initiation.

The purpose of this thesis is to functionalize natural and synthetic polymers through radiation-induced graft polymerization techniques, such as simultaneous and pre-irradiation grafting, and to evaluate the effects of RAFT chain transfer agent in the emulsion phase graft polymerization. The applications of the graft copolymers in adsorbing different heavy and rare earth metals, and in imparting hydrophobic surface are also explored. **Chapter 1** explores the solution- and emulsion-mediated radiation-induced graft polymerization of the oxirane group-containing monomer glycidyl methacrylate (GMA) on microcrystalline cellulose, delignified water hyacinth fibers and abaca/polyester nonwoven fabrics. These trunk polymers were radiation grafted using the proposed technique for the first time; hence their successful epoxide group functionalization opens doors to a variety of new applications. The conventional "grafting from" approach was utilized and both simultaneous irradiation and pre-irradiation methods for grafting were employed in synthesizing the grafted cellulosic and lignocellulosic materials, emphasizing on the effects of the reaction parameters on the amount of grafted chains. The radiation-grafted water hyacinth fibers and abaca/polyester polymers were tested for their heavy metal adsorption capacity, while the radiation-grafted microcrystalline cellulose was tested for its wettability in two immiscible solvents. The techniques utilized in Chapter 1 primarily proceed through the free radical polymerization process, which suffers from lack of control on the molecular weight and molecular weight distribution of the graft chains. We imparted control to the radiation-grafting process by addition of RAFT agent to the monomer

mixture to suppress irreversible termination reactions. **Chapter 2** analyzes, for the first time, the effects of adding RAFT agent in the industry relevant emulsion-mediated radiation-induced graft polymerization of glycidyl methacrylate (GMA) on the synthetic polymer backbone polyethylene/polypropylene. The union of the two techniques, i.e. RAFT-mediation and radiation induced grafting in emulsion phase, was motivated by the prospective combination of the merits and advantages offered by the individual methods. Both simultaneous irradiation and pre-irradiation techniques were applied and the results, in terms of the amount of grafted polymer chain and molecular weight distribution of homopolymers, from the two techniques were discussed. **Chapter 3** focuses on the comparison of the chemical reactivity and the europium adsorption capacity of the poly(glycidyl methacrylate) (PGMA) modified polymers prepared in emulsion phase via RAFT-mediated radiation-induced grafting with those synthesized using the conventional radiation-induced grafting. The synthesized radiation-grafted polymers are suitable as precursor material and it can be tailor fit to meet the desired properties of the target applications, which in this case, as rare earth element adsorbent. All the results and important insights were synthesized in **Chapter 4**, together with the recommendations and suggestions for future research.

REFERENCES:

1. Nasef, M.M.; Güven, O. *Prog. Polym. Sci.* **2012**, *37*, 1597-1656.
2. Madrid, J.F.; Nuesca, G.M.; Abad, L.V. *Radiat. Phys. Chem.* **2014**, *97*, 246-252.
3. Madrid, J.F.; Ueki, Y.; Seko, N. *Radiat. Phys. Chem.* **2013**, *90*, 104-110.
4. Seko, N.; Ueki, Y.; Hoshina, H.; Tamada, M. *J. Ion Exch.* **2007**, *18*, 232-235.
5. Hoshina, H., Ueki, Y., Saiki, S., Seko, N. *Int. J. Org. Chem.* **2014**, *4*, 195-200.
6. Kavaklı, P.A.; Kavaklı, C.; Seko, N.; Güven, O. 2016. *Radiat. Phys. Chem.* **2016**, *127*, 13-20.
7. Nasef, M.M.; Gürsel, S.A.; Karabelli, D.; Güven, O. *Prog. Polym. Sci.* **2016**, *63*, 1-41.
8. Ueki, Y.; Saiki, S.; Shibata, T.; Hoshina, H.; Kasai, N.; Seko, N. *Int. J. Org. Chem.* **2014**, *4*, 91-105.
9. Akiyama, Y.; Kushida, A.; Yamato, M.; Kikuchi, A. and Okano, T. *J. Nanosci. Nanotech.* **2007,** *7*, 796-802.
10. Biazar, E.; Zeinali, R.; Montazeri, N.; Pourshamsian, K.; Behrouz, M.J.; Asefnejad, A.; Khoshzaban, A.; Shahhosseini, G.; Soleimannejad, M.; Najafabadi, Abyani, R.; Jamalzadeh, H.; Fouladi, M.; Hagh, S.R.; Khamaneh, A.S.; Kabiri, S.; Keshel, S.H.; Mansourkiaei, A. *Int. J. Nanomed.* **2010**, *5*, 549-556.
11. Wojnarovits, L.; Foldvary, Cs.M.; Takacs, E. *Radiat. Phys. Chem.* **2010**, *79*, 848-862.
12. Roy, D.; Semsarilar, M.; Guthrie, J.T.; Perrier, S. *Chem. Soc. Rev.* **2009**, *38*, 2046-2064.
13. Nasef, M.M.; Hegazy, E.S.A. *Prog. Polym. Sci.* **2004,** *29*, 499-561.
14. Nasef, M.M. *Polym. Int.* **2001**, *50*, 338-346.
15. Franks, F. *Water A Comprehensive Treatise: Volume 4: Aqueous solutions of amphiphiles and macromolecules, Plenum Press, New York, USA*, **1975**, 585-586.
16. Wada, Y.; Tamada, M.; Seko, N.; Mitomo, H. *J. Appl. Polym. Sci.* **2008**, *107*, 2289-2294.
17. Vosloo, J.J.; De Wet-Ross, D.; Tonge, M.P.; Sanderson, R.D. *Macromolecules* **2002,** *35*, 4894-4902.
18. Grasselli, M.; Betz, N. *Nucl. Instrum. Meth. B* **2005**, *236*, 201-207.
19. Matyjaszewski, K. and Spanswick, J. *Mater. Today* **2005**, *8*, 26-33.

20. Rizzardo, E.; Chong, Y.K.; Evans, R.; Moad, G. and Thang, S.H. *Macromol. Symp.* **1996**, *111*, 1-11.
21. Boutevin, B. *Adv. Polym. Sci.* **1990**, *94*, 69.
22. Davis, T.P.; Kukulj, D.; Haddleton, D.M.; Maloney, D.R. *Trends Polym. Sci.* **1995**, *3*, 365-373.
23. Gaynor, S.C.; Wang, J.S.; Matyjaszewski, K. *Macromolecules* **1995**, *28*, 8051-8056.
24. Moad, G.; Chiefari, J.; Chong, Y.K.; Krstina, J.; Mayadunne, R.T.A.; Postma, A.; Rizzardo, E.; Thang, S.H. *Polym. Int.* **2000**, *49*, 993-1001.
25. Yu, W.; Kang, E.; and Neoh, K. *Langmuir* **2005**, *21*, 450-456.
26. Yoshikawa, C., Goto, A., Tsujii, Y., Fukuda, T., Yamamoto, K., and Kishida, A. *Macromolecules* **2005**, *38*, 4604-4610.
27. Wang, W.; Neoh, K.; Kang, E. *Macromol. Rapid Comm.* **2006**, *27*, 1665-1669.
28. Millard, P.E.; Barner, L.; Reindhardt, J.; Buchmeiser, M.; Barner-Kowollik, C.; Muller, A. *Polymer* **2010**, *51*, 4319-4328.
29. Barsbay, M.; Güven, O. *Polymer* **2013,** *54*, 4838-4848.
30. Moad, G.; Rizzardo, E.; Thang, S.H. *Aust. J. Chem.* **2005,** *58*, 379–410.
31. Barsbay, M.; Güven, O.; Stenzel, M.H.; Davis, T.P; Barner-Kowollik, C.; Barner, L. *Macromolecules* **2007,** *40*, 7140–7147.
32. Barsbay, M.; Güven, O. *Radiat. Phys. Chem.* **2009,** *78*, 1054–1059.

CHAPTER 1

RADIATION-INDUCED GRAFT POLYMERIZATION IN SOLUTION AND EMULSION PHASE: MODIFICATION OF CELLULOSIC AND LIGNOCELLULOSIC POLYMERIC MATERIALS

1.1 INTRODUCTION

Cellulose is a natural polymer and it constitutes the most abundant and renewable biopolymer resource available worldwide. Natural sources of cellulose include several agricultural products and byproducts, such as cotton, abaca, sugar cane bagasse, jute, rice straw [1 – 3], some animals and in some cases, bacteria and fungi [4 – 6]. Cellulose is one of the raw materials with high potential for the modern industry. It is a carbohydrate composed of β-D-glucopyranose units joined together by β-1,4-glycosidic linkages, as illustrated in Figure 1.1. The glucose units in cellulose are oriented in a way, which produces long, and unbranched chains, allowing the cellulose molecules to develop highly ordered structures. Cellulose samples normally include both amorphous and crystalline regions.

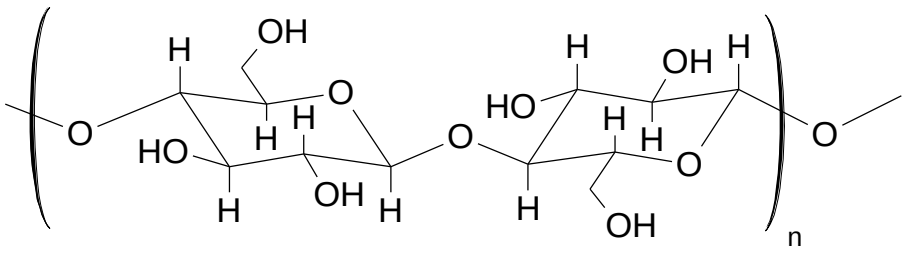

Figure 1.1 Cellobiose unit: two β-D-glucopyranose units joined together by β-1,4-glycosidic linkages.

In nature, cellulose is normally intimately associated with lignin and hemicelluloses, and some protein, lipids, wax, etc. [7] and the structure of this biomass is normally referred to as lignocellulose. The relative proportion of the three main components (i.e. cellulose, hemicellulose and lignin) of lignocellulose is dependent on the plant source [8]. Hemicelluloses are branched carbohydrates, comprised of five- and six-carbon sugars such as arabinose, galactose, mannose and

xylose, with lower degree of polymerization than cellulose. Lignin, on the other hand, is a branched, three-dimensional, complex polymer with both aromatic, such as *p*-coumaryl alcohol, coniferyl alcohol and sinapyl alcohol and aliphatic components. Both hemicelluloses and lignins can be eliminated from the raw material source by alkali hydrolysis [9].

Radiation processing of natural materials to modify their properties has been studied for several applications [3, 10 – 19]. Radiation interacts with matter to create excited or ionized atoms or molecules, followed by a rapid train of processes involving definable intermediates (ions, electrons, free radicals) leading to chemical change. The free radicals generated in the amorphous regions of cellulose decay fast, while others that are located in the crystalline and in the boundary of amorphous and crystalline areas of cellulose structure decay more gradually. The long-lived radicals may give rise to further degradation [20] and may also initiate graft polymerization in the presence of a different type of monomer to impart new functionalities.

In recent years, radiation-induced graft polymerization is considered as an important research subject, because it has been shown as a good method for the modification of chemical and physical properties of polymeric material [3, 19, 21 – 27]. The process of radiation-induced grafting has advantages over chemical grafting. The most pronounced is the absence of chemical initiators, which are, most of the time, unnecessary in the final product. Residual initiators slowly leach out when the polymers are in use and thus are not desirable for biomaterials and for polymers which are targeted for environmental applications [3, 10]. Another advantage is that high temperature is not necessary for radiation-induced grafting; hence heat sensitive monomers can be polymerized or grafted safely [3, 10]. In order to obtain different kinds of functional polymers, grafting of monomers that have various types of functional group or those which are straightforwardly transformed to other functional chemical groups have been tried. Radiation-induced grafting has also been shown to impart important properties to cellulosic materials; such properties include flame retardancy, high absorbency, water impermeability, abrasion resistance, anti-crease properties, rot resistance, thermo-responsive property and properties for bio-medical applications [25].

Graft polymerization of various monomer molecules from cellulose and lignocellulosic materials may be performed via mutual/simultaneous grafting or pre-irradiation grafting techniques. In the simultaneous grafting technique, the monomer and the trunk polymer are simultaneously irradiated to create initiation sites (i.e. free radicals) for graft polymerization. Most researches used monomer solutions instead of pure monomers in the simultaneous grafting technique. During irradiation, free radicals are generated from the decomposition of solvent, monomer, and trunk polymer. Generally, the solution consists of more solvent than monomer molecules and as approximation, it may be assumed that the bulk of high-energy radiation is absorbed by the solvent and the generated free radicals from solvent molecules radiolysis react with both the monomer and the trunk polymer [3]. An increase in the irradiation dose boosts the generation of free radicals on the cellulose and lignocellulose materials, and consequently, the number of active sites that may initiate graft polymerization also increases leading to increased grafting yield. In pre-irradiation grafting of cellulose, 10-40 kGy absorbed doses are utilized and in this range, the degree of grafting increases with absorbed dose [28].

In this chapter, the modification of microcrystalline cellulose and two lignocellulosic biomasses, namely water hyacinth and abaca fibers, by radiation grafting is discussed. Microcrystalline cellulose (MCC) is a plant-derived form of cellulose and it has advantage of high surface area compared to other conventional cellulose fibers. Moreover, it has good mechanical properties, making it a very promising cellulosic reinforcement in polymeric matrices [29]. However, the inherent hydrophilicity of microcrystalline cellulose limits its dispersion and compatibility with hydrophobic matrices. This results to low interface bonding strength which affects the properties of composites containing MCC. Consequently, modification of MCC to enhance its hydrophobicity is of interest in order to improve its compatibility with various hydrophobic matrices. Water hyacinth (*Eichhornia crassipes)* is a waterweed that rapidly propagates causing congestion of waterways. In 2011, several parts of Mindanao area in the Philippines were heavily flooded due to water hyacinth infestation of major river systems. In most cases, the plants are just allowed to rot and thrown away. Recently, the fibers from water hyacinth plants at the Philippines have been used to produce textiles, bags and footwear. The Philippines remains the world's largest producer of fibers from abaca plant (*Musa textilis)*. As such, the industry

continues to contribute and sustain the country's economic growth and development. There are plenty of applications for abaca fibers worldwide. Some of these include the use of abaca fiber in the automotive industry and the use of enzyme from abaca in cosmetics. However, continuous development of new end-use of abaca fiber should be done to further heighten the country's competitive advantage in the world market.

The purpose of this chapter is to investigate the conventional radiation-induced grafting of the epoxide-containing monomer glycidyl methacrylate on microcrystalline cellulose and two lignocellulosic biomasses, abaca and water hyacinth fibers, which are present in large amounts in the Philippines. The abundance of these materials presents an advantage for the Filipinos; hence, it is necessary to try and explore possibilities for new applications of these natural polymers. This chapter discusses in detail the implementation of simultaneous and pre-irradiation grafting techniques for the modification of the chosen trunk polymers. The grafted lignocellulosic materials were tested for their metal ion adsorption capability. On the other hand, the change in the hydrophilic character of microcrystalline cellulose was evaluated after grafting it with poly(glycidyl methacrylate) (PGMA). The effects of various grafting parameters on the amount of grafted chains were systematically studied and discussed.

1.2 EXPERIMENTAL

1.2.1 Materials

The delignified water hyacinth fibers (WHF) and needle-punched abaca-polyester nonwoven fabrics (APNWF) were given in kind by the Philippine Textile Research Institute (PTRI) while the microcrystalline cellulose (MCC), with a density of 1.5 g/cm^3, was obtained from Merck. The WHF were cleaned by soaking in methanol for an hour. These were then washed repeatedly with deionized water and air dried at room temperature. Final drying was performed in an oven at 40 °C for 72 hours. Analytical grade glycidyl methacrylate (GMA, >97%, Aldrich or Tokyo Chemical Industry Co.), methanol (>99.8%, Tedia), dimethylformamide (DMF, >99.8%, RCI Labscan), acetone (> 99.5%, Univar), isopropanol (IPA, >99%, Tedia), ethylenediamine (EDA, >99%, Aldrich or Kanto Chemical Co.), sulfuric acid (>98%,

Univar), polyoxyethylene sorbitan monolaurate (Tween 20, Kanto Chemical Co.), were used as received. The Pb^{2+}, Cu^{2+}, Cr^{3+} and Ni^{2+} solutions for ion adsorption studies were prepared from either from 1000 ppm Titrisol standard solutions (Merck, for adsorption by grafted WHF) or from the metal ion salts $Ni(CH_3COO)_2 \cdot 4H_2O$ (>98.0%) and $CuSO_4 \cdot 5H_2O$ (>99.5%, Kanto Chemical Co., for adsorption by grafted APNWF). Deionized water was obtained from an ultra-pure water system Milli-Q plus (Millipore).

1.2.2 Radiation-induced grafting

In the γ-radiation-induced grafting of WHF and MCC, the monomer GMA was dissolved in suitable solvents (e.g. methanol, acetone, DMF, water/methanol mixture) to prepare the monomer solution. A weighed amount of WHF or MCC was mixed with the GMA solution, and then the mixture was deoxygenated by bubbling with high purity N_2 gas for 10 minutes. The samples were irradiated by ^{60}Co gamma rays (absorbed dose 2-30 kGy, dose rate 8 kGy $hour^{-1}$) in the Philippine Nuclear Research Institute (PNRI) Gamma Irradiation Facility at room temperature. After irradiation, the grafted WHF and MCC were filtered from the mixture. The homopolymers and unreacted monomers adhered on the grafted samples were removed by extraction with acetone in a Soxhlet extraction set-up for 5 hours. The samples were then dried in a convection oven at 40 °C for 24 hours. The absorbed dose was determined by an ethanol-chlorobenzene dosimetry system, which is traceable to the National Physical Laboratory, United Kingdom and prepared using ASTM 51538.

In the electron beam-induced grafting of APNWF, the APNWF was first cut into 3 cm x 3 cm square pieces and were placed in polyethylene bags. The air inside the polyethylene bags was displaced with high-purity nitrogen gas. The samples were then irradiated at dry ice temperature with electron beam of 2 MeV energy and 3 mA current up to absorbed doses of 50, 100 and 200 kGy. The absorbed dose of the samples irradiated with electron beam was evaluated from the response of cellulose triacetate dosimeter. The irradiated APNWF samples were placed in a glass ampoule that was immediately evacuated of air using a vacuum line. Afterwards, a previously deaerated emulsion composed of GMA and Tween20 in deionized water was drawn into the glass ampoule. The emulsion grafting was carried out by keeping the glass

ampoule in a thermostatic water bath at 40 °C for 1 – 4 hours. After the desired reaction time, the grafted APNWF pieces were washed repeatedly with methanol, to remove the remaining non-reacted GMA and adhered Tween 20, and then dried *in vacuo*.

The amount of grafted poly(glycidyl methacrylate) (PGMA) chains on the cellulosic and lignocellulosic trunk polymers were expressed as degrees of grafting (*Dg*) and the values were calculated gravimetrically using the following equation:

$$Dg\,[\%] = \frac{W_g\text{-}W_o}{W_o} \times 100 \qquad (1.1)$$

where W_g is the weight of trunk polymer after grafting and W_o is the weight of pristine trunk polymer.

1.2.3 Post-grafting functionalization

The epoxide groups in the water hyacinth fibers-g-poly(glycidyl methacrylate) (WHF-g-PGMA) were converted into amino functional groups by reaction with EDA solution in IPA. Approximately 0.1 gram of the WHF-g-PGMA was mixed in the ethylenediamine solution for 24 hours with continuous shaking at 30 °C. The functionalized WHFs were washed repeatedly with deionized water and then dried in a convection oven at 40 °C for 48 hours. The dried functionalized fibers were kept in a desiccator prior to characterization and adsorption experiments. The EDA group density, expressed in mmol EDA group per gram adsorbent, was determined gravimetrically and calculated using the equation:

$$EDA\ group\ density\ [\text{mmol/g}] = [(W_f - W_g)/W_f] \times (1000/MW) \qquad (1.2)$$

where W_f is the weight of the EDA functionalized WHF, W_g is the weight of the WHF-g-PGMA and *MW* is the molecular weight of EDA.

In the same way as WHF amination, abaca polyester nonwoven fabric-g-poly(glycidyl methacrylate) (APNWF-g-PGMA) was also reacted with EDA to introduce amino functional groups on the abaca-containing polymer backbone. A solution of EDA in IPA was added to a glass ampoule containing the sample. The amination reaction was performed for 15 – 180 minutes in a thermostatic water bath at 60 °C. After the desired reaction time, the aminated APNWF-g-PGMA was removed from the solution and then washed thoroughly with methanol. After drying *in vacuo,*

the EDA group density was determined using two methods. The first method was similar to the one described above (through Equation 1.2) and the other method was based on the nitrogen content that was determined using an elemental analyzer.

1.2.4 Adsorption experiments

The effects of pH, initial metal ion concentration and contact time in the adsorption capacity of the synthesized adsorbents were evaluated. A weighed amount of the sample (e.g. pristine polymer backbone, aminated WHF, aminated APNWF) was mixed in a solution of the target metal ion. The mixture was stirred for a pre-determined adsorption time; afterwards, an aliquot was withdrawn from the solution and filtered with 0.45 μm syringe membrane filter. The filtrate was analyzed for metal ion concentration using atomic emission spectrophotometry. The amount of metal ion adsorbed by the synthesized adsorbent was reported either as percentage removal/adsorption:

$$\textit{percentage removal/adsorption}\ [\%] = (C_o - C_t)/C_o \times 100 \qquad (1.3)$$

where C_o is the initial ion concentration (ppm) and C_t is the ion concentration (ppm) of the solution at time t; or as q_t:

$$q_t\ [\text{mg metal ion/g-adsorbent}] = (C_o - C_f) \times V/W \qquad (1.4)$$

where C_o and C_f are the initial and final concentrations (ppm) of the metal ion in the aqueous phase, V is the volume of the solution (L) and W the mass (g) of the synthesized adsorbents.

The kinetic model that would better describe the adsorption of the target ions on the adsorbents was determined by fitting the obtained data into two kinetic models: the first order model [3] proposed by Lagergren and the pseudo-second order model developed by Ho and McKay [30]. The LINEST function from Microsoft Excel 2007 was used to get linear regression parameters such as r^2 and slope. The first-order rate constant of adsorption, k_1, was obtained from the slope of the plot of log $(q_e - q_t)$ versus time, where q_e and q_t are the amount of metal ion adsorbed at equilibrium and at time "t", respectively. The pseudo-second-order rate constant of adsorption, k_2, was computed from the slope of the plot of $1/q_t$ versus 1/t.

1.2.5 Characterization of grafted material

Fourier transformed infrared spectroscopy (FTIR) analysis of the pristine, grafted and functionalized samples were carried out using a Spectrum Frontier FTIR Spectrometer System (Perkin Elmer) with Single Reflection Diamond Universal Attenuated Total Reflection (ATR) accessory (Golden Gate Single Reflection Diamond ATR, Specac-Teknokroma). Samples were scanned in the range 600-4000 cm^{-1}, with a resolution of 4 cm^{-1}.

The morphology of the polymer substrates was investigated by Scanning Electron Microscopy (SEM) using a Hitachi TM 3000 (Hitachi, Japan) microscope at acceleration voltage of 15 kV and magnification of 1500X. It is equipped with Quantax 70 (Bruker-Nano, Germany) energy dispersive X-ray (EDX) spectrometer for elemental analysis.

Thermogravimetric measurement of the polymer samples was carried out using a Shimadzu TGA-50 instrument with platinum cell. The samples were heated from 25-950 ^{o}C at a rate of $10^{o}C$ per minute and maintained under nitrogen atmosphere at flow rate of 50 mL min^{-1}.

Metal ion concentrations before and after adsorption were determined using a Perkin Elmer Inductively Coupled Plasma-Optical Emission Spectrometer (ICP-OES) Optima 4300 DV or a Shimadzu AA-6300 double beam atomic absorption spectrophotometer. The concentrations of the metal ions from the adsorption experiments were calculated from their respective calibration curve.

The X-ray diffraction (XRD) patterns were taken using an X-ray diffractometer set-up, with Siemens Kristalloflex 760 X-ray Generator with Cu as anode material and Philips PW 1050/80 vertical goniometer equipped with a detector assembly, graphite crystal secondary monochromator and collimators. The X-ray diffractometer was set at 34 kV and 20 mA. Samples were scanned from $2\theta = 10°$ to 30° using the Cu Kα radiation ($\lambda = 1.54$ Å). The crystallinity index, I_C, was calculated according to Segal empirical equation:

$$I_C = (I_{002} - I_{am})/I_{002} \quad (1.5)$$

where I_{002} is the maximum intensity of diffraction of the (0 0 2) lattice peak at a 2θ angle between 22° and 23° and I_{am} is the intensity of diffraction of the amorphous material, which is taken at a 2θ angle between 18° and 19° where the intensity is at a minimum [31].

The procedure for wettability test was adopted from Namazi and Dadkah (2010). A 5 mg sample was mixed in a vial containing two immiscible solvents, water and dichloromethane, to observe the wettability of the sample with the two solvents [32].

The nitrogen content of APNWF and aminated APNWF was analyzed with a Perkin Elmer Series II CHNS/O Analyzer 2400. Samples weighing 2.5-3 mg were sealed in tin caps for analysis. Acetanilide (Perkin Elmer, C = 71.09%, H = 6.71%, N = 10.36%) was used as standard.

1.3 RESULTS AND DISCUSSION

The degree of radiation-induced graft polymerization, whether it is implemented using simultaneous or pre-irradiation method, is a function of different experimental variables such as absorbed dose, monomer concentration, solvent composition, ambient conditions and other technique-dependent factors. In order to find the optimum radiation-induced grafting conditions, the different grafting parameters were systematically varied and the effects on the amount of grafted polymer, expressed as degree of grafting (*Dg*), were studied. The optimum *Dg* value depends on the intended application of the final material. For preparation of biocompatible surface, grafting of 2-4% may be sufficient, for fuel cell and battery separator applications grafting of 20-50% would be desired and for adsorption applications even grafting of 100-150% would be preferred [33].

1.3.1 Effect of solvent

It is known that the use of solvents in radiation induced graft polymerization enhances the accessibility of monomer to the grafting sites due to the ability of the solvent to swell the polymer backbone [3]. The nature of solvent also influences the grafting kinetics for simultaneous grafting because of the indirect effect of solvent

radiolysis in the production of active sites (i.e. free radicals) on the macromolecular structure of the polymer backbone. The solubility of the monomer in the solvent must also be considered. Dimethylformamide [34], methanol, methanol-water mixtures [24, 35] and water-surfactant mixtures [36, 37] were used for this purpose.

Figure 1.2 shows the effect of solvents on *Dg* for the γ-radiation induced graft polymerization of GMA from delignified WHF. It was found that the *Dg* of GMA was dependent on the type of solvent used during grafting. Graft levels of GMA increased in the order of 1:4 H_2O/CH_3OH < acetone < dimethylformamide < 1:2 H_2O/CH_3OH < 1:3 H_2O/CH_3OH < methanol.

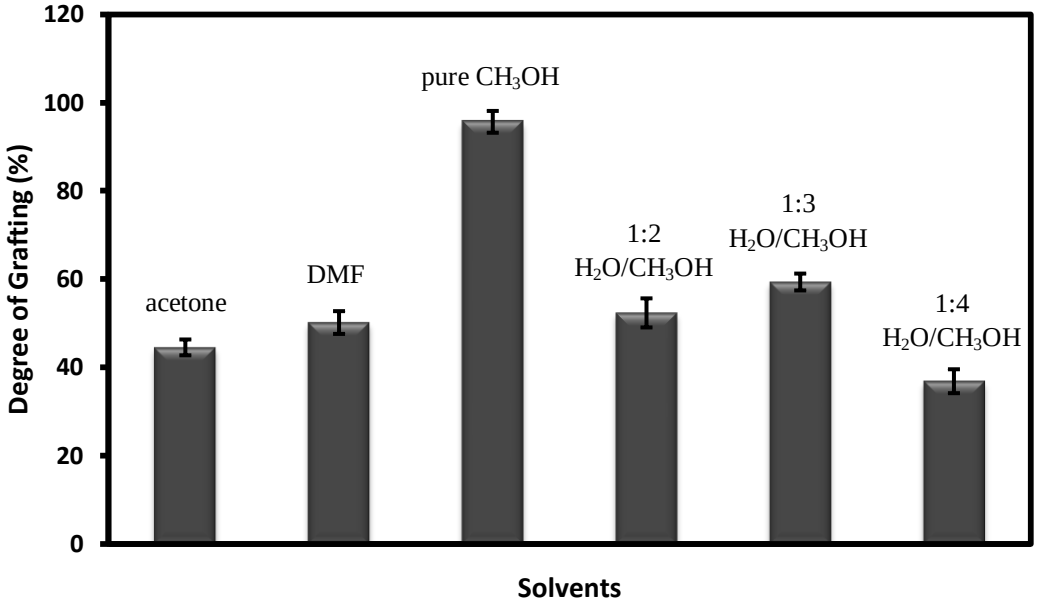

Figure 1.2 Effect of solvent on degree of grafting in the radiation-induced graft polymerization of GMA from WHF. Grafting conditions: 30 kGy, 8 kGy $hour^{-1}$, 5% GMA, 3 trials.

Results indicate that among the solvents studied for the radiation-induced grafting of GMA on WHF, methanol yielded the highest calculated *Dg* (~95%). However, the resulting grafted fibers were brittle and white flakes covered the fibers surface. This may be homopolymers that were not removed even after an extended Soxhlet extraction. The presence of homopolymer on the surface may have rendered the obtained *Dg* inaccurate. Methanol is not a good swelling agent for cellulose [38],

so the GMA monomer was not able to effectively penetrate the fiber's interior and most of the radiation-induced reactions proceeded only from the exposed surface. When DMF, acetone, or water/methanol solutions were used as solvent, the grafted fibers were not brittle and the previously adhered white flakes were not observed. Water and DMF are known to be good swelling agents for cellulose [39]. Variation of the water and methanol contents of the monomer solution affects the balance between the swelling ability of WHF in water and the dissolution of GMA by methanol. Sufficient amount of methanol ensures that more GMA reach the initiating free radicals, which were generated from the direct effect of radiation and from the indirect effects of solvent radiolysis, and propagating graft polymer chains. Water, on the other hand, swells the WHF, which increases the number of available sites for reactions within the lignocellulosic portion of the fiber. The optimum ratio among the different water/methanol mixtures for the radiation-induced grafting of GMA on WHF was found to be 1:3 water/methanol.

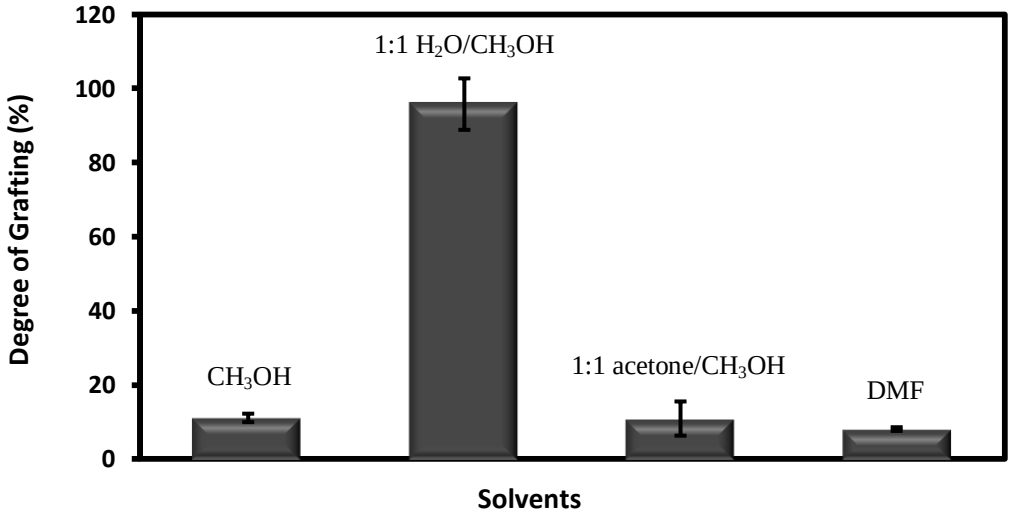

Figure 1.3 Effect of solvent on the degree of grafting in the radiation-induced graft polymerization of GMA from MCC. Grafting conditions: 10 kGy, 8 kGy hour^{-1}, 7% GMA, 2 trials.

Figure 1.3 demonstrates the variation of *Dg* with type of solvent for grafting of GMA on MCC in methanol, 1:1 water/methanol solution, 1:1 water/acetone solution, and DMF. Similar to the trend observed in Figure 1.1, the grafting of GMA on MCC exhibited solvent dependence. Graft levels of GMA increased in the order of DMF < 1:1 acetone/H_2O ~ methanol << 1:1 CH_3OH/H_2O. The results indicated that the

maximum weight increment was achieved when 1:1 CH_3OH/H_2O was used as the solvent for GMA. However, the obtained *Dg* might not be accurate because there were visible homopolymers attached to some of the grafted MCC even after more than 24 hours extraction with acetone. Although 1:1 CH_3OH/H_2O solvent system resulted to the highest *Dg* after grafting, it was not chosen for the subsequent grafting experiments because of too much homopolymer formation.

The celluloses used in this study have microcrystalline and lignocellulosic forms. Cellulose is a carbohydrate comprising of β-D-glucopyranose units bonded together by β-1,4-glycosidic linkages. The glucose units are oriented with $–CH_2OH$ groups alternating above and below the plane of rings; thus producing long and unbranched chains. In crystalline cellulose, the chains are connected primarily by hydrogen bonding. In addition to hydrogen bonding, van der Waals force has significant contribution to the lattice energy [3]. Highly ordered regions in cellulose substrates are packed so tightly that even small molecules such as water cannot penetrate these highly organized structural entities. The limited accessibility to these regions leads to alteration of their reactivity to swelling [40] which results in decreased number of accessible active sites for graft polymerization.

The radiolysis of methanol, which has been reported as a very useful solvent in the radiation-grafting of GMA [41], yields primary reactive intermediates solvated electron (e_{me}^-), hydrogen atom (H·) and hydroxymethyl radical (·CH_2OH) [42]. On the other hand, water radiolysis yields hydroxyl radical (·OH), hydrogen atom (H·) and hydrated electron (e_{aq}^-) reactive intermediates [3]. Hydroxyl (from water radiolysis) and hydroxymethyl radicals (from methanol radiolysis), and with smaller rate, hydrogen atoms (from both water and methanol radiolysis) are capable of abstracting hydrogen atoms from cellulose producing free radicals on cellulose chains [3, 10]. All three intermediates (hydroxyl and hydroxymethyl radicals, and hydrogen atoms) may react with the cellulose and GMA yielding radicals that can take part both in grafting and homopolymer formation, resulting in the high *Dg* observed in Figure 1.3. However, the obtained weight increment may be a combination of both grafted polymers and unremoved homopolymers from the grafted MCC, as stated in the previous paragraph; therefore the water/methanol solvent mixture was not chosen as the solvent for the succeeding experiments.

The radiolysis of acetone and dimethylformamide were not as widely studied compared to methanol, but it has been established that the amount of radicals created by irradiation of methanol is greater than the amount of radicals from acetone and dimethylformamide radiolysis [10]. This partly explains the higher *Dg* values calculated for WHF and MCC grafted in methanol based solvents, as shown in Figure 1.3. Based on available literature, the major primary reactive intermediates produced in the gamma irradiation of acetone are solvated electrons and methyl radical [43]. Products of the γ-radiolysis of dimethylformamide suggest that fission of the carbonyl-nitrogen and nitrogen-methyl bonds are the most probable reactions [44]. Solvated electrons react slowly, if at all, with common carbohydrates and the hydrated electron had been found to have low reactivity toward carbohydrates [3, 10].

Water is known to be a good swelling agent for cellulose [35]. Adding water to methanol and acetone solvents affect the balance between the dissolution of GMA by methanol/acetone and the swelling ability of water for cellulose. Methanol and acetone dissolves and facilitate the diffusion of GMA to the surface of MCC. Water on the other hand swells MCC to increase the number of available sites for reactions. However, the high number of radicals produced in water-based solvents contributed significantly to the formation of large amounts of homopolymers in the grafting mixture during irradiation. The difficulty of removing the homopolymers from the grafted MCC rendered the use of water/methanol solvent impractical; therefore methanol was used as the solvent for the succeeding experiments.

1.3.2 Effect of absorbed dose

In both simultaneous and pre-irradiation grafting methods, the number of free radicals generated in the sample during irradiation increases with increment in the energy absorbed by the irradiated materials (i.e. absorbed dose). Consequently, the degree of grafting increases with absorbed dose because of the increase in number of initiation sites on the polymer backbone. As expected, higher degrees of grafting were obtained at higher absorbed doses in the γ-radiation induced grafting of WHF and MCC, as shown in Figures 1.4 and 1.5, respectively. For WHF-g-PGMA, the *Dg* increased with increasing absorbed dose, which eventually leveled off at 10 to 20 kGy. A similar increasing trend of *Dg* with absorbed dose was observed for MCC-g-PGMA; however, the *Dg* did not attain a constant value even after irradiation at 20

kGy. The *Dg* value could have leveled off at higher absorbed dose, but no attempt was made to irradiate the MCC in the monomer solution beyond 20 kGy because of too much homopolymer formation in the solution. Therefore, subsequent preparation of WHF and MCC were performed at 10 kGy absorbed dose.

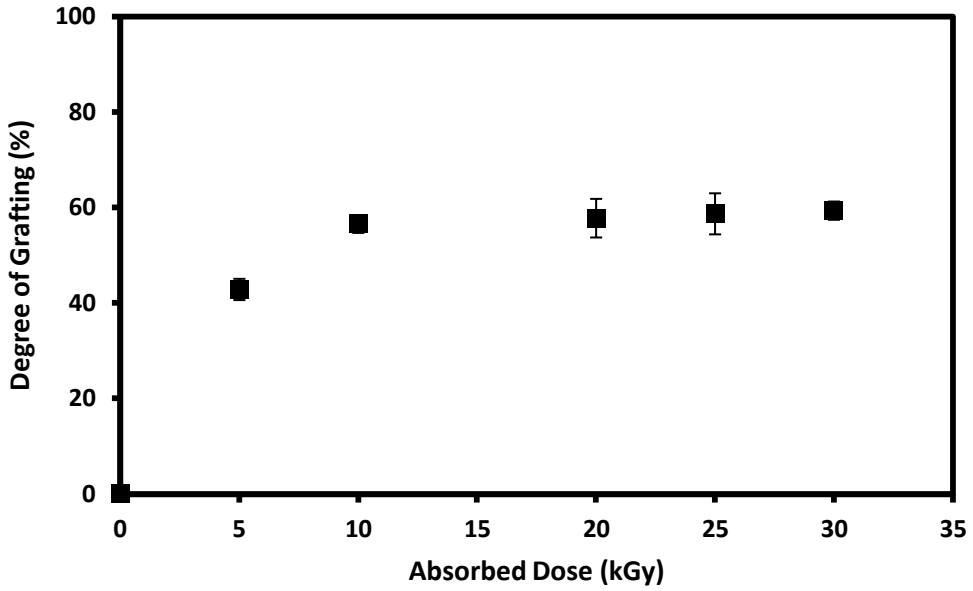

Figure 1.4 Effect of absorbed dose on degree of grafting in the radiation-induced graft polymerization of GMA from WHF. Grafting conditions: 5% GMA, 8 kGy hour^{-1} dose rate, 1:3 water/methanol, 3 trials.

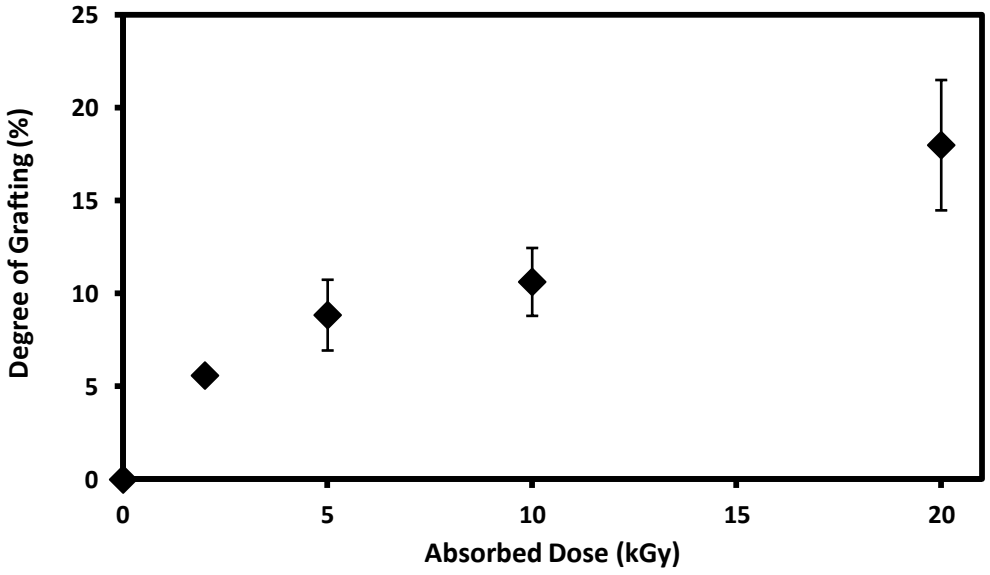

Figure 1.5 Effect of absorbed dose on degree of grafting in the radiation-induced graft polymerization of GMA from MCC. Grafting conditions: 7% GMA, 8 kGy hour^{-1} dose rate, methanol, 2 trials.

The amount of free radicals formed by interaction with radiation increases in a linear fashion with absorbed dose and then reaches a certain limiting value at higher absorbed doses. At higher absorbed doses, the degree of grafting tended to level off because of the recombination of some free radicals before they can initiate graft polymerization. The leveling off could be attributed to the fact that at higher degree of grafting values, the polymerization becomes a diffusion-controlled process [45]. The almost constant grafting extent at high absorbed doses may also be attributed either to monomer exhaustion or to the increased viscosity of the bulk of grafting mixture which restricts the glycidyl methacrylate diffusion to the grafter chains.

The number of free radicals created in the grafting mixture increased at higher absorbed dose. The radicals produced upon interaction of radiation with the sample were generated from GMA, trunk polymer (i.e. WHF and MCC) and solvent molecules because the grafting method used in the above discussions was simultaneous grafting. The free radicals from monomer and solvent can react with the trunk polymers to generate additional active sites on WHF and MCC, which lead to the higher Dg. Therefore, grafting of GMA on WHF and MCC, was enhanced at higher absorbed dose. However, larger amounts of homopolymers were also formed when higher absorbed doses were utilized because the monomer molecules were also exposed to γ-radiation.

The dose rate dependence of the degree of grafting was observed in several studies [10, 46]. Table 1.1 shows that decreasing the dose rate from 8 kGy $hour^{-1}$ to 1.4 kGy $hour^{-1}$ resulted in a 6% increase in *Dg*. High dose rates produce higher free radical density, which may favor recombination of radicals generated in close vicinity or faster generation of the homopolymer in bulk and this effect may lessen the available monomer available for grafting. However, the decrease in dose rate translated to six additional hours of irradiation time. The small increment in *Dg* did not compensate the added irradiation time so 8 kGy $hour^{-1}$ was the preferred dose rate.

Table 1.1 Effect of dose rate on degree of grafting for the radiation-induced graft polymerization of GMA from WHF. Grafting conditions: 5% GMA, 1:3 water/methanol, 10 kGy absorbed dose, nitrogen atmosphere.

Dose Rate	Degree of grafting
8 kGy $hour^{-1}$	58%
1.4 kGy $hour^{-1}$	64%

The achieved *Dg* values in the grafting of WHF are comparable with the values obtained by other researches that utilized grafted lignocellulosic and cellulosic materials. Sokker *et al*. (2009), used cotton fabric wastes as polymer backbone in the radiation-induced graft polymerization of GMA. After optimizing the grafting conditions, they were able to achieve around 80% *Dg*, but the monomer concentration used in their study is four times the optimum concentration in radiation grafting of WHF [18]. In the study of Khan (2005), he achieved 53% *Dg* in the pre-irradiation grafting of emulsified methyl methacrylate from γ-irradiated jute fibers [47]. Abdel-Aal *et al*. (2005), performed radiation-induced graft copolymerization of maize starch/acrylic acid, but they did not report the degree of grafting values [48]. Although the *Dg* values calculated from the grafted MCC were less than the values from grafted WHF and other lignocellulosic materials discussed here, it is already sufficient to change the surface property of MCC, as shown in the wettability test.

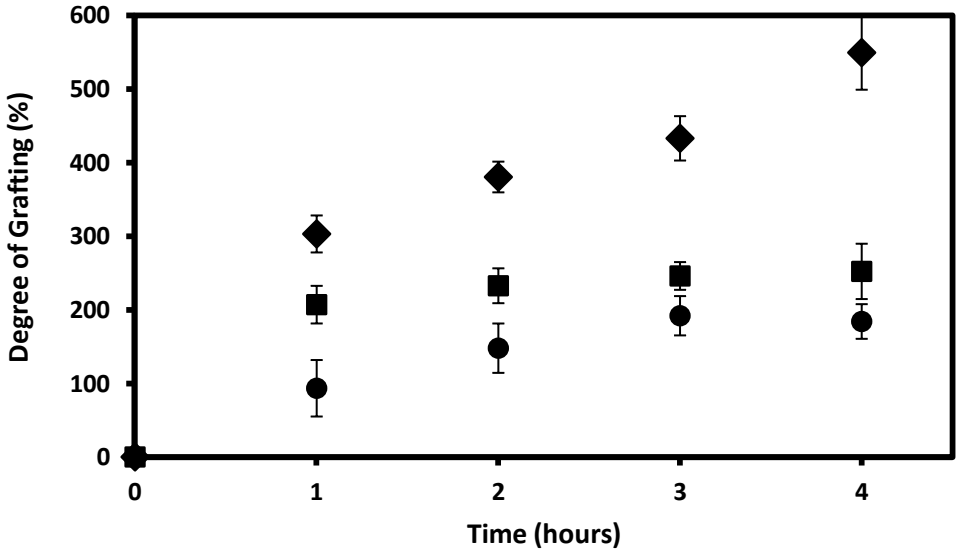

Figure 1.6 Effect of absorbed dose on degree of grafting at different reaction times for graft polymerization of GMA from electron beam pre-irradiated APNWF. Grafting conditions: 5% GMA, 0.5% Tween 20, 200 kGy (◆), 100 kGy (■) and 50 kGy (●) absorbed doses, 5 trials.

The *Dg* of grafted polymers increased with increasing absorbed dose in the pre-irradiation grafting of APNWF with GMA monomer (Figure 1.6), similar to the trend observed from the previous discussion of results from simultaneous grafting of GMA onto WHF. The trunk polymer contains abaca fibers, which are inherently tough even in its processed form. The interaction of electron beams with APNWF resulted in the production of free radicals. Higher absorbed dose yielded higher free radical concentration that translated to higher number of initiation sites for graft polymerization. Figure 1.6 shows the relationship between *Dg* and grafting time at different absorbed doses. It can be observed from Figure 1.6 that at a fixed reaction time, higher absorbed dose gave APNWF-g-PGMA with higher *Dg*. APNWF exposed to a pre-irradiation dose of 200 kGy gave a 303% *Dg* after an hour of reaction with 5% GMA emulsion and this increased to 550% after 4 hours of reaction time. However, the APNWF-g-PGMA obtained at these conditions was brittle because of the very high amount of PGMA graft chains. The brittleness made the handling of the grafted APNWF difficult for the subsequent processes. With an absorbed dose of 100 kGy, the *Dg* increased from 207% to 252% when the reaction time was increased from 1 to 4 hours. At both absorbed doses, prolonged contact of the irradiated APNWF with the GMA emulsion resulted in higher *Dg*. This can be attributed to the fact that an increase in reaction time allows more GMA molecules to react with the active sites (i.e. free radicals initiation sites) on the surface of irradiated APNWF. Prolonged contact with the GMA emulsion also enhanced the propagation of the PGMA chains, resulting in higher *Dg*.

According to Sekine *et al*. (2010), a *Dg* greater than 100% is preferable for synthesis of a metal ion adsorbent via chemical modification [36]. APNWF exposed to 50 kGy irradiation dose gave 93% *Dg* after an hour of contact with the GMA emulsion. Similar to the results observed before, the *Dg* increased with increasing grafting time. An almost constant *Dg* value of 180% was achieved after 3 hours of reaction time and this is sufficient for preparation of metal ion adsorbent. A 180% Dg corresponds to an epoxide group density of 4.5 mmol/gram-adsorbent. The grafted APNWF obtained at these conditions was more flexible compared to those exposed at higher irradiation dose. Attaining a sufficient *Dg* after irradiation at a low dose of 50 kGy is valuable for development of a metal ion adsorbent. It was found that irradiation at higher doses results in degradation of the molecular chain of the

polymeric material that leads to easy fiber-breaking [28]. Irradiation at lower absorbed dose also gives economic advantage for the process.

1.3.3 Effect of GMA concentration

The graft polymerization of GMA from WHF (simultaneous grafting), MCC (simultaneous grafting) and APNWF (pre-irradiation grafting) exhibited monomer concentration dependence, as shown in Figures 1.7 – 1.9. Higher grafting yields were obtained at higher monomer concentration because at any instant the free radicals generated on the polymer backbone surface and the free radical ends of propagating graft polymer chains, have higher chance of interaction with more monomer molecules. For graft polymers prepared using simultaneous method, however, significant formation of ungrafted PGMA homopolymers accompanied the increase in *Dg*. This was expected because the monomer was also exposed to γ-radiation. It was difficult to retrieve the grafted WHF and MCC from the sticky homopolymers. Thus, for practical reasons, the range of studied GMA concentrations was limited from 1% to 10%. It was observed that at 7% and 10% GMA concentrations, the amount of homopolymers on the surface of WHF and MCC became significant that even after acetone extraction, portions of the surface was covered with a gel-like material. This insoluble portion present on the surface may be crosslinked PGMA.

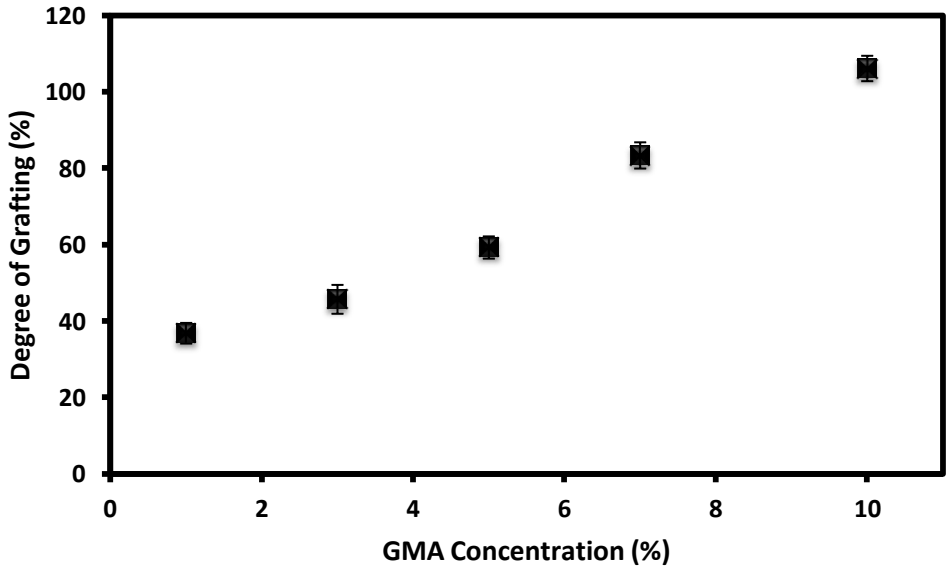

Figure 1.7 Effect of monomer concentration on degree of grafting in the radiation-induced graft polymerization of GMA from WHF. Grafting conditions: 10 kGy, 8 kGy hour^{-1}, 1:3 water/methanol, 3 trials.

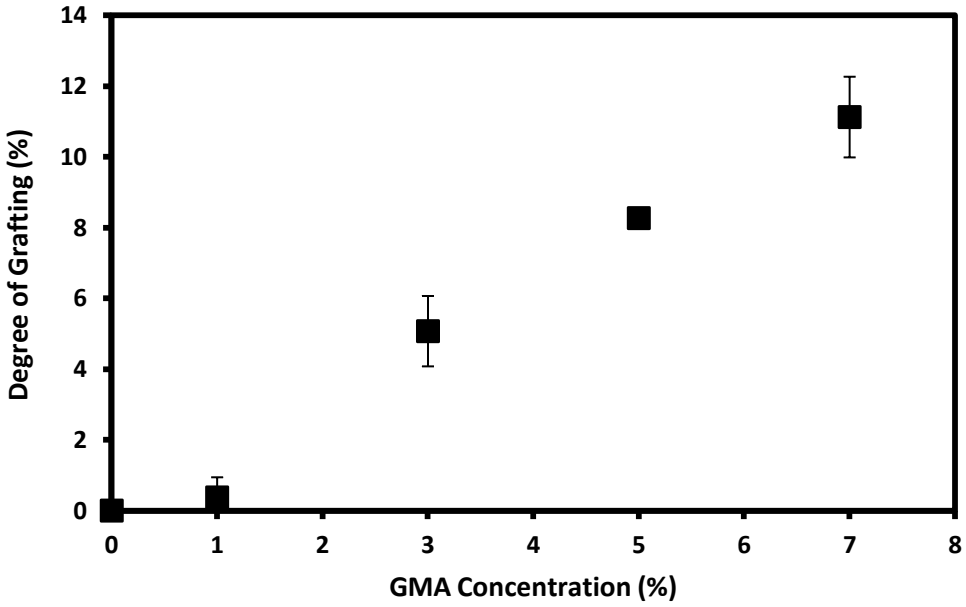

Figure 1.8 Effect of monomer concentration on degree of grafting in the radiation-induced graft polymerization of GMA from MCC. Grafting conditions: 10 kGy, 8 kGy hour^{-1}, methanol, 2 trials.

A study had shown accelerated grafting at high monomer concentrations [45]. This phenomenon was attributed to the increase in the viscosity of the medium due to formation of homopolymers. The study stated that bimolecular termination of the growing chain is hindered at high viscosity. On the other hand, the other steps in graft polymerization process such as initiation, propagation and radical chain processes are not affected to the same extent. This resulted in increased *Dg* at higher monomer concentrations, as exhibited in Figures 1.7 and 1.8, in spite of higher extent of homopolymerization.

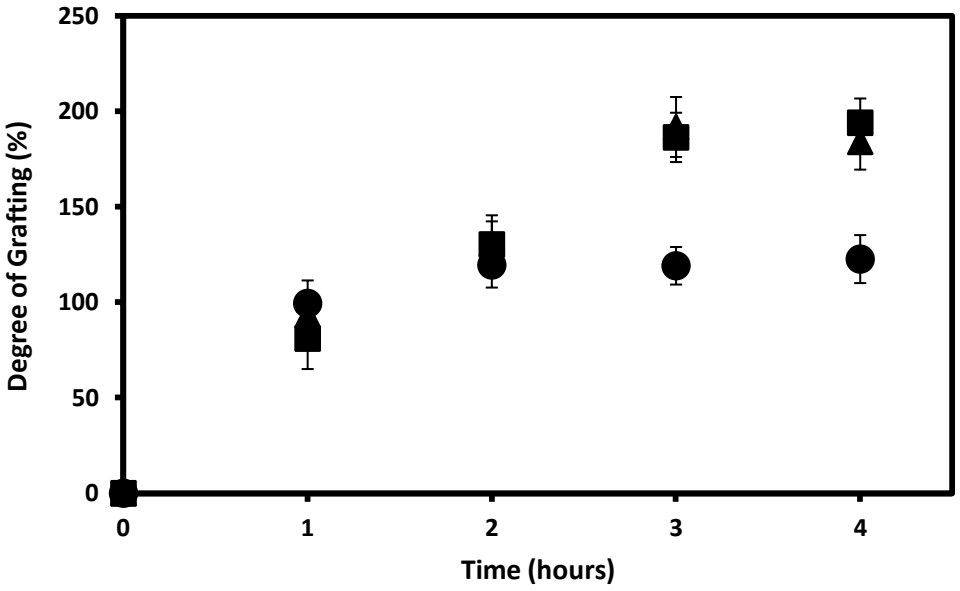

Figure 1.9 Effect of monomer concentration on degree of grafting at different reaction times for graft polymerization of GMA from electron beam pre-irradiated APNWF. Grafting conditions: 0.5% Tween 20, 50 kGy absorbed dose, 7% (■), 5% (◆) and 3% (●) GMA, 5 trials.

Figure 1.9 shows the effect of GMA concentration on *Dg* at different reaction times in the pre-irradiation grafting of GMA from APNWF. It can be observed from Figure 1.9 that an increase in GMA concentration from 3% to 5% resulted in a significant increase in *Dg* after 3 hours of reaction time. As expected, higher *Dg* was obtained at higher GMA concentration because more monomers were able to interact with the radicals and propagating polymer chains on the APNWF. Further increase in GMA concentration from 5% to 7% GMA did not result in any significant increase in *Dg*. Figure 1.9 also shows that the *Dg* reached an almost constant value faster at lower GMA concentration, i.e. the *Dg* of the grafted material reached 120% after 2 hours of reaction with 3% GMA while at 5% GMA, a higher *Dg* of 180% was attained after 3 hours. Increasing the reaction times beyond these values did not result in further increase in *Dg*. The retardation in *Dg* increase might be due to the fact that at high *Dg*, the reaction became a diffusion-controlled process [45]. The grafted PGMA chains on the surface might slowed down or prevented further diffusion of more monomers to the available active sites which resulted in an almost constant *Dg* despite the increase in reaction time. The results also showed that the prepared GMA emulsions with 10:1 monomer/surfactant ratio were stable while being deaerated

using nitrogen gas and during grafting at 40^{o}C. The emulsions were in a milky state and no phase separation was observed throughout the experiments. This is in concurrence with a previous research which showed that an aqueous emulsion with 5% GMA and 0.5% Tween 20 are stable up to 48 hours [49].

1.3.4 Amination of APNWF-g-PGMA and WHF-g-PGMA

The chemical structure of the GMA monomer (Figure 1.10) indicates that it contains a pendant epoxide group that acts as a "molecular anchor" and permits binding of reactive groups to the polymer backbone from which its polymerized form was grafted to. The epoxide ring can be chemically modified by various post-grafting reactions to generate new functional groups for various target applications. These reactions allow the conversion of the epoxide group to another functional group such as amines [36, 50], imidazole [51 – 53], alcohols [21], phosphonic acid [54], etc. that are capable of selective adsorption of metal ions and other compounds.

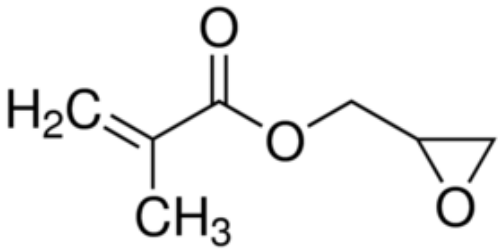

Figure 1.10 Chemical structure of the monomer glycidyl methacrylate (GMA).

The APNWF-g-PGMA polymers, with approximately 160-180% Dg, were functionalized by reacting with ethylenediamine (EDA). This process resulted in the introduction of amino functinal groups by ring opening reaction of the epoxide group in GMA. The effects of contact time and EDA concentration on the EDA group density were studied. Figure 1.11 shows the EDA group density of the aminated APNWF-g-PGMA as a function of reaction time at different EDA concentrations. It can be observed from Figure 1.11 that the EDA group densities obtained gravimetrically were almost the same with the values determined using an elemental analyzer for the APNWF-g-PGMA that were reacted with 15% and 30% EDA.

However, significant differences between the EDA group densities calculated from the two methods were observed starting at 120 and 60 minutes of reaction with 50% and 70% EDA, respectively. The EDA group density derived from the elemental analyzer reached an almost constant value while the values obtained through the gravimetric method decreased with increasing reaction time. The decrease in EDA group density indicated that the weight of the APNWF-g-PGMA decreased after amination due to prolonged contact with 50% and 70% EDA solutions. The observed decrease in weight was attributed to the degradation of APNWF-g-PGMA in contact with high EDA concentration solutions at higher reaction times. Therefore, for consistency, the results derived from the elemental analyzer will be used for succeeding discussions of aminated APNWF-g-PGMA.

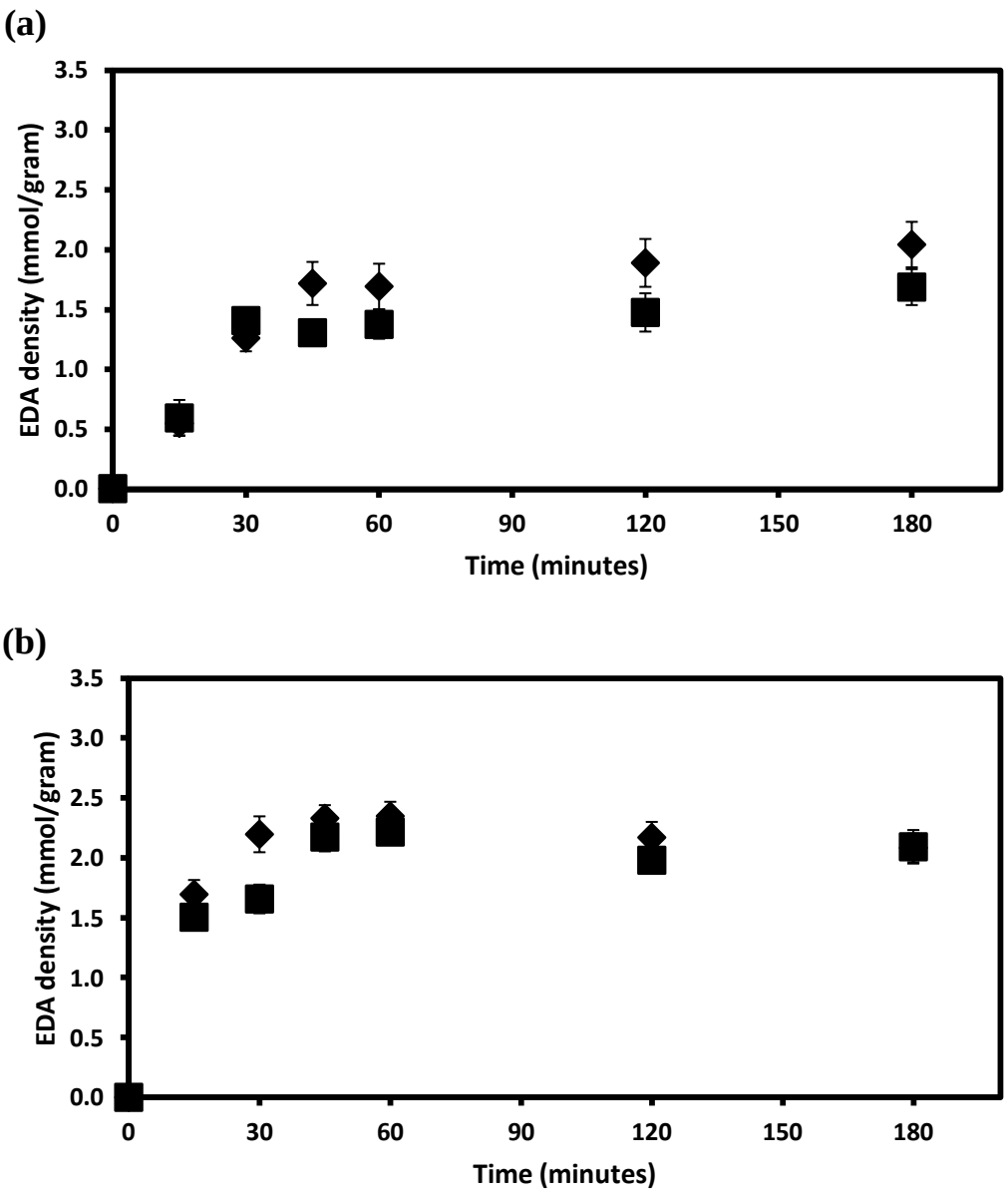

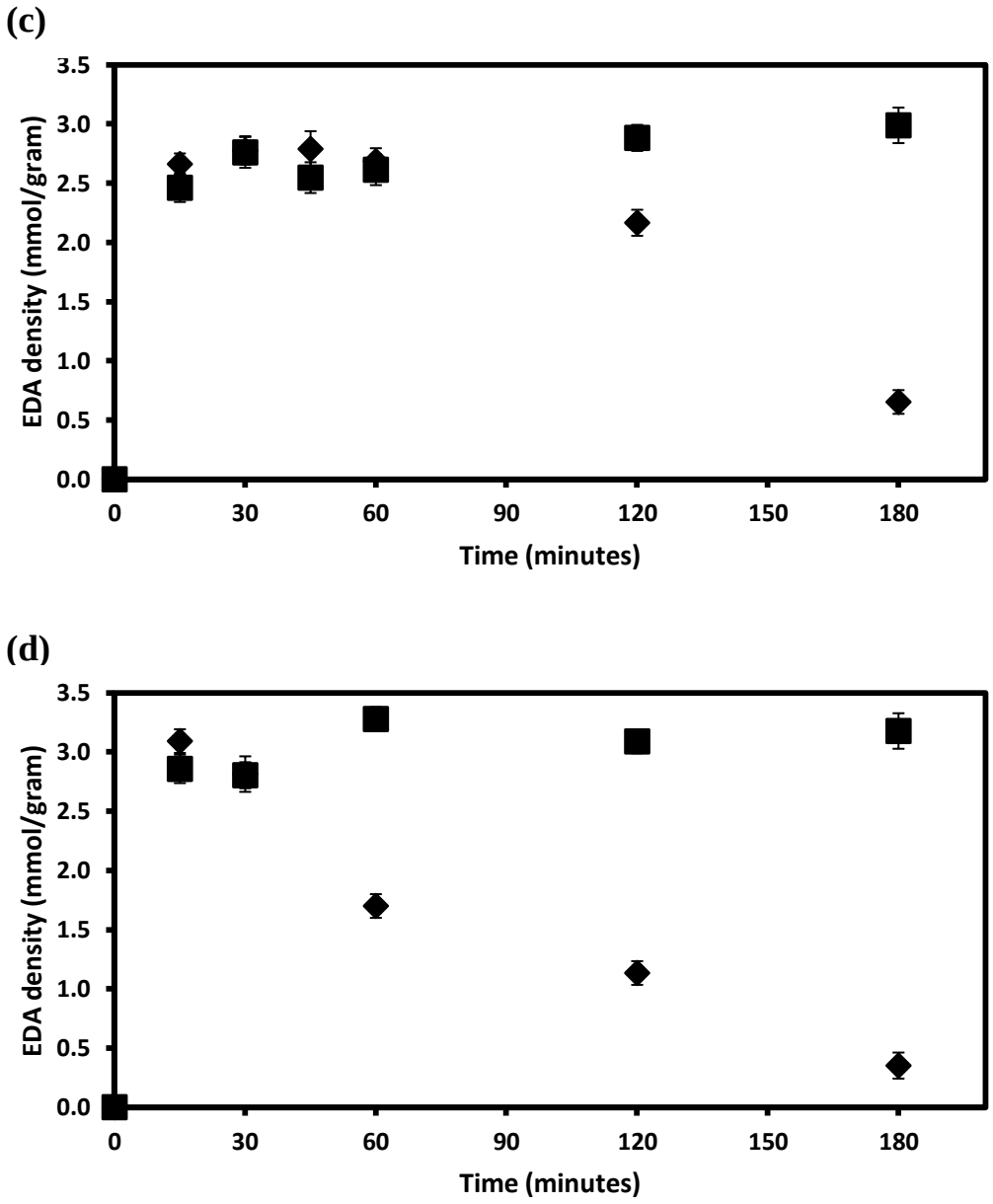

Figure 1.11 Variation of EDA group density with reaction time at (a) 15%, (b) 30%, (c) 50% and (d) 70% (wt/wt) EDA concentration. EDA group density was determined gravimetrically (◆) and by an elemental analyzer (■), 3 trials.

The plots shown in Figure 1.11 indicate that the amount of incorporated EDA groups increased with reaction time. The EDA group density reached almost constant values of 1.50, 2.10 and 2.70 mmol/gram-adsorbent after 120, 45 and 30 minutes of reaction with 15%, 30% and 50% EDA, respectively. This signified that increasing the concentration of EDA allowed the amination process to reach an equilibrium state faster. It can also be noted from Figure 1.11 that at a given reaction time, higher EDA

group density was achieved at higher EDA concentration. At a fixed reaction time, higher EDA concentration solutions have more EDA molecules that can react with the epoxide groups in APNWF-g-PGMA, resulting in enhanced conversion (i.e. ring opening reactions of epoxide group to give amino functional groups) and higher EDA group density.

All synthesis experiments that involved APNWF in this study showed that the optimum conditions for the preparation of an amino-type adsorbent from APNWF were as follows: pre-irradiation of APNWF up to 50 kGy absorbed dose, reaction with aqueous emulsion consisted of 5% GMA and 0.5% Tween 20 at 40^{o}C for 3 hours, and amination with 50% EDA at 60^{o}C for 30 minutes. These conditions allowed the synthesis of APNWF-g-PGMA with approximately 150% *Dg*, sufficient for the target adsorption application, which after amination gave 2.7 mmol EDA groups for every gram of adsorbent. Based from literature search, this is the first attempt on grafting a nonwoven fabric made of natural and synthetic polymer components.

Table 1.2 EDA group densities of aminated WHF-g-PGMA at different EDA concentrations. IPA solvent, 30 °C

EDA Concentration (%)	EDA Group Density (mmol/g)
100	-
70	1.03
50	1.78
30	0.75
10	-

Data from the amination of APNWF-g-PGMA showed that the EDA group densities that were calculated gravimetrically were comparable with the values obtained from the more accurate method, which is through nitrogen elemental analysis, especially at low reaction times and low EDA concentrations. Hence, in the amination reaction of WHF-g-PGMA, the weights of the grafted and aminated WHF were used in the calculation of the EDA group density. The results in Table 1.2 showed that the solution with 50% EDA in IPA yielded the highest EDA functional group density, 1.78 mmol/gram adsorbent, as compared with the other mixtures. Thus, this EDA concentration was used in the preparation of the amino-type fibrous WHF

adsorbent for the metal ion uptake studies. The data also showed that using too high (100%) or too low (10%) EDA concentration resulted in fibers with very low (< 0.05 mmol/g) EDA group density. This might be due to inefficient interaction between the EDA molecules and the epoxide groups on the WHF-g-PGMA at low concentrations or probable degradation of the fibers at very high concentrations.

1.3.5 Characterization of pristine and grafted cellulosic and lignocellulosic polymers

1.3.5.1 FTIR Analysis

Most researches utilized Fourier transform infrared (FTIR) spectroscopy to follow grafting and post-grafting reactions. The traditional transmission (KBr pellet) method is useful for obtaining data about the changes caused by the grafted polymer chains, both on the surface and those inside the fibrils. The attenuated total reflectance (ATR) method is a useful technique to study modifications in surface structure. The succeeding discussions will focus on the ATR-FTIR analysis of the pristine, grafted and functionalized cellulosic and lignocellulosic polymers.

(i) FTIR-ATR Analysis of WHF-g-PGMA and aminated WHF-g-PGMA

FTIR spectroscopy was performed to analyze the pristine WHF, PGMA homopolymers and WHF-g-PGMA with 58% *Dg* to investigate the graft polymerization of GMA on the lignocellulosic polymer backbone. The results of the FTIR spectroscopic analysis, in ATR mode, of the pristine and grafted WHF are shown in Figure 1.12. The FTIR spectrum of WHF exhibited the O-H stretching absorption at 3335 cm^{-1}, C-H stretching at 2890 cm^{-1}, C=C stretch from the lignin part at 1611 cm^{-1}, and C-O stretch from the cellulose units at 1027 cm^{-1}. For the PGMA homopolymer, the peaks at 1722 cm^{-1} and 1147 cm^{-1} are assigned to the C=O and C-O stretching vibrations, indicating the presence of the ester group -COO-. The peaks at 1253, 905, 843 cm^{-1} correspond to the characteristic peaks of the epoxide group. Similar characteristic peaks were observed by other researchers [3, 24]. Peaks from both WHF and PGMA were observed from the FTIR spectrum of the grafted fibers, WHF-g-PGMA, which indicates successful grafting.

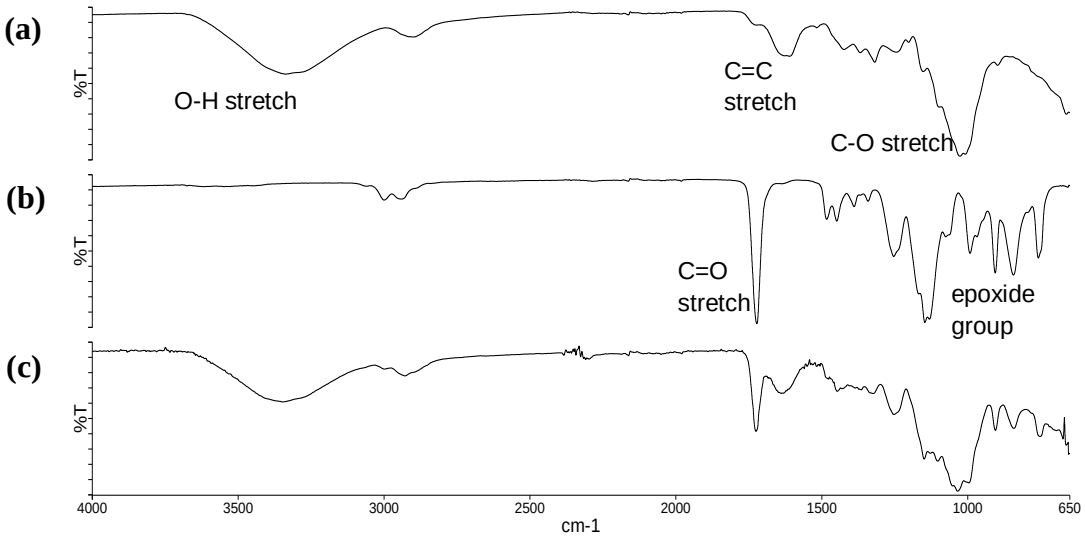

Figure 1.12 FTIR-ATR spectra of (a) pristine WHF, (b) PGMA homopolymers and (c) WHF-g-PGMA with 58% degree of grafting.

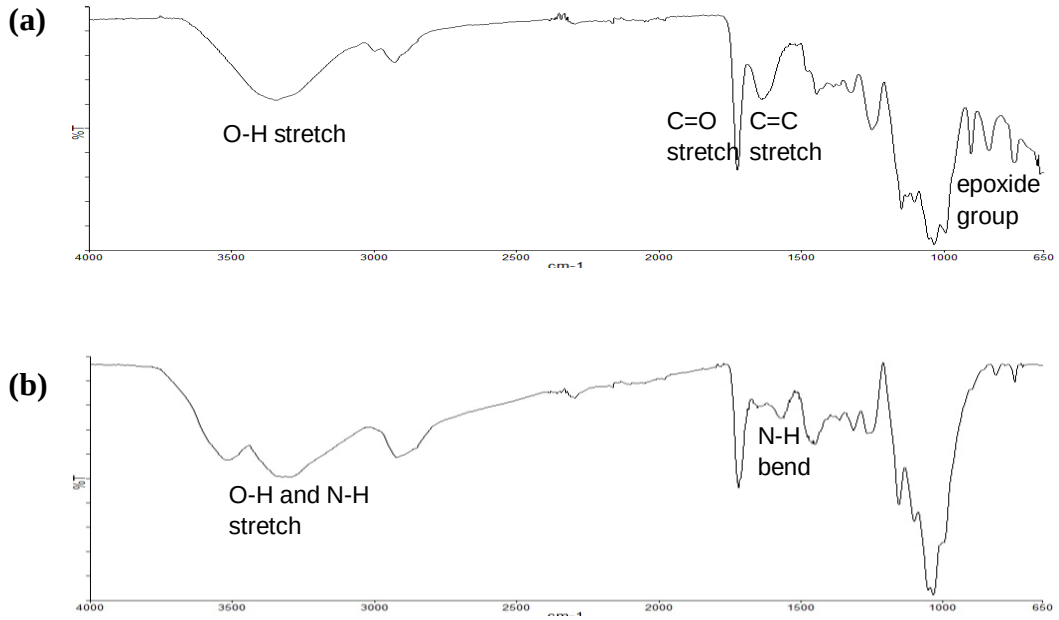

Figure 1.13 FTIR-ATR spectra of (a) WHF-g-PGMA with 58% degree of grafting and (b) EDA functionalized WHF-g-PGMA.

Figure 1.13 shows the FTIR-ATR spectra of WHF-g-PGMA and EDA functionalized WHF. Comparison of the two spectra reveals that new peaks appeared after the reaction of WHF-g-PGMA with EDA solution. The FTIR spectrum of WHF-

g-PGMA was analyzed and discussed above. Some of the peaks observed from the WHF-g-PGMA were retained after its reaction with EDA. The peak at 3510 cm^{-1}, overlapping with the -OH stretch peak at 3296 cm^{-1}, was due to the -NH_2 and -NH stretches, while the peak observed at 1568 cm^{-1} is attributed to the N-H bend. The peaks on Figure 1.13a that correspond to the epoxide group of GMA were almost absent in Figure 1.13b. This was expected because the epoxide groups in the PGMA graft chains opened upon reaction with EDA. The absence of the characteristic peaks from the epoxide group and the presence of new peaks corresponding to N-H and C-N stretches confirm the successful EDA functionalization of the WHF-g-PGMA.

(ii) FTIR-ATR Analysis of APNWF-g-PGMA and aminated APNWF-g-PGMA

The grafting of GMA from irradiated APNWF and the incorporation of EDA groups by reaction of EDA with the epoxide groups on APNWF-g-PGMA was verified using FTIR analysis. Figure 1.14 shows the spectra from the FTIR analysis of pristine APNWF, APNWF-g-PGMA and aminated APNWF-g-PGMA. The FTIR spectrum of APNWF (Figure 1.14a) exhibited absorptions corresponding to the abaca lignocellulose portion: O-H stretch at 3334 cm^{-1}, C-H stretch at 2887 cm^{-1}, glycosidic C-O-C stretch at 1100 cm^{-1}, C-OH stretch at 1017 cm^{-1}; and absorptions due to the polyester region : C=O stretch at 1712 cm^{-1}, C-O stretch at 1241 cm^{-1}. After grafting to a *Dg* of 150%, the FTIR spectrum of APNWF-g-PGMA (Figure 1.14b), showed the presence of characteristic peaks at 1255, 904, 843 cm^{-1} corresponding to the IR absorption of the epoxide group vibrations of GMA. Similar characteristic peaks were observed by other researchers [3, 24] and also in the WHF-g-PGMA discussed above. Besides the epoxide group absorption frequencies, peaks from APNWF were observed on the FTIR spectrum of APNWF-g-PGMA, which indicates successful graft polymerization of GMA from pre-irradiated APNWF.

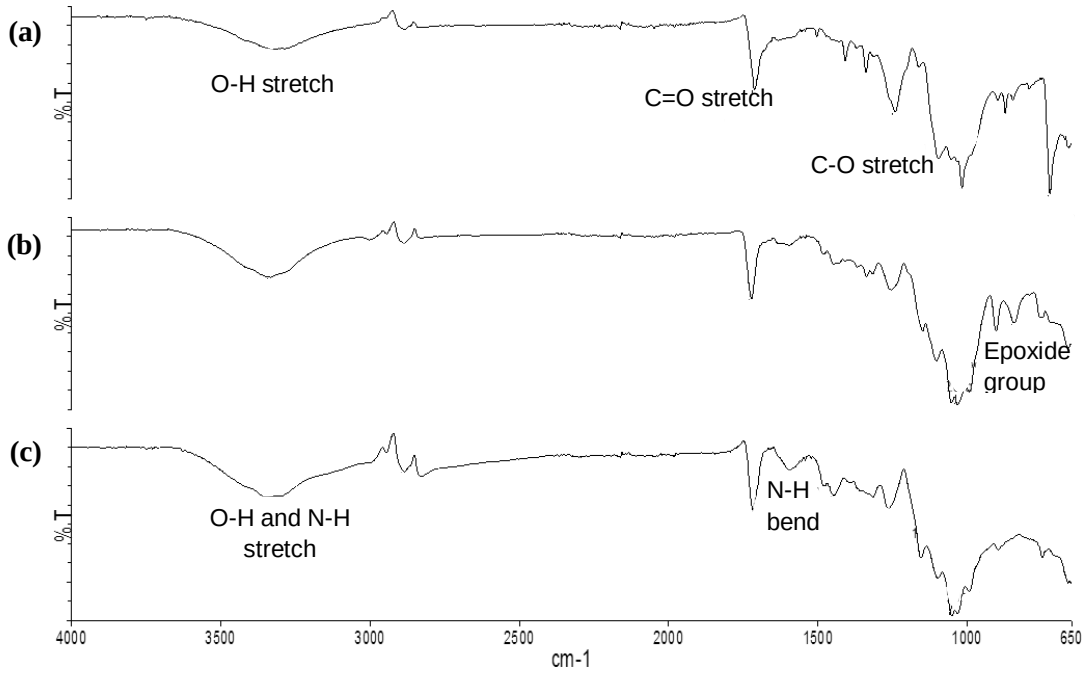

Figure 1.14 FTIR-ATR spectra of (a) pristine APNWF, (b) APNWF-g-PGMA with 150% degree of grafting and (c) EDA functionalized APNWF-g-PGMA.

Figure 1.14c shows the FTIR spectrum of the aminated APNWF-g-PGMA. Some of the peaks observed from Figure 1.14b remained after the EDA reaction. The peak at 3342 cm^{-1}, due to the O-H stretch peak from abaca has a small shoulder overlapping at around 3421 cm^{-1}, and this corresponds to the -NH_2, -NH stretches from the imparted amino groups of EDA. The peak at 1595 cm^{-1} is attributed to the N-H bend while the C-N absorption gave a peak at around 1156 cm^{-1}. The peaks that correspond to the epoxide group from GMA from Figure 1.14b were almost absent in Figure 1.14c. This observation was similar to what happened after the amination of WHF-g-PGMA with EDA: the epoxide groups opened upon reaction of APNWF-g-PGMA with EDA, resulting in the disappearance of the epoxide peaks. The absence of the characteristic peaks for the epoxide group and the presence of new peaks corresponding to N-H and C-N stretches confirmed the successful amination of the APNWF-g-PGMA.

(iii) FTIR-ATR Analysis of MCC and MCC-g-PGMA

Figure 1.15 illustrates the FTIR-ATR spectra of pristine MCC and grafted MCC with different *Dg* values. The IR spectrum of pristine MCC exhibited O-H

stretching absorption at 3335 cm^{-1}, C-H stretching at 2899 cm^{-1}, and C-O stretch from the cellulose units at 1030 cm^{-1}. After γ-radiation induced grafting of GMA from MCC, a new peak at 1726 cm^{-1} appeared which was assigned to the C=O stretching vibration of the grafted PGMA. Moreover, new peaks at 1251, 902, and 845 cm^{-1} appeared and these were attributed to the frequencies for the vibration of the epoxide group, indicating the successful grafting of GMA onto MCC.

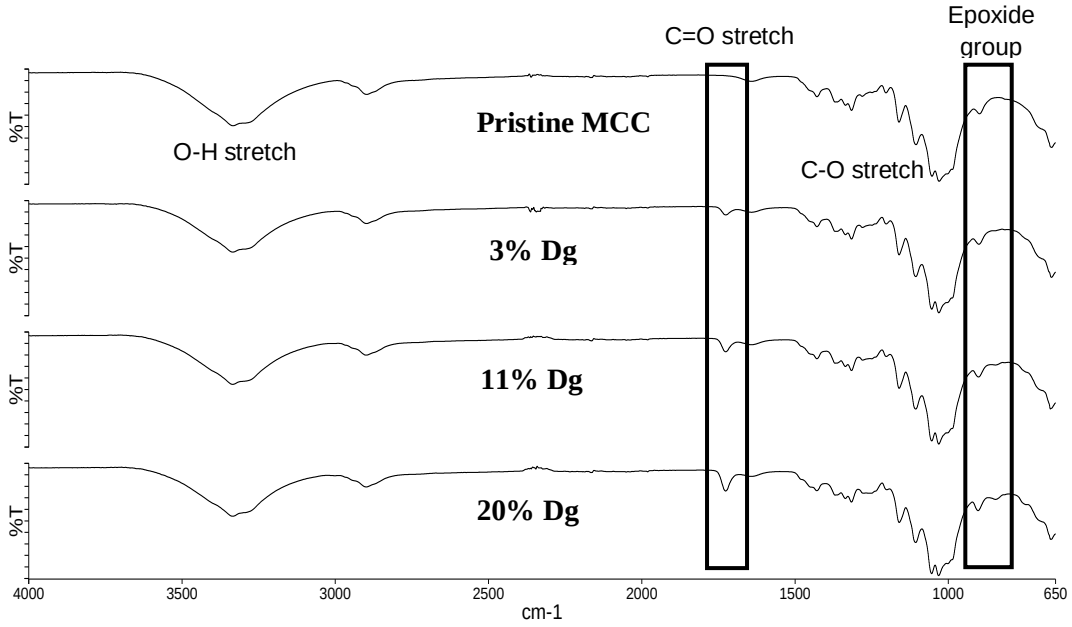

Figure 1.15 FTIR-ATR spectra of pristine MCC and MCC-g-PGMA with different degrees of grafting.

The data from FTIR-ATR spectra in Figure 1.15 shows that the intensity of the peak at 1726 cm^{-1} corresponding to C=O stretching vibration increases with *Dg*. The same trend was observed by Takacs *et al*. (2012) in the radiation-induced grafting of GMA from fibers, wherein they employed FTIR in diffuse reflectance mode (DRS) to follow the graft polymerization: the peak intensity of C=O from glycidyl methacrylate is proportional to the degree of grafting [55]. High *Dg* polymers have higher C=O concentration and according to Beer-Lambert Law, its corresponding absorbance must also increase.

1.3.5.2 SEM-EDX Analysis

The surface and in some cases the cross-section morphology of the pristine and grafted polymers were examined mostly by scanning electron microscopy (SEM).

The images captured by the SEM equipment may show if there were non-uniform grafting or if homopolymers were embedded on the grafted polymer macrostructure, which indicates the sufficiency of the cleaning process. The surface chemistry may be analyzed in micro scale with SEM equipped with an energy dispersive X-ray spectrometer (EDX). EDX also allows the qualitative and quantitative studies of adsorbed metal ions on the grafted polymers.

(i) SEM Analysis of WHF-g-PGMA

The surfaces of both grafted and unmodified WHF were analyzed by SEM and the results are shown on Figure 1.16. A clear difference in the surface morphologies of the pristine WHF sample and WHF-g-PGMA can be seen from the SEM pictures. From Figure 1.16a, the surface shows prominent ridges parallel to the length of the fiber. After graft polymerization of GMA on the fibers, the morphology of the bulk changed quite uniformly even at low *Dg* (Figure 1.16b). At higher grafting yields (Figure 1.16c and Figure 1.16d), the picture of the grafted polymer becomes more different from the pristine fibers and the grafted PGMA becomes visibly uniform. Patches of the grafted PGMA were visible from the surface of the fiber with 93% *Dg* at higher magnification (Figure 1.16e). These pictures are evidences that PGMA was successfully grafted from WHF using γ-radiation induced graft polymerization technique.

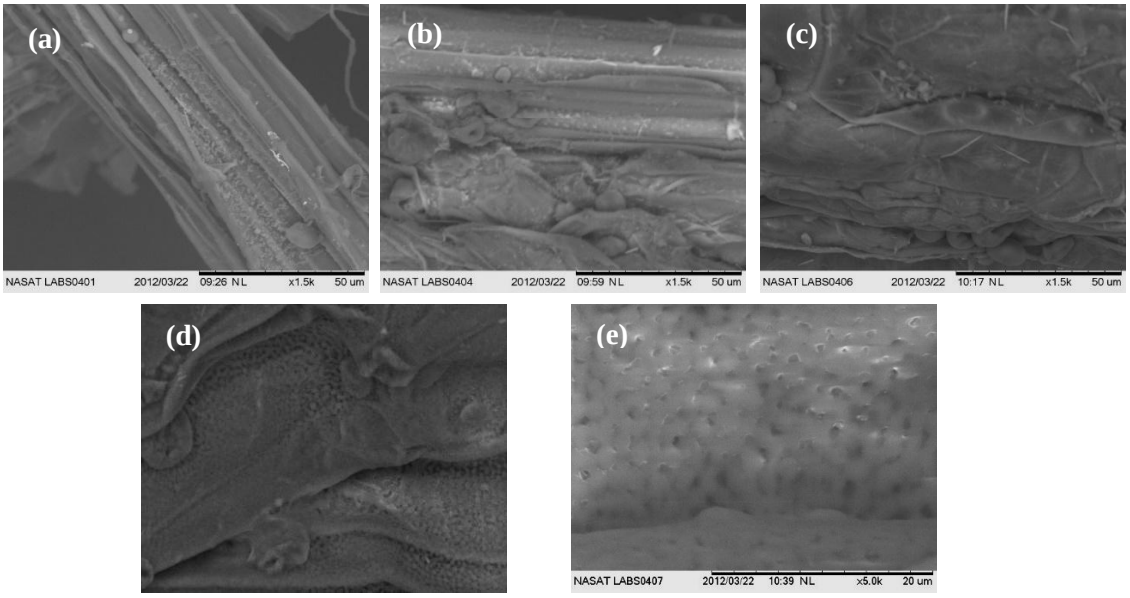

Figure 1.16 SEM photographs of (a) pristine WHF, WHF-g-PGMA with (b) 32% *Dg*, (c) 58% *Dg*, (d) 93% *Dg* (1500x magnification) and (e) 93% *Dg* (5000x magnification).

(ii) EDX Analysis of WHF and WHF-g-PGMA

EDX analysis of the pristine WHF showed that its surface is comprised mostly of carbon and oxygen, as shown in Figure 1.17a, with peaks at energies of 0.28 keV and 0.53 keV, respectively. This result was expected because of the lignocellulosic nature of the WHF polymer backbone. Other elements, such as potassium, calcium, and chlorine, with peaks at 3.31 keV, 3.69 keV and 2.82 keV energies, respectively, were also detected from the EDX data. This reflected the presence of other compounds on the WHF surface.

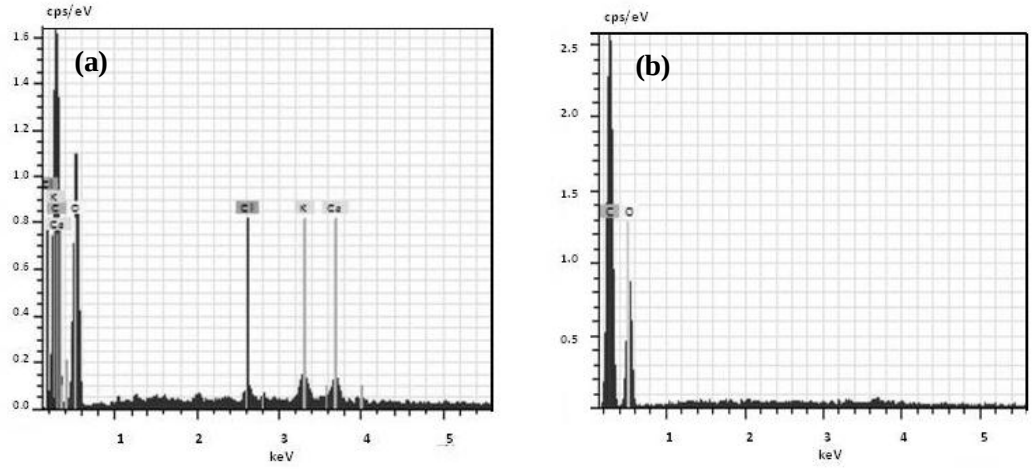

Figure 1.17 EDX spectrum of (a) water hyacinth fibers and (b) 58% grafted fibers.

After γ-radiation induced graft polymerization of GMA from WHF, with around 60% *Dg* (Figure 1.17b), only the elements carbon and oxygen were detected from the surface. Other elements probably also existed on the WHF-g-PGMA surface but had concentrations that were below the detection limit of the instrument. The detection of C and O are from the lignocellulosic nature of the WHF polymer backbone and from the PGMA grafted onto the fibers.

(iii) EDX Analysis of aminated WHF-g-PGMA

Nitrogen mapping of the aminated WHF-g-PGMA was performed using EDX spectroscopy. The result is shown in Figure 1.18. The nitrogen mapping from the EDX analysis indicates that the nitrogen distribution was non-homogeneous. The surface of the WHF-g-PGMA has uneven morphology (Figures 1.16b-d) prior to its reaction with EDA. This might have caused the uneven diffusion of EDA in its

reaction with the epoxide groups on the WHF-g-PGMA, making the distribution of nitrogen from the functionalized portions of fibers non-homogeneous. The EDX spectrum of the aminated fibers showed carbon and oxygen, with peaks at 0.28 keV and 0.53 keV, respectively, as the major elements. The nitrogen peak at around 0.39 keV, which was absent from the WHF-g-PGMA, became apparent on the EDX spectrum of the aminated WHF-g-PGMA.

Figure 1.18 Nitrogen elemental map from the EDX analysis of the aminated WHF with 1.78 mmol/gram amino functional group density.

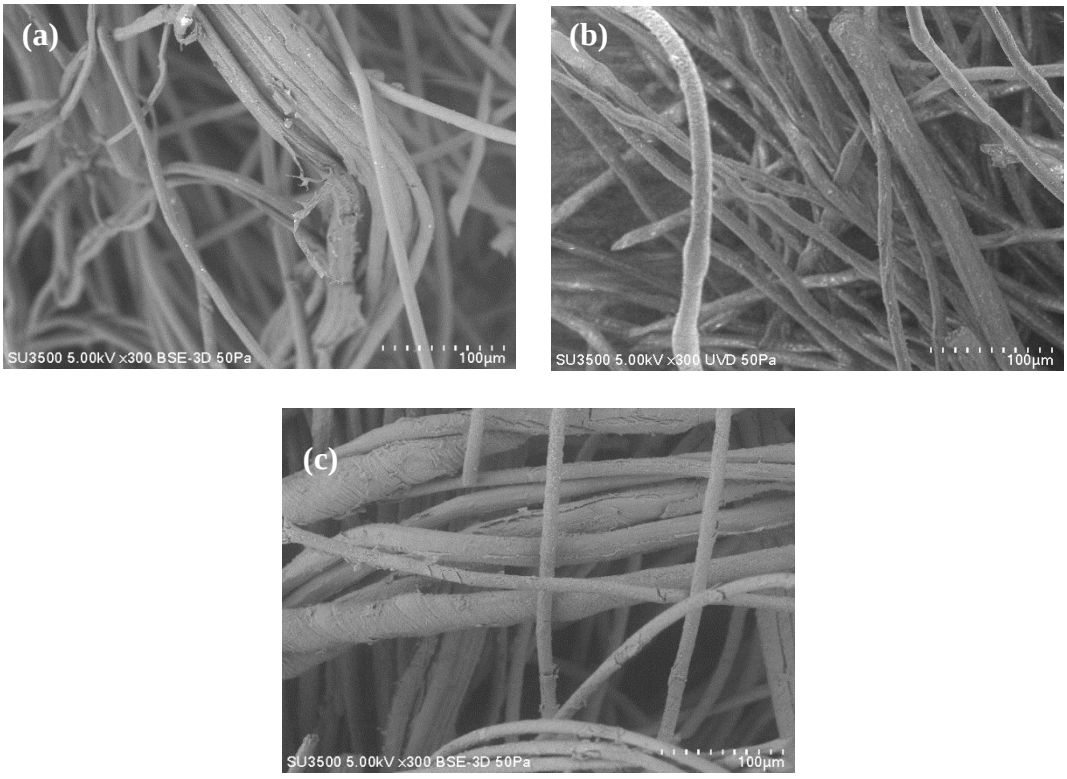

Figure 1.19 SEM photographs of (a) pristine APNWF, (b) APNWF-g-PGMA with 140% *Dg* and (c) aminated APNWF-g-PGMA.

(iv) SEM Analysis of APNWF-g-PGMA and aminated APNWF-g-PGMA

Figure 1.19a shows that the pristine APNWF was porous and consisted of two types of fibers with different properties: the larger and rougher fibers are from the natural fiber component of the NWF, i.e. abaca fibers, while the thin fibers are from the synthetic component, i.e. polyester. The SEM image of APNWF-g-PGMA and aminated APNWF showed that the grafted and functionalized materials remained porous and consisted of fibers with larger diameter and rougher morphology compared to the pristine NWF. The thicker fibers were due to the addition of grafted PGMA layer to the pristine APNWF. Both the grafted and EDA functionalized APNWF fibers were intact and comparable with the pristine NWF. This indicates that the graft polymerization and subsequent reaction with ethylenediamine did not result in any significant physical damage to the fibers. No homopolymers were observed from the SEM images of grafted NWF, demonstrating that the modified fibers were cleaned properly.

(v) SEM Analysis of MCC and MCC-g-PGMA

Figures 1.20a and 1.20b show the SEM pictures of pristine MCC and MCC-g-PGMA. Both samples were composed of particles with different shapes and sizes. The MCC-g-PGMA did not show any significant morphological changes from the pristine polymer backbone, probably because of the low *Dg* attained during the graft polymerization. No gelatinous lumps of PGMA homopolymers were observed from the grafted MCC, indicating that the homopolymer extraction procedure was successfully carried out.

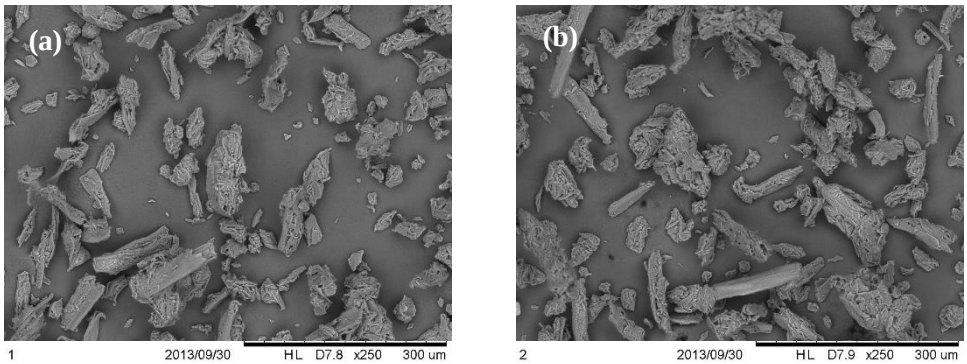

Figure 1.20 SEM photographs of (a) pristine MCC and (b) MCC-g-PGMA with 12% *Dg*.

1.3.5.3 Thermogravimetric Analysis

Radiation-induced grafting introduce new chemical bonds from the grafted polymer chains into the polymer backbone, thus it is expected that the thermal properties of the grafted polymer will be different from the polymer backbone. Thermogravimetric analysis (TGA) may be used to evaluate the thermal stability of the pristine and grafted samples, and to get information on the oxidative and non-oxidative decomposition of the polymers. In some cases, enhancement of the thermal stability after grafting was observed.

(i) Thermogravimetric Analysis of WHF-g-PGMA and aminated WHF-g-PGMA

Thermal analysis of the unmodified WHF, WHF-g-PGMA and aminated WHF-g-PGMA was carried out under dynamic nitrogen at a heating rate of 10^{o}C $minute^{-1}$ and the results are shown in Figure 1.21. All samples exhibited initial weight loss from 25 to 120 °C, which was attributed to loss of adsorbed water. In the TG curve of pristine WHF, the weight loss from 200 to around 350 °C was attributed to the volatilization of organic compounds and the decomposition of celluloses and hemicelluloses [56]. Compared with the pristine WHF, a greater mass loss was observed at the 200-350 °C temperature range in the TG curve of WHF-g-PGMA. Choi *et al*. (2004), stated that the decomposition of the ester group, 2,3-epoxidepropyl group, from glycidyl methacrylate occurs from ~220 to 300 °C [57]. Hence, the observed increase in mass loss can be ascribed to the decomposition of the PGMA graft chains. The degradation temperature shifted to higher temperature after grafting. This indicated that radiation induced grafting of WHF had increased its thermal stability. This trend was also observed by other researchers [3, 56]. Lignin is more stable and consequently decomposed at higher temperatures, and this is seen as a weight loss at around 500 °C on the thermographs of WHF and WHF-g-PGMA.

Functionalization of the WHF-g-PGMA was expected to change the grafted fibers thermal stability. The TG curve for the EDA functionalized WHF-g-PGMA polymers is shown also in Figure 1.21. The degradation of the EDA functionalized fibers started at a lower temperature compared to the degradation of WHF-g-PGMA. The TGA thermograph of EDA functionalized WHF-g-PGMA showed an initial weight loss from 25 °C to 120 °C and this can be attributed to loss of adsorbed water from the functionalized sample. After the initial weight loss from 25 °C to 120 °C, the

material showed another degradation step from 223 °C to around 500 °C. The relative mass loss in this temperature range was 58% and this amount was considerably lower than the mass loss at the same temperature range for the WHF-g-PGMA. The difference can be attributed to the presence of terminal $–NH_2$ in the aminated fiber which was derived from the reaction of the epoxide groups with EDA. The $–NH_2$ could have played as a radical scavenger during the fiber decomposition that slowed down the degradation of EDA functionalized water hyacinth fibers in nitrogen atmosphere [58]. This explains the lower mass loss that was observed after introducing $–NH_2$ groups to the WHF-g-PGMA.

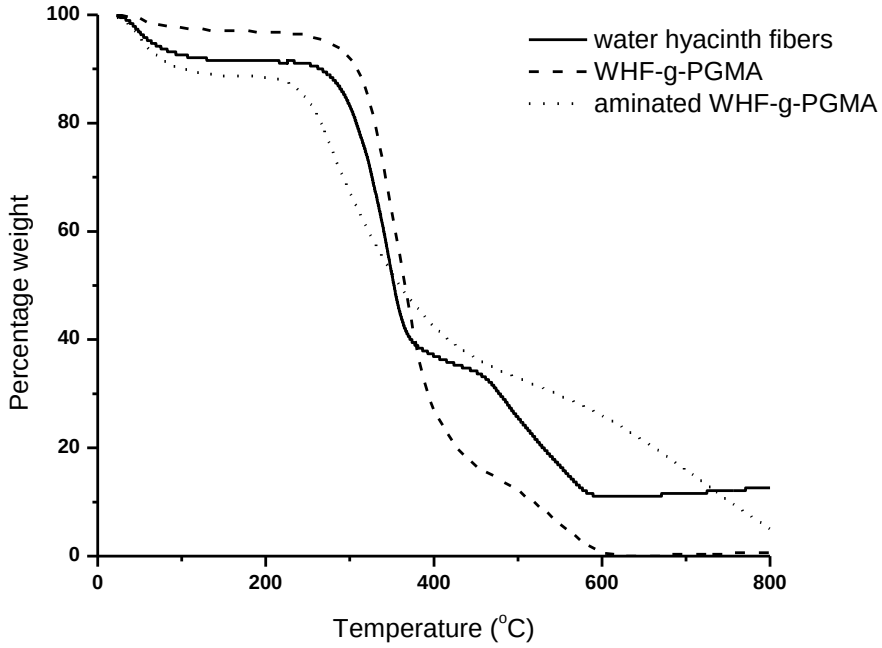

Figure 1.21 TGA thermographs of pristine WHF, WHF-g-PGMA with 58% degree of grafting and aminated WHF-g-PGMA.

(ii) Thermogravimetric Analysis of APNWF-g-PGMA and aminated APNWF-g-PGMA

Thermal analysis of the pristine and modified abaca/polyester NWF were carried out and the results are shown in Figure 1.22. All samples exhibited partial

weight loss from 25 to 120 °C. This was attributed to the loss of adsorbed water. The pristine APNWF showed a two-step thermal decomposition profile: the first weight loss started at around 300 °C and continued until 380 °C with a maximum weight loss at around 350 °C while the second step weight loss began at 380 °C and ended at 470 °C with a maximum weight loss at 425 °C. The first portion of the thermal decomposition profile may be associated with the decomposition of the abaca constituents including lignin, cellulose and hemicelluloses [59] while the second step may be attributed to the decomposition of the polyester component of the APNWF [60].

The APNWF-g-PGMA showed an almost similar thermal decomposition profile as that of the pristine NWF. However, the abaca/polyester-g-PGMA started to degrade at a lower temperature and it showed greater weight loss compared with the pristine NWF in the temperature range 300 °C to 380 °C, the same range of temperature where the abaca constituents are known to thermally decompose. Zulfiqar *et al*. (1990) determined that PGMA decomposition profile proceeds in two steps: the initial degradation step was ascribed to the depolymerization from the unsaturated chain ends and decomposition of the ester group, while the second degradation step with weight loss above 300 °C was associated with degradation by random chain scission [61]. Hence, the greater weight loss observed from 300 to 380 °C was due to the combined contributions from the degradation of both the abaca component of the trunk material and the grafted chains, i.e. PGMA. The second step may be associated with the decomposition of the polyester component of the NWF.

The thermograph of the APNWF-g-PGMA reacted with ethylenediamine showed a continuous weight loss even at low temperature that can be attributed to loss of adsorbed water from the sample. Afterwards, the material showed a significant weight loss from 220 to 410 °C. It can be observed that the EDA functionalized NWF exhibited slightly lower weight loss compared with APNWF-g-PGMA at temperatures greater than 300 °C, similar to the observation mentioned above for aminated WHF-g-PGMA. This observation may also be attributed to the presence of terminal $–NH_2$ that were imparted to the abaca/polyester-g-PGMA after the functionalization step. The $–NH_2$ could play as a radical scavenger during the thermal decomposition that slowed down the degradation of EDA functionalized abaca/polyester-g-PGMA in nitrogen atmosphere [58].

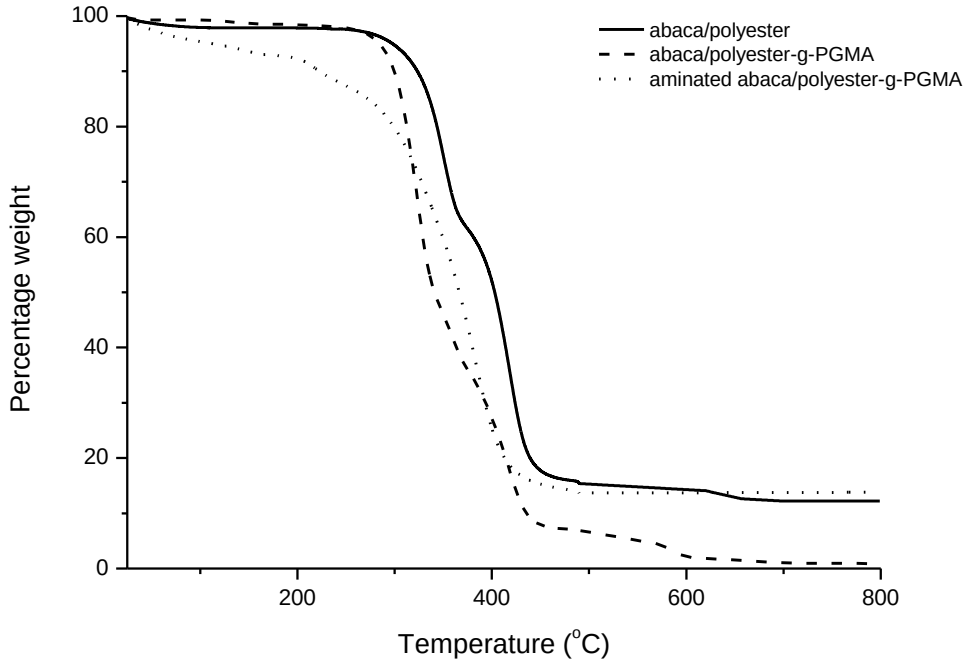

Figure 1.22 TGA thermographs of APNWF, APNWF-g-PGMA and aminated APNWF-g-PGMA.

(iii) Thermogravimetric Analysis of MCC and MCC-g-PGMA

Figure 1.23 shows the first derivative thermograph plot from the thermogravimetric analysis of the pristine and grafted MCC polymers with 11% and 18% *Dg*. All three samples exhibited a small decrease in mass after heating to 100 °C. This mass loss was attributed to the removal of adsorbed water. Cellulose is a highly hydrophilic polymer; hence water is present on its surface most of the time. MCC lost most of its mass, i.e. maximum degradation, at 345 °C. Grafting MCC with PGMA improved its degradation temperature, shifting to higher temperatures of 376 °C and 380 °C for *Dg* values of 11% and 18%, respectively. The change in decomposition temperature signified that the MCC base polymer had been successfully modified through grafting which resulted in the change in its decomposition behavior. The shift in decomposition temperature after grafting was also observed by other researchers [62].

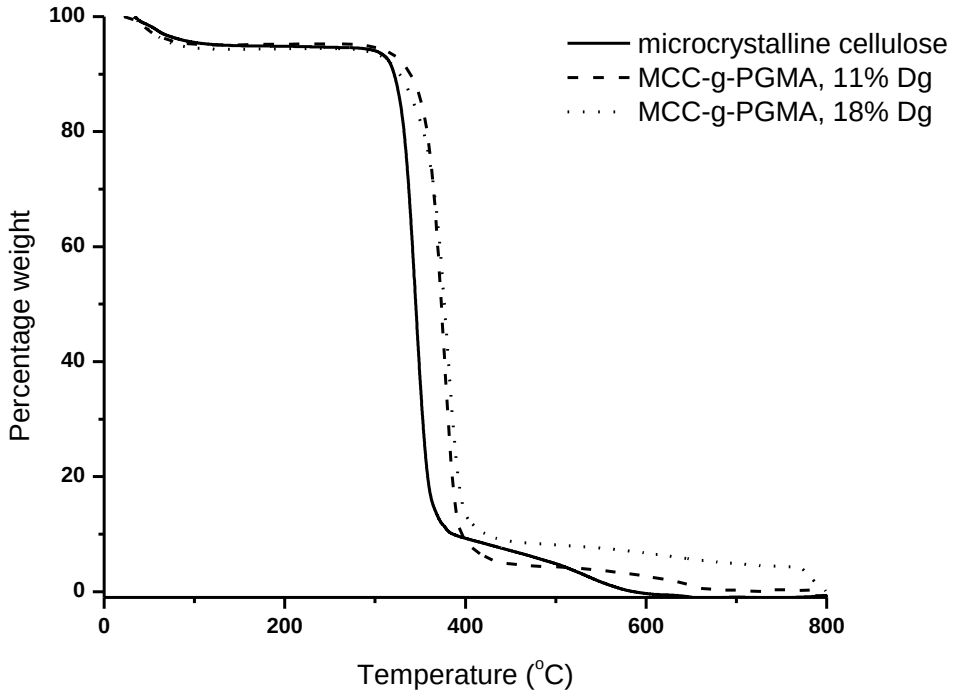

Figure 1.23 TGA thermographs of pristine MCC, and MCC-g-PGMA with 11% and 18% degrees of grafting.

1.3.5.4 XRD Characterization of MCC and MCC-g-PGMA

The X-ray diffraction (XRD) pattern of cellulosic materials remains basically the same after graft polymerization. However, grafting from a trunk polymer dilutes the mass of the trunk polymer because of the addition of new graft polymers, and the mass fraction of the trunk polymer crystalline phase decreases. Therefore, after graft polymerization the intensity of the reflection peak attributed to the crystalline organization of the trunk polymer decreases.

Figure 1.24 shows the X-ray diffractogram of the grafted (*Dg* = 18%) and pristine MCC. Both samples showed a similar diffraction pattern with peaks at 14.7°, 16.4° and 22.5° corresponding to the (1 0 1), (1 0 $\bar{1}$) and (0 0 2) crystallographic planes, respectively [63]. The XRD patterns indicated that grafting of GMA onto MCC, up to Dg of 18%, did not destroy the crystalline structure in MCC. This observation is valuable because the crystallinity of MCC has been shown to

significantly contribute in the properties of composites such as lower water uptake and moisture absorbability [64], and improved mechanical properties [65, 66].

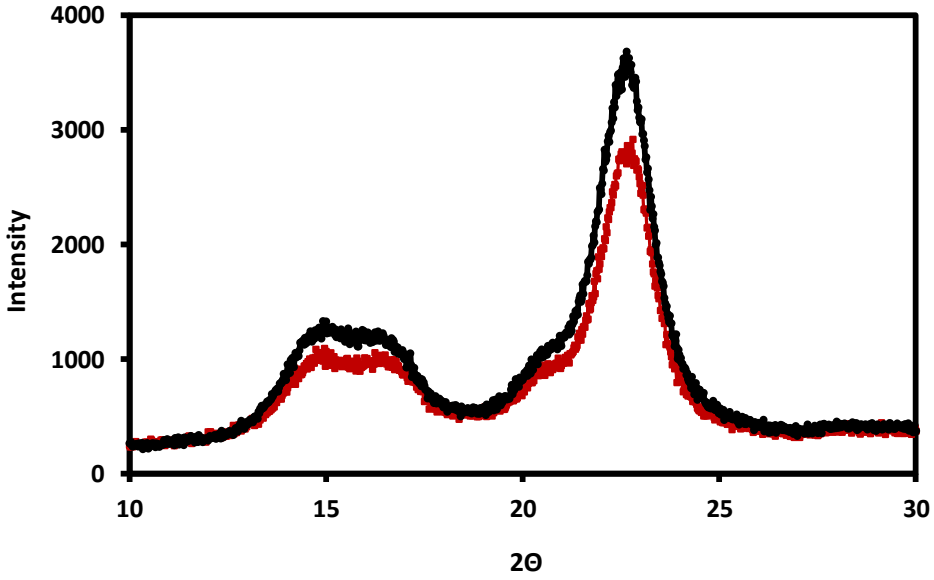

Figure 1.24 X-ray diffraction patterns of pristine MCC (black) and MCC-g-PGMA (red).

The crystallinity index, I_C, was calculated using the Segal empirical equation. The calculated I_C's for pristine and grafted MCC were 86.3% and 83.6%, respectively, indicating a small decrease in crystallinity after grafting, probably because of the dilution of the crystalline portion after grafting. This was also reflected by the decrease in peak intensities from the XRD diffraction patterns after grafting of MCC. The results implied that the crystallinity of MCC was not adversely affected after grafting with GMA under the conditions used in this study.

1.3.6 Characteristics and kinetics of heavy metal uptake

1.3.6.1 Aminated WHF-g-PGMA as adsorbent

The Philippines is one of the countries in the world with severely polluted bodies of water and land areas. The pollutants came from malpractices of different industries such as tanneries (Cr), lead-acid battery recycling operators and other industries (Pb) or accidents in mining sites (Cu and Ni). All options to minimize the negative effects of these pollutants are being tried and evaluated, including the development and synthesis of various heavy metal adsorbents.

(i) Effect of pH on metal ion adsorption

In order to determine the effect of pH on Pb^{2+}, Cu^{2+}, and Cr^{3+} removal by the EDA functionalized fibers, batch adsorption experiments were conducted using 50 ppm of each metal. The effect of the solution's pH on metal adsorption is illustrated in Figure 1.25.

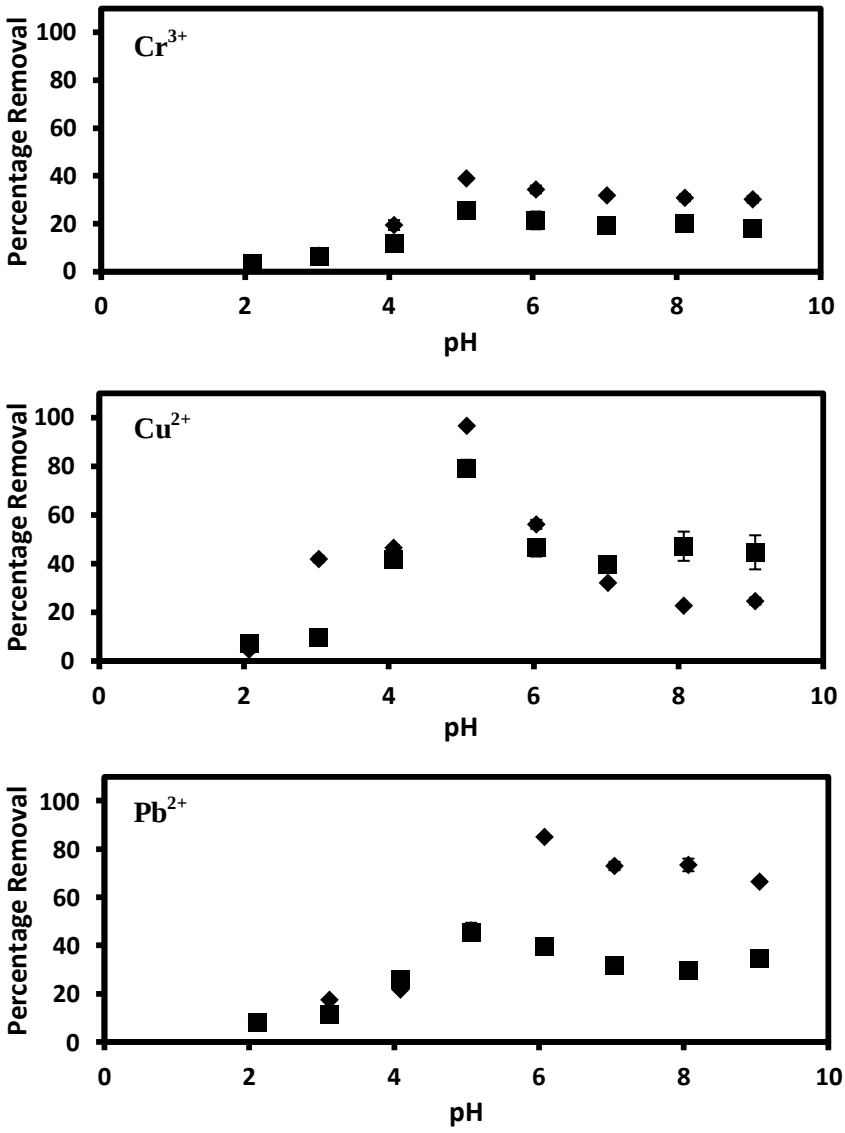

Figure 1.25 Effect of pH on the removal of Cr^{3+}, Cu^{2+} and Pb^{2+} by the EDA functionalized WHF-g-PGMA (◆) and pristine WHF (■), 3 trials.

It can be observed from the three plots on Figure 1.25 that negligible amounts of metal ions were adsorbed from solutions with pH 2 and 3. The same trend was observed in EDA functionalized cotton [67]. At low pH values, the H^+ concentration

of the solution was too high and most of the EDA amino groups were protonated. This caused an electrostatic repulsion between the positively charged metal ion in the solution and the adsorbent, resulting in the decreased sorption of the metal ions. As the pH increases, the amount of adsorbed metal ions also increased. The maximum adsorption of the metals by the EDA functionalized fibers was found to occur at pH 6.0 for Pb^{2+} and at pH 5.0 for both Cr^{3+} and Cu^{2+} while the unmodified water hyacinth fibers showed maximum removal of metals ions around pH 5.0. Beyond these optimum pH values, the removal of the metal ion from the solution by the EDA modified water hyacinth fibers decreased and precipitation of the metal hydroxide took place.

(ii) Effect of contact time on Cr^{3+}, Cu^{2+} and Pb^{2+} adsorption

Adsorption time is significant in determining the efficiency of new adsorbents. It is particularly important in evaluating the efficiency of adsorption and it helps to determine the effluent flow rate for optimum removal of target materials such as heavy metal ions or organic compounds from aqueous solutions. Reports have shown that the water hyacinth biomass is capable of adsorbing heavy metals from polluted waters [68 – 70]. However, none of these previous researches used water hyacinth fibers specifically for removing heavy metals from aqueous solutions. The effect of contact time and the initial concentration of the solution on the adsorption of Pb^{2+}, Cu^{2+}, and Cr^{3+} by water hyacinth fibers and EDA functionalized fibers were studied and the results for the adsorption using 150 ppm metal ion solutions are shown in Figure 1.26. Experiments were done at a sorbent dose of approximately 0.8 grams of adsorbent per liter of metal solution. The pH of each solution was adjusted to the optimum pH determined from the previous experiment.

For the adsorption of Pb^{2+}, Cu^{2+} and Cr^{3+} onto aminated WHF-g-PGMA, the results showed that the uptake of Cu^{2+} and Pb^{2+} increased very rapidly up, almost achieving equilibrium values after just 15 minutes while the adsorption of Cr^{3+} required about 2 hours. After these contact times, the adsorption slowly reached a constant value beyond which only small changes in metal concentration were observed. A quasi-stationary state was obtained within 4 hours of shaking, regardless of initial concentration. For practical consideration, the 4 hour time was recognized to represent the time after which the adsorption of metal ions achieve equilibrium.

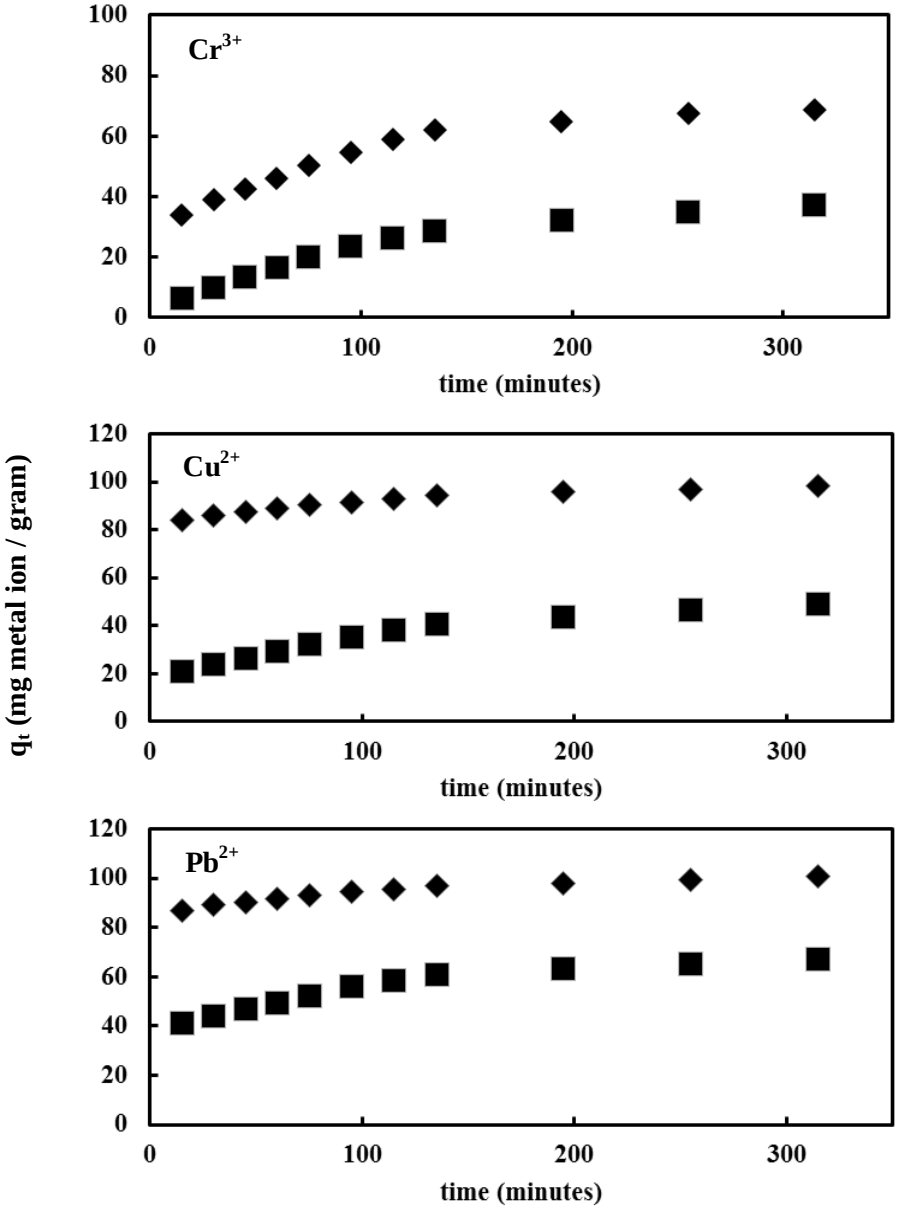

Figure 1.26 Time profiles for the adsorption of Cr^{3+}, Cu^{2+}, and Pb^{2+} from 150 ppm solutions onto EDA functionalized WHF-g-PGMA (◆) and pristine WHF (■).

When the initial concentration of Cu^{2+} was raised from 25 to 150 ppm, the equilibrium adsorption capacity, q_e, increased from 24.6 mg $gram^{-1}$ to 97.6 mg $gram^{-1}$, but the removal efficiency decreased from 97.1% to 68.2%. For Pb^{2+}, an increase in the initial concentration from 25 to 150 ppm resulted to an increase in q_e from 24.7 mg $gram^{-1}$ to 100 mg $gram^{-1}$, but a decrease in removal efficiency from 98.2% to 72.6%. The same trend was also observed for Cr^{3+}. An increase in initial concentration from 25 to 150 ppm resulted to an increase in q_e from 14.5 mg $gram^{-1}$ to

68.0 mg gram^{-1} but a decrease in removal efficiency from 62.4% to 49.7%. These results indicated that the uptake of Pb^{2+}, Cu^{2+} and Cr^{3+} by the aminated WHF-g-PGMA was concentration dependent. These observations may be attributed to the fixed number of binding sites on the adsorbent so the amount of adsorbate that it can remove from the metal ion solution at equilibrium was limited; hence the amount of metal ion that the grafted material can remove relative to its initial amount in the solution decreased with increasing metal ion concentration.

The same tendency was observed for the adsorption of Pb^{2+}, Cu^{2+} and Cr^{3+} onto pristine WHF. The amount of metal adsorbed at equilibrium by water hyacinth fibers is dependent on the initial concentration. When the initial concentration of Cu^{2+} was raised from 25 to 150 ppm, q_e increased from 11.5 mg gram^{-1} to 47.7 mg gram^{-1}, but the removal efficiency decreased from 46.2% to 33.3%. For Pb^{2+}, an increase of the initial concentration from 25 to 150 ppm resulted to an increase in q_e from 17.3 mg gram^{-1} to 66.2 mg gram^{-1}, but a decrease in removal efficiency from 67.7% to 48.5%. The same trend was also observed for Cr^{3+}, an increase of initial concentration from 25 to 150 ppm resulted to an increase in q_e from 7.1 mg gram^{-1} to 36.0 mg gram^{-1} but a decrease in removal efficiency from 30.0% to 27.0%.

From the data presented, it can be concluded that generally, the adsorption of the studied metal ions onto EDA functionalized WHF-g-PGMA reached equilibrium faster than the adsorption of metals onto pristine WHF. At the same time, the amounts of Pb^{2+}, Cu^{2+} and Cr^{3+} adsorbed by pristine WHF were less than the amount adsorbed by the EDA functionalized WHF at equilibrium. This implied that the γ-radiation induced grafting of GMA and subsequent functionalization enhanced the overall adsorption capacity of the WHF.

(iii) Adsorption Kinetics

Evaluation of the kinetic parameters and determination of changes in adsorption with time were done by fitting the data into two adsorption kinetic equations: a first-order kinetic model developed by Lagergren and a pseudo-second-order kinetic model described by Ho and McKay [30, 71]. From these equations, k_1 is the adsorption first-order rate constant and k_2 is the adsorption pseudo-second order

rate constant [72]. The kinetic parameters of these models applied to EDA functionalized WHF-g-PGMA and pristine WHF for different concentrations were calculated from the slope and intercept of the linear plots of log ($q_e - q_t$) versus time and $1/q_t$ versus 1/t. The results for adsorption of Cr^{3+}, Cu^{2+} and Pb^{2+} from 75 ppm are given at Table 1.3.

Based on the results for all the concentrations studied, it was found that the adsorption of Pb^{2+}, Cu^{2+}, and Cr^{3+} onto aminated WHF-g-PGMA and pristine WHF can be best described by the first order kinetic model by Lagergren. The first order Lagergren kinetic model is based from the Lagergren rate equation:

$$\frac{dq_t}{dt} = k_1(q_e - q_t) \tag{1.6}$$

Table 1.3 Kinetic parameters for the adsorption of Cr^{3+}, Cu^{2+}, and Pb^{2+} ions from 75 ppm solutions onto EDA functionalized WHF and pristine WHF.

Concentration (ppm)	q_e (mg g^{-1})	First-order		Pseudo-second order	
		k_1 (min^{-1})	r^2	k_2 (g mg^{-1} min^{-1})	r^2
Amine-type					
Cr^{3+}	32.3	0.0187	0.955	1.87×10^{-4}	0.990
Cu^{2+}	65.5	0.0149	0.987	7.21×10^{-3}	0.830
Pb^{2+}	73.5	0.0173	0.959	0.0741	0.715
Unmodified					
Cr^{3+}	20.5	0.0125	0.993	5.07×10^{-4}	0.982
Cu^{2+}	24.7	0.0122	0.988	2.25×10^{-3}	0.861
Pb^{2+}	42.6	0.0127	0.988	0.0048	0.745

This first order differential equation indicates that the higher the difference between the amount of adsorbed metal at equilibrium, q_e, and the amount of adsorbed metal at time t, q_t, the greater the rate of adsorption. Using the calculated k_1, it is possible to calculate the amount of adsorbed material at any time provided that the amount adsorbed at equilibrium is known. The results indicate that the first order rate constant for the adsorption of Pb^{2+}, Cu^{2+}, and Cr^{3+} onto EDA functionalized WHF-g-PGMA were generally higher than the first order rate constant for the adsorption of Pb^{2+}, Cu^{2+}, and Cr^{3+} onto pristine WHF at most of the concentrations studied. This

must be due to the higher number of available binding sites which resulted from the graft polymerization of GMA and its subsequent modification with EDA. The lignocellulosic WHF contain mostly cellulose and lignin, which might have been responsible for binding the metals. Grafting increased the available binding sites, resulting in the faster removal of the metal ions from the solution. This was reflected by the higher k_1 values obtained for the adsorption of Pb^{2+}, Cu^{2+}, and Cr^{3+} onto EDA functionalized WHF-g-PGMA than the first order rate constant for the adsorption of Pb^{2+}, Cu^{2+}, and Cr^{3+} onto pristine WHF.

(iv) SEM-EDX analysis of metal loaded EDA functionalized WHF

The distribution of adsorbed metals on the surface of EDA functionalized fibers was determined using energy dispersive X-ray spectroscopy (EDX). Based from the obtained elemental maps, the distribution of the metals on the surface is non-uniform. This can be attributed to the uneven distribution of available binding sites on the surface of the EDA functionalized water hyacinth fibers as shown in Figure 1.18. The EDX spectrum of the metal-loaded amino-type adsorbent show the presence of Cr, Cu and Pb with peaks at 0.57 keV and 5.41 keV, 0.95 keV and 8.04 keV, and 2.35 keV, respectively. The amounts of Pb^{2+}, Cu^{2+}, and Cr^{3+} on the surface were quantified using EDX. The results in descending order were as follows: Pb^{2+}, 5.97 ($\pm$ 0.23) % ≈ Cu^{2+}, 5.83 ($\pm$ 0.21) % > Cr^{3+}, 2.75 ($\pm$ 0.10) %. These numbers correlated well with the amount of each metal adsorbed at equilibrium at different concentrations given on Table 1.3. From the results, it can be concluded that at all concentration ranges, Pb^{2+} and Cu^{2+} were adsorbed in almost equal amounts at equilibrium and these metals were adsorbed in greater amounts than Cr^{3+}. Overall, the results also indicated that the EDA functionalized WHF-g-PGMA has enhanced adsorbing capacity than pristine WHF. Furthermore, the kinetics and EDX data showed that the synthesized adsorbent has greater affinity for Pb^{2+} and Cu^{2+} than Cr^{3+}.

1.3.6.2 Aminated APNWF-g-PGMA as adsorbent

(i) Effect of pH on Cu^{2+} and Ni^{2+} adsorption

The adsorptive property of modified adsorbents towards metal ions was found to be related to the pH value of the original solution [36, 73, 74]. In order to evaluate

the effect of pH on Cu^{2+} and Ni^{2+} uptake by the aminated APNWF-g-PGMA, batch adsorption experiments were performed using 50 ppm of each metal. Figure 1.27 illustrates the relationship between the amount of metal adsorbed and the initial pH of the solution.

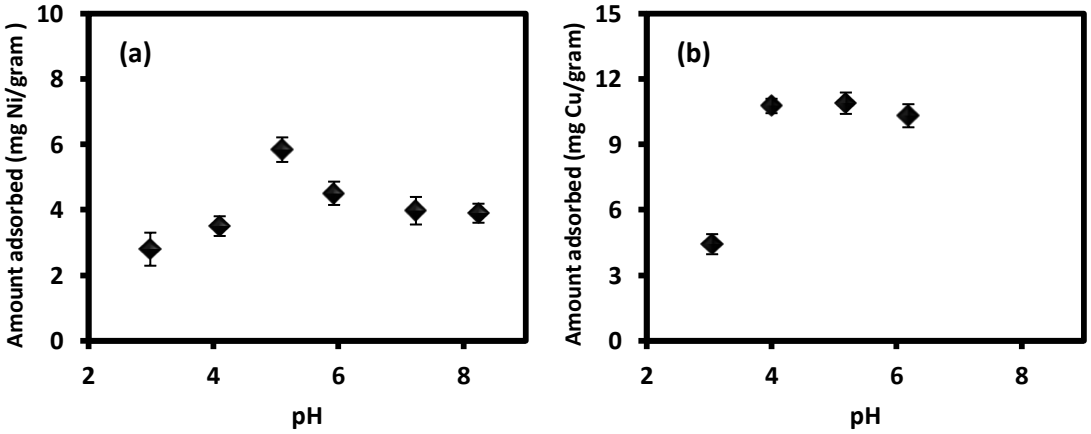

Figure 1.27 Effect of pH on amount of (a) Ni^{2+}, (b) Cu^{2+} ions adsorbed by the aminated APNWF-g-PGMA, 3 trials.

The batch adsorption tests showed that the aminated APNWF had poor affinity for both Cu^{2+} and Ni^{2+} at very low pH values. A similar trend was observed above with the aminated WHF-g-PGMA. The low adsorption may be attributed to either competition of H^+ for the adsorption sites or electrostatic repulsion between the protonated amino groups and the metal ions. The high H^+ concentration of low pH solutions causes most of the amino groups to be protonated and this resulted in electrostatic repulsion between the positively charged metal ions and the adsorbent. The amount of adsorbed metal ions increased with pH of the solution. The maximum adsorption of the metals by the aminated APNWF-g-PGMA was found to occur at pH 5 for Ni^{2+} and between pH 4-5 for Cu^{2+}. At pH higher than these optimum values, the amount of adsorbed metal ion decreased and the metal ions started to precipitate out of the solution.

(ii) Effect of initial concentration on metal ion uptake

Figure 1.28 shows the dependence of the amount of adsorbed metal on the initial concentration of the metal in the solution. The quantity of adsorbate on the solid phase increased with the initial amount of the metal ion in the original solution. However, the amount of removed metal expressed in terms of percentage removal, decreased with increasing initial concentration. When the amount of Cu^{2+} was raised from 10 to 1000 ppm, the adsorption capacity increased from 2.3 to 141.9 mg/gram-adsorbent but the percentage removal decreased from 99.4 to 52.0%. The same trend was observed for Ni^{2+}. A similar increase in initial Ni^{2+} concentration resulted in an increase in adsorption capacity from 2.7 to 31.5 mg/gram-adsorbent but a decrease in percentage removal from 96.2 to 16.0%. In contrast to the performance of grafted APNWF, the pristine APNWF was able to remove only 15% and 8% of Cu^{2+} and Ni^{2+} from 10 ppm solutions, significantly lower than the values obtained at the same concentration as reported above. This data emphasizes the importance of functionalization through grafting to improve the adsorption performance of polymers.

The data showed that the Ni^{2+} and Cu^{2+} uptake was concentration dependent. The available metal ion adsorption sites of the aminated APNWF became fewer at higher initial concentrations. The total available adsorption sites were limited so increasing the amount of metal ion in the solution did not result in the complete removal of the metal ions. This caused a decrease in percentage removal when the initial sorbate concentration was increased.

The performance of the aminated APNWF-g-PGMA towards adsorption of Ni^{2+} and Cu^{2+} was compared with a commercial resin, DIAION WA20 (Figure 1.29). This commercial resin has amino functional groups almost similar to EDA. From elemental analysis, it has 3.66 mmol amino groups for every gram of resin when calculated in moisture-free basis. This number is larger than the 2.70 mmol/gram amino group density of aminated APNWF-g-PGMA. Weighed amounts of the commercial adsorbent, with similar functional group content as the aminated APNWF used in the initial concentration tests, were added to solutions containing different concentrations of Cu^{2+} and Ni^{2+}. The batch adsorption tests were conducted at

conditions similar to the tests using aminated APNWF-g-PGMA. Results of the experiment are also shown in Figure 1.28.

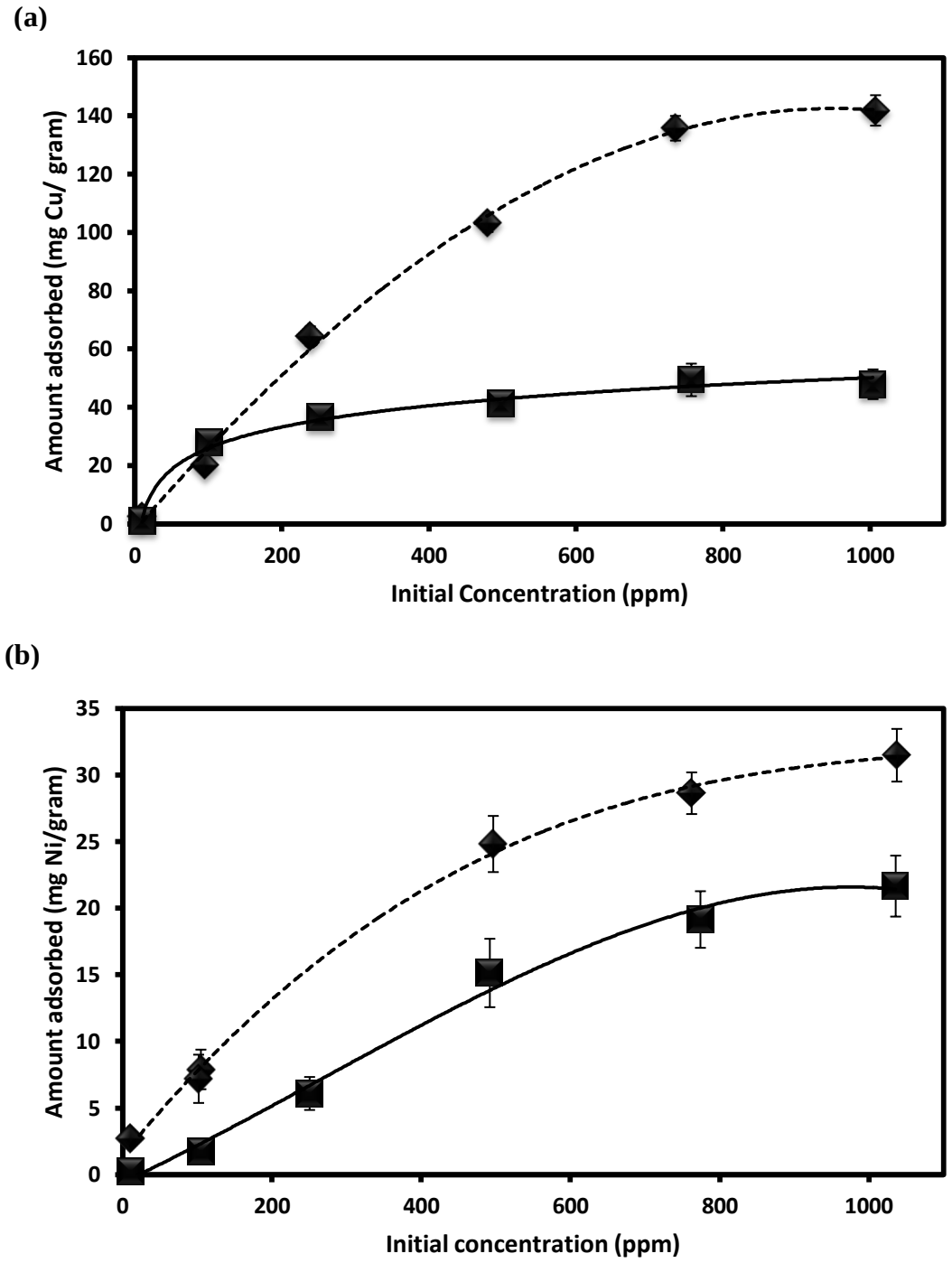

Figure 1.28 Effect of initial concentration on the adsorption of (a) Cu^{2+} and (b) Ni^{2+} ions by the aminated APNWF-g-PGMA (◆) and DIAION WA20 (■) at 30 °C and initial pH of 5, 2 trials.

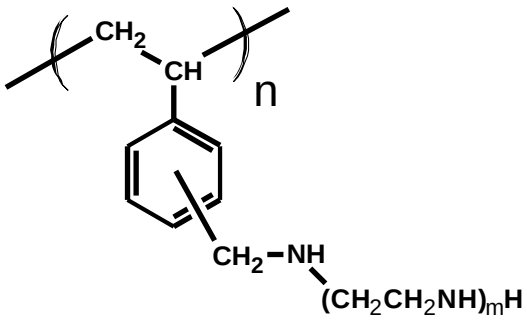

Figure 1.29 Chemical structure of DIAION WA20.

Both the aminated APNWF-g-PGMA and DIAION WA20 followed the same trend for the adsorption of metal ions. The Ni^{2+} adsorption capacity was calculated to be 31.5 and 21.7 mg/gram-adsorbent for APNWF-g-PGMA and DIAION WA20, respectively. These values were lower compared to the Cu^{2+} adsorption capacity of both adsorbents, which were determined to be 141.9 and 49.4 mg/gram-adsorbent for APNWF-g-PGMA and DIAION WA20, respectively. The results showed that both adsorbents have higher Cu^{2+} than Ni^{2+} adsorption capacity. Specifically, the adsorption capacity of the synthesized aminated APNWF was four times greater for Cu^{2+} ions compared to Ni^{2+} ions. The data also showed that at the specified conditions, the adsorption capacity of the synthesized adsorbent for both Cu^{2+} and Ni^{2+} was greater than that of DIAION WA20 commercial resin.

(iii) Adsorption kinetics

Adsorption kinetics is important in determining the efficiency of new adsorbents. Kinetics studies are significant in evaluating the adsorption efficiency. It also helps to determine the effluent flow rate to achieve maximum removal of target metal ions or organic compounds from solutions. The effect of contact time on the adsorption of Cu^{2+} and Ni^{2+} ions by the aminated APNWF and DIAION WA20 were investigated and the results are shown in Figure 1.30.

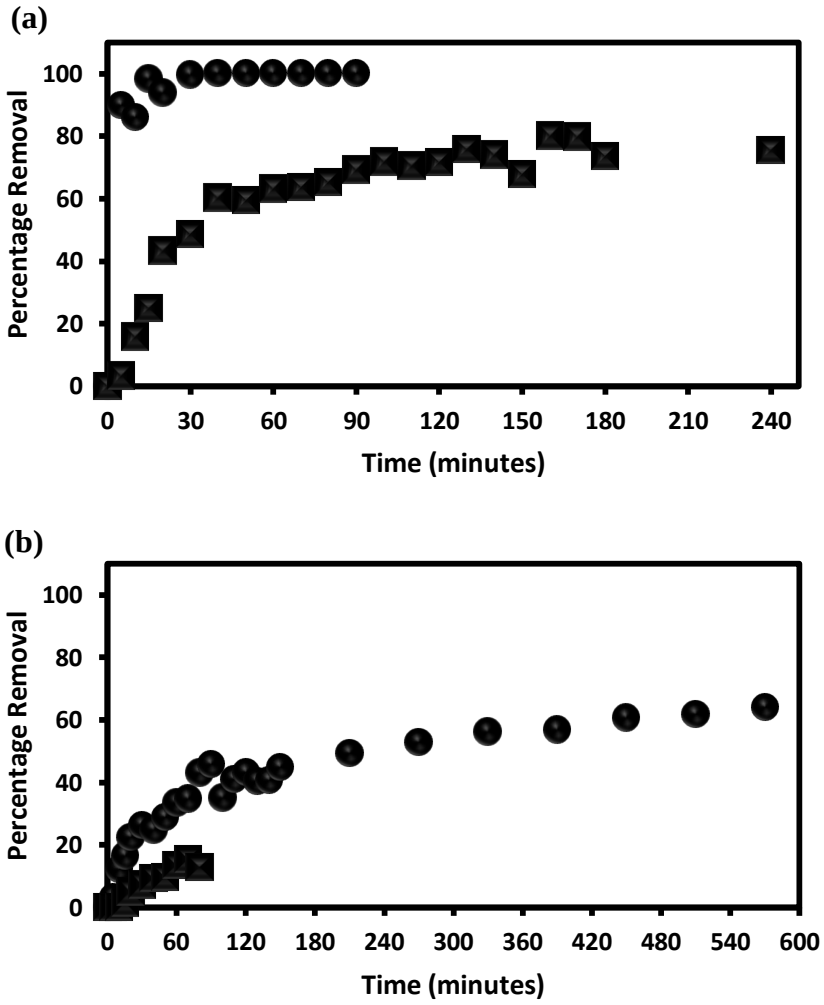

Figure 1.30 The relative amount of (a) Cu^{2+} and (b) Ni^{2+} ions removed from 10 ppm solutions as a function of time by aminated APNWF-g-PGMA (●) and DIAION WA20 (■) at pH 5 and 30^{o}C.

Figure 1.30a shows that the aminated APNWF-g-PGMA removed almost 90% of the Cu^{2+} ions after 5 minutes of contact with the solution. This percentage removal was significantly higher compared to the 3.3% removed by the commercial resin DIAION WA20 in the same period of contact time. Complete uptake of Cu^{2+} ions in the solution by the aminated APNWF-g-PGMA was achieved after stirring for 30 minutes. The amount of Cu^{2+} removed from the solution by DIAION WA20 increased fast, reaching 60.2% after 40 minutes, followed by a slow steady increase until it reached an almost constant value of 77.2% after 130 minutes of stirring.

A trend similar to that of Cu^{2+} adsorption was observed for Ni^{2+} ion removal by both the synthesized adsorbent and the commercial resin. It can be seen from Figure 1.30b that the amount of Ni^{2+} ions removed by the aminated APNWF increased up to 33.4% after 60 minutes of stirring. Afterwards, gradual increments in Ni^{2+} removal were observed until the percentage removal leveled at approximately 62.1% after 450 minutes. DIAION WA20 showed even lower adsorption of Ni^{2+} ions. It adsorbed negligible amounts of Ni^{2+} for the first 20 minutes and reached only 13.8% removal after 60 minutes of adsorption.

The kinetics experiments revealed important things about the aminated APNWF-g-PGMA. The aminated APNWF-g-PGMA removed Cu^{2+} faster than Ni^{2+} ions from the solution. After 30 minutes of contact time, the aminated APNWF had removed almost 100% of the Cu^{2+} ions from the solution while the amount of Ni^{2+} ions was reduced by only 26.3%. Also, the results of the kinetics experiment indicated that the ion sorption ability of the aminated APNWF-g-PGMA was greater than the commercial resin DIAION WA20, corroborating the results obtained from the previous section. The swiftness of Cu^{2+} adsorption by the aminated APNWF-g-PGMA was significantly greater than that of DIAION WA20. The aminated APNWF-g-PGMA required 30 minutes to completely remove the Cu^{2+} ions from a 100 mL of 7 ppm solution while at the same amount of contact time and solution, the percentage removal attained by DIAION WA20 was 48.5%, less than half the amount removed by the aminated APNWF-g-PGMA. It is known that the rate-limiting step in ion sorption by spherical resins in a well-stirred system is either intraparticular diffusion (i.e. the transfer from the surface to the intraparticular active sites) or chemical reaction (i.e. uptake of ions by the adsorption sites) [74]. Both the aminated APNWF-g-PGMA and commercial resin, DIAION WA20, have almost similar amino groups on the surface; hence chemical reactivity can be assumed to be similar for both cases. Indeed, this was seen from the results as both adsorbents showed higher adsorption capacity for Cu^{2+} than Ni^{2+}. Fibrous adsorbents have small fiber diameter size which is typically ten times smaller than the size of spherical resin adsorbents [36], making the diffusion rate of metals into fibrous adsorbents higher compared to its spherical resin counterpart. This resulted in the observed faster ion uptake by the aminated APNWF-g-APNWF than the commercial resin, DIAION WA20.

1.3.7 Wettability test of MCC-g-PGMA

The introduction of hydrophobic polymer on the surface of MCC would alter its surface properties. Wettability is a basic property that is related to the physical and chemical properties of polymers. The wettability test performed in this study was a simple procedure that can determine the affinity between the MCC-g-PGMA and solvents with different polarity [32]. Water and dichloromethane were used as the immiscible solvents.

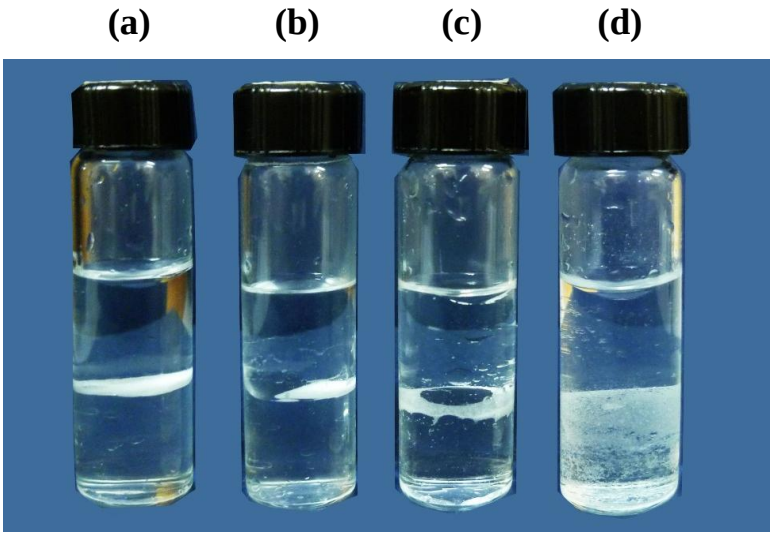

Figure 1.31 Wettability tests of (a) pristine MCC and MCC-g-PGMA with (b) 6%, (c) 10% and (d) 18% degree of grafting values.

Owing to the presence of hydroxyl groups along the cellulose chain, MCC is a highly hydrophilic material. Obviously, MCC particles (Figure 1.31a) were not able to migrate to the dichloromethane layer due to its higher affinity with water. On the other hand, the grafted MCCs behaved differently. After adding the MCC-g-PGMA (Figure 1.31b-d) with 6%, 10% and 18% *Dg* values in the mixture, migration of the grafted MCC particles to the dichloromethane layer was observed. Furthermore, samples with higher Dg showed better dispersion in the dichloromethane layer. These results showed that graft polymerization of GMA from MCC modified its hydrophobicity and dispersion in a non-polar solvent.

1.4 CONCLUSIONS

The facile process of radiation-induced grafting of dissolved and emulsified GMA monomer from cellulosic and lignocellulosic materials were carried out using simultaneous and pre-irradiation grafting techniques under controlled reaction parameters. Based from our literature survey, these are the first reports on the modification of APNWF, WHF and MCC via radiation grafting. The pre-irradiation grafting of APNWF was initiated using electron beams while γ-irradiation was employed in the simultaneous irradiation grafting of WHF and MCC in GMA solution. The grafted PGMA chains from WHF-g-PGMA and APNWF-g-PGMA were further functionalized with EDA in a one-step process. Based from the gathered data, the optimum conditions for the synthesis and subsequent functionalization of the cellulosic and lignocellulosic backbone polymers were as follows: (a) for WHF – 10 kGy absorbed dose (γ-radiation), 8 kGy $hour^{-1}$ dose rate, 5% GMA, 1:3 H_2O/CH_3OH solvent, 50% EDA; (b) for APNWF – 50 kGy absorbed dose (2 MeV electron beam), 3 hours reaction time at 40 °C in 5% GMA stabilized with 0.5% Tween 20 for grafting, 30 minutes at 60 °C in 50% EDA for functionalization; (c) for MCC – 10 kGy absorbed dose (γ-radiation), 8 kGy $hour^{-1}$ dose rate, 7% GMA, CH_3OH solvent.

The FTIR-ATR spectra, TGA thermographs, SEM images and EDX plots and maps of the pristine, grafted and functionalized WHF, APNWF and MCC confirmed the successful graft polymerization and functionalization of GMA on the polymer backbones. It was established that the adsorption process using the synthesized amino-type adsorbents were dependent on contact time, initial pH and concentration of the solution. The amount of adsorbed metal ion increased with increasing initial metal ion concentration and contact time, but the relative amount of metal ion removed from the original solution decreased with increasing initial metal ion concentration. Moreover, the aminated WHF-g-PGMA and APNWF-g-PGMA exhibited different affinities towards different metal ion adsorbates. The results of adsorption experiments, coupled with kinetics and comparison with control resins experiments, indicate the very high potential of applying the functionalized polymers for removing heavy metals (Cu^{2+}, Cr^{3+}, Pb^{2+} and Ni^{2+}) from aqueous solutions. The wettability test showed that the grafted MCC was more hydrophobic than the pristine MCC, making it more compatible with non-polar solvent. The hydrophobic character that was imparted to the otherwise strongly hydrophilic MCC may be useful in its

application as compatibilizer or reinforcing agent in composites comprised of two materials with different wetting characteristics (i.e. different polarities).

1.5 REFERENCES

1) Eichhorn, S.J.; Baillie, C.A.; Zafeiropoulos, N.; Mwaikambo, L.Y.; Ansell, M.P.; Dufresne, A. *J. Mater. Sci.* **2001**, *36*, 2107–31.
2) Klemm, D.; Heublein, B.; Fink, H.F.; Bohn, A. *Angew. Chem. Int. Edit.* **2005,** *44*, 3358–3393.
3) Wojnarovits, L.; Foldvary, Cs.M.; Takacs, E. *Radiat. Phys. Chem.* **2010,** *79*, 848-862.
4) Klemm, D.; Schumann, D.; Kramer, F.; Hessler, N.; Hornung, M.; Schmauder, H.P.; Marsch, S. *Polysaccharides* **2006,** *205*, 49–96.
5) Henriksson, M.; Berglund, L.A. J. *Appl. Polym. Sci.* **2007,** *106*, 2817–2824.
6) Iwamoto, S.; Nakagaito, A.N.; Yano, H. *Appl. Phys. A-Mater. Sci. Process* **2007,** *89*, 461–466.
7) Vaughan, T.; Seo, C.W.; Marshall, W.E. *Biores. Technol.* **2001,** *78*, 133–139.
8) Rubin, E.M. *Nature* **2008,** *454*, 841-845.
9) Bhatnagar, A., Sain, M. *J. Reinf. Plast. Compos.* **2005**, *24*, 1259–1268.
10) Swallow, A.J. *Radiation Chemistry: An Introduction* **1973**, Halsted Press: USA.
11) Boto, B.; Pawlowski, L. *Wastewater Treatment by Ion Exchange*, **1987,** Chapman and Hall, New York.
12) Wang, S.W.; Jang, F.Y. *Heavy Metal Wastewater Treatment Technique* **1993**, Metallurgy Technology Press: Beijing.
13) Eilbeck, W.; Mattock, G. *Chemical Process in Water Treatment*, **1996**, John Wiley and Sons, New York.
14) Chauhan, G.; Mahajan, S.; Guleria, L. *Desalination* **2000,** *130*, 85-88.
15) Chauhan, G.; Mahajan, S.; Guleria, L. *Desalination* **2001**, 141, 325-329.
16) Chauhan, G.; Mahajan, S. *J. Appl. Polym. Sci.* **2002**, 86, 667-671.
17) Yun, Y.; Volesky, B. *Environ. Sci. Technol*. **2003**, 37, 3601-3608.
18) Sokker, H.; Badawy, S.; Zayed, E.; Eldien, F.; Farag, A. *J. Haz. Mat.* **2009,** *168*, 137-144.
19) Xie, G.; Shang, X.; Liu, R.; Hu, J.; Liao, S. *Carbohydr. Polym.* **2011**, 84, 430-438.
20) Yang, C.P.; Shen, Z.Q.; Yu, G.C.; Wang, J.L. *Biores. Technol.* **2008,** *99*, 6240–6245.

21) Kim, M.; Saito, K.; Furusaki, S.; Sugo, T.; Okamoto, J. *J. Membr. Sci.* **1991,** *56*, 289–302.

22) Choi, S.; Nho, Y., *Kor. J. Chem. Eng.* **1999,** *16*, 241–247.

23) Kumar, V.; Bhardwaj, Y.; Rawat, K.; Sabharwal, S. *Radiat. Phys. Chem.***2005**, 73, 175 – 182.

24) Sokker, H.; Badawy, S.; Zayed, E.; Eldien, F.; Farag, A. *J. Haz. Mat.* **2009,** *168*, 137-144.

25) Fujiwara, K.; Masubuchi, T.; Miyata, K.; Shiozawa, M.; Takato, T.; Harakawa, H. *Radiat. Phys. Chem.* **2010**, 79, 238–240.

26) Chaudhari, C.V.; Paul, J.; Panicker, L.; Dubey, K.A.; Kumar, V.; Goel, N.K.; Bhardwaj, Y.K.; Sabharwal, S. *Envi. Prog. Sustain. Energy* **2012,** *31*, 77-88.

27) Ueki, Y.; Saiki, S.; Shibata, T.; Hoshina, H.; Kasai, N.; Seko, N. *Int. J. Org. Chem.***2014,** *4*, 91-105.

28) Takacs, E.; Wojnarovits, L.; Borsa, J.; Papp, J.; Hargittai, P.; Korecz, L. *Nucl. Instrum. Methods Phys. Res. B* **2005,** *236*, 259–265.

29) Wittaya, T. *Int. Food Res. J.* **2009**, *16*, 493-500.

30) Ho, Y.; McKay, G. *Water Res.* **2000,** *34*, 735-742.

31) Rosa, S.M.L.; Rehman, N.; De Miranda, M.I.G.; Nachtigall, S.M.B. and Bica, C.D. *Carbohydr. Polym.* **2012,** *87*, 1131–1138.

32) Namazi, H. and Dadkah, A. *Carbohyd. Polym.* **2010**, *79*, 731-737.

33) Bhardwaj, Y.; Tamada, M.; Nho, Y-C.; Nasef, M.; Güven, O. *Harmonized Protocol for Radiation-Induced Grafting*, **2014**, IAEA, Vienna.

34) Reddy, P.R.S.; Agathian, G.; Kumar, A. *Radiat. Phys. Chem.* **2005,** *72*, 511-516.

35) Desmet, G.; Takacs, E.; Wojnarovits, L.; Borsa, J. *Radiat. Phys. Chem.* **2011,** *80*, 1358-1362.

36) Sekine, A.; Seko, N.; Tamada, M.; Suzuki, Y. *Radiat. Phys. Chem.* **2010,** *79*, 16-21.

37) Seko, N.; Ninh, N.T.Y.; Tamada, M. *Radiat. Phys. Chem.* **2010**, *79*, 22-26.

38) Lauer, K.; Ayer, J.E.; Seoud, A.L.A. *J. Polym. Sci., Part A: Polym. Chem.* **1957,** *24*, 67-74.

39) Desmet, G.; Takacs, E.; Wojnarovits, L.; Borsa, J. *Radiat. Phys. Chem.* **2011,** *80*, 1358-1362.

40) Arantes, V. and Saddler, J. *Biotechnol. Biofuels*, **2010,** *3*, 4.

41) Yamagishi, H.; Saito, K.; Furusaki, S.; Sugo, T. *Ind. Eng. Chem. Res.* **1990,** *30*, 2234-2237.

42) Baxendale, J.H.; Wardman, P. *The Radiolysis of Methanol: Product Yields, Rate Constants, and Spectroscopic Parameters of Intermediates*, **1975,** National Bureau of Standards: USA.

43) Gerin, J.; Fraser, M.; Swiderek, P.; Michaud, M.; Ferradini, C.; Sanche, L. *Radiat. Phys. Chem.* **1997**, *50*, 263-265.

44) Colebourne, N.; Collinson, E.; Dainton, F. **1963**, *59*, 886-894.

45) Hebeish, A.; Kantouch, A.; Khalil, M.; El-Rafie, M. *J. App. Polym. Sci.* **1973,** *17*, 2547-2556.

46) Chaudhari, C.V.; Guin, J.P.; Dubey, K.A.; Bhardwaj, Y.K.; Varshney, L. *Polym. Bull.* **2016**, *73*, 2907-2926.

47) Khan, F. *Macromol. Biosci.* **2005,** *5*, 78-89.

48) Abdel-Aal, S.; Gad, Y.; Dessouki, A. *J. Appl. Polym. Sci.* **2006**, *99*, 2460-2469.

49) Seko, N.; Bang, L.T.; Tamada, M. *Nucl. Instrum. Meth. B* **2007**, *265*, 146-149.

50) Anirudhan, T.; Jalajamony, S.; Divya, L. *Ind. Eng. Chem. Res.* **2009,** *48*, 2118-2124.

51) O'Connell, D.; Birkinshaw, C.; O'Dwyer, T. *J. Appl. Polym. Sci.* **2006a,** *99*, 2888-2897.

52) O'Connell, D.; Birkinshaw, C.; O'Dwyer, T. *Adsorption Sci. Technol.* **2006b**, *24*, 337-347.

53) O'Connell, D.; Birkinshaw, C.; O'Dwyer, T. *J. Chem. Technol. Biotechnol.* **2006c,** *81*, 1820-1828.

54) Choi, S-H.; Nho, Y. *Kor. J. Chem. Eng.* **1999**, *16*, 241–247.

55) Takacs, E.; Wojnarovits, L.; Horvath, E.K.; Fekete, T.; Borsa, J. *Radiat. Phys. Chem.* **2012,** *81*, 1389-1392.

56) Luo, G.; Strong, J.; Wang, H.; Ni, W.; Shi, W. *Bioresour. Technol.* **2011,** *102*, 6990 – 6994.

57) Choi, S.; Lee, K.; Kang, H.; Park, H. *Macromol. Research* **2004,** *12*, 586 – 592.

58) Zaharescu, T.; Jipa, S.; Setnescu, R.; Wurm, D.; Brites, M.; Esteves, M. *Polym. Degrad. Stab.* **2000**, *68*, 83.

59) Agung, E.H.; Sapuan, S.M.; Hamdan, M.M.; Zaman, H.M.D.K.; Mustofa, U. *Int. J. Phys. Sci.* **2011**, *6*, 2100-2106.

60) Zohdy, M.H.; Sahar, S.M.; Hassan, M.S.; Khalil, E.M.; El-Hossamy, M.; El-Naggar, A.M. *Polym. Deg. And Stab.* **1999**, *63*, 187-193.

61) Zulfiqar, S.; Zulfiqar, M.; Nawaz, M. *Polym. Deg. And Stab.* **1990**, *30*, 195-203.

62) Solpan, D.; Torun, M.; Guven, O. *Radiat. Phys. Chem.* **2010**, *79*, 250-254.

63) Sun, Y.; Lin, L.; Deng, H.; Li, J.; He, B.; Sun, R. and Ouyang, P. *BioResources* **2008**, *3*, 297-315.

64) Awa, K.; Shinzawa, H. and Ozaki, Y. *AAPS Pharm. Sci. Tech.* **2015,** *16*, 865-870.

65) Mathew, A.; Oksman, K.; Sain, M. *J. Appl. Polym. Sci.* **2004,** *97*, 2014-2025.

66) Ni'mah, H.; Ningrum, E.O.; Sumarno; Rizkiyah, D.N.; Divta, I.; Meiliefiana; Subaghio, M.A. *AIP Conf. Proc.* **2017,** *1840*, 090009.

67) Ghali, A.; Baouab, M.; Roudesli, M.; *Chem. Eng. J.* **2011**, *174*, 18-26.

68) Low, K.; Lee, C.; Tan, K. *Bioresour. Technol.* **1995,** *52*, 79-83.

69) Low, K.; Lee, C., *Pertanika J. Sci. and Tech.* **1997,** *5*, 147-155.

70) Sarkar, D.; Das, S.; Mukherjee, P.; Bandyopadhyay, A. *Clean – Soil, Air, Water* **2010,** *38*, 764–770.

71) O'Connell, D.; Birkinshaw, C.; O'Dwyer, T. *Bioresour. Technol.* **2008,** *99*, 6709 – 6724.

72) Shibi, I.; Anirudhan, T. *Chemosphere* **2005,** *58*, 1117-1126.

73) Ma, H.; Morita, K.; Hoshina, H.; Seko, N. *Mater. Sci. Appl.* **2011,** *2*, 777-785.

74) Lee, S.; Mi, F.; Shen, Y.; Shyu, S. *Polymer* **2001,** *42*, 1879-1892.

75) Chapiro, A. *Radiaiton Chemistry of Polymeric Systems*, **1962,** John Wiley and Sons, Inc., Great Britain.

CHAPTER 2

RAFT-MEDIATED GRAFT POLYMERIZATION IN EMULSION PHASE: ELECTRON BEAM AND γ-RADIATION INITIATION

2.1 INTRODUCTION

Fabrication of chemically modified polymers via graft polymerization is one of the most versatile approaches to impart new functionalities, such as enhanced hydrophilicity [1], cation or anion adsorption property [2 – 3], biocompatibility [5] and conductivity [6], to the currently available polymers. Unlike physisorption of materials on polymers for surface modification, graft polymerization results to covalent attachment, which can avoid desorption issues and provide a robust bond between the grafted polymer chains and base polymer surface. Surface graft polymerization requires the generation of active species, such as carbon-centered radicals, peroxide or hydroperoxide, on the base polymer surface. These active species, which serve as initiation sites for graft polymerization, can be generated effectively by plasma or high energy radiation, such as electron beam, γ-ray and heavy ion-beam. Through proper choice of monomers with appropriate functional groups, new functionalities can be imparted onto the activated base polymer surface under relatively mild conditions.

Radiation-induced graft polymerization (RIGP) method has advantages such as simplicity, control over the process and adjustment of the materials composition and structure. Moreover, this method allows graft polymerization of monomers without adding chemical initiators and sensitizers [7]. Non-polar monomers are generally dissolved in organic solvents before reaction with the pre-irradiated polymer surface. This process generates organic solvent wastes which pose handling and storage difficulties. The use of surface active agents, i.e. surfactants, allowed the dispersion of organic monomers in water, a more environment friendly solvent for graft polymerization. Moreover, water provides an almost ideal solvent medium because unlike many organic solvents, it is highly resistant to attack by free radicals so that chain transfer to the solvent can be kept to a minimum [8]. It has been shown that radiation-induced grafting of monomer in emulsion state resulted in grafted

materials with significant amount of grafted polymers even at low monomer concentration [8 – 11]. These merits of pre-irradiation grafting in emulsion state continue to attract the interest of researchers worldwide.

Electron beams and γ-radiation are examples of high-energy radiation that are used by researchers worldwide to initiate graft polymerization from solid polymer surfaces, which generally proceeds via free radical polymerization process. However, irreversible termination of propagating polymer chains and chain transfer are features intrinsic to the process of free radical polymerization. Irreversible termination of propagating radicals and chain transfer reactions both result in loss of control over molecular weight and chain structure as well as broadening of the molecular weight distribution [12 – 14]. These drawbacks have inspired the research field of controlled free-radical polymerization (CRP) which essentially employs chain transfer agents. It has been established that chain transfer agents (CTA) have profound effects in free radical polymerization processes. Chain transfer processes can be utilized to control the polymer architecture and to reduce polydispersity [15]. Developments in the field of chain transfer polymerizations include the use of conventional transfer agents [16], catalytic transfer agents based on cobalt complexes [17], degenerative transfer [18], and chain transfer by reversible addition-fragmentation (RAFT) [13, 19 – 24].

Among the CRP methods, chain transfer by reversible addition-fragmentation (RAFT) is one of the most adaptable techniques for providing pseudo-living properties to free radical polymerization [12, 25, 26]. RAFT-mediated graft polymerization at ambient conditions through γ-radiation has been successfully conducted for an array of monomers [27]. In this technique, thiocarbonyl organic compounds such as dithioesters and trithiocarbonates are employed as chain transfer agents. During RAFT-mediated γ-radiation initiated grafting, propagation of the grafted polymer (covalently linked to the surface), and ungrafted polymer (in the bulk) are regulated by the same RAFT agent simultaneously. Therefore, the molecular weights and molecular weight distributions of grafted and ungrafted polymers should be comparable when the grafting occurs from the surface of the trunk polymer [25].

Conventional free radical polymerization is commonly employed in the commercial production of a wide range of synthetic materials. Approximately 50% of these free radical polymerization processes are performed in emulsions. In order to

achieve industrial acceptance, RAFT-mediated polymerization and other CRP methods must be viable in emulsion, particularly in water-based emulsion system [12]. Besides being an environment friendly solvent, the use of water-based emulsions offers additional benefits such as easier handling of the product material. Though there are a number of publications dealing with synthesis of graft copolymers from synthetic and natural fibers through conventional radiation-induced grafting in emulsion phase [10, 11, 28, 29], to the best of our knowledge there have been no report on electron beam- and γ- initiated RAFT-mediated graft polymerization of monomers in emulsion from synthetic polymers. Polyethylene (PE), polypropylene (PP) and polyethylene coated polypropylene (PE/PP) fibers are important synthetic fibers that are commercially available and have been used as trunk materials after functionalization in many applications. These synthetic fibers themselves cannot be used as plain materials for special applications because they lack functional groups for the target function.

This chapter discusses the results from the study of electron beam and γ-radiation initiated graft polymerization of emulsified glycidyl methacrylate (GMA) from polyethylene/polypropylene (PE/PP) trunk polymer in the presence of the RAFT agent 4-cyano-4-((phenylcarbonothioyl)thio) pentanoic acid (CPPA). The effects of various experimental parameters to the degree of grafting were evaluated. CPPA has a carboxylic group which allows good solubility in aqueous solutions and it has been shown to control the polymerization of methacrylate monomers, such as 2-(dimethylamino)ethyl methacrylate and oligo(ethylene glycol) methacrylate, in aqueous media with addition of small amount of organic solvent [24]. The reactive oxirane group of GMA can be reacted with various reagents to impart new functionalities. This provides versatility to the grafted polymer that can be useful for different applications.

2.2 EXPERIMENTAL

2.2.1 Materials

The RAFT agent used in this study, 4-cyano-4-((phenylcarbonothioyl)thio) pentanoic acid (CPPA, > 97%), was purchased from STREM Chemicals, USA. Glycidyl methacrylate (GMA, >95.0%, TCI) was deinhibited by percolation through a column of activated basic alumina (Ecochrom) and then stored at 4 °C. The

surfactant, polyoxyethylene sorbitan monolaurate (Tween 20), tetrahydrofuran (THF, HPLC grade, > 99.8%) and methanol (HPLC grade, > 99.8%) were supplied by Kanto Chemical Co., Japan and were used as received. Nonwoven fabrics with fibers made of polypropylene coated with polyethylene (PE/PP) were provided by Kurashiki Sen-I Kako Co. Okayama, Japan and were used as polymeric substrates for the grafting experiments.

2.2.2 Irradiation

The ^{60}Co irradiation facility and electron beam (2 MeV) facility in Takasaki Advanced Radiation Research Institute, Japan were used for the irradiation of samples. All irradiation experiments were carried out in inert conditions to prevent radical scavenging resulting from contact with atmospheric oxygen.

2.2.3 Graft polymerization

2.2.3.1 Pre-irradiation grafting

The PE/PP nonwoven fabric, which was cut into 2 cm x 2 cm square pieces, was irradiated at dry ice temperature and nitrogen atmosphere with electron beam of 2 MeV energy and 3 mA current. The absorbed dose was evaluated from the response of a cellulose triacetate dosimeter.

In a typical graft polymerization procedure, a mixture composed of GMA, Tween 20 and CPPA RAFT agent in deionized water was homogenized at 6000 rpm and deoxygenated by bubbling with high purity nitrogen gas for an hour. The irradiated PE/PP sample was placed in a glass ampoule which was immediately evacuated of air using a vacuum line. After reaching a pressure of 3 Pa, approximately 10 g of the previously deoxygenated monomer emulsion was drawn into the glass ampoule. The reaction was carried out by keeping the glass ampoule in a thermostatic water bath at 40 ℃ from 30 minutes to 4 hours. After grafting, the polyethylene/polypropylene-g-poly(glycidyl methacrylate) (PE/PP-g-PGMA) was washed repeatedly with methanol and THF to remove non-reacted GMA and “free” PGMA homopolymers and then dried overnight under reduced pressure at 35 ℃. The “free” PGMA homopolymer was recovered by precipitating the polymerization mixture and washings in excess methanol. The amount of PGMA grafted onto PE/PP,

expressed as degree of grafting, *Dg*, was calculated from the increment in weight after the grafting reaction using equation (2.1):

$$Dg\ [\%] = \frac{w_g - w_o}{w_o} \times 100 \qquad (2.1)$$

where w_g is the weight of PE/PP after grafting and w_o is the weight of pristine PE/PP. The overall conversion was determined gravimetrically and calculated using equation (2.2):

$$\text{overall conversion } [\%] = \frac{(w_g - w_o) + w_{\text{free PGMA}}}{w_{\text{monomer}}} \times 100 \qquad (2.2)$$

where $w_{\text{free PGMA}}$ is the weight of the PGMA homopolymers formed in the mixture and w_{monomer} is the weight of the monomer at the start of the reaction. Conventional grafting studies were also performed wherein PE/PP substrates were grafted identically with PGMA except that no RAFT agent was added to the emulsion.

2.2.3.2 Simultaneous grafting

In a typical RAFT-mediated grafting, the trunk polymer PE/PP with 1 cm x 3 cm dimensions and a mass of approximately 0.02 g was mixed into the grafting solution (~8 g) produced by homogenizing GMA, CPPA and Tween 20 in water at 6000 rpm for 15 minutes. The polymerization mixture in glass vial capped with self sealing septum was connected to N_2 bubbling at room temperature for 10 minutes, and then placed in γ-irradiator chamber. After the graft polymerization was carried out at room temperature for the prescribed time, the polymerization was stopped by removing it from the ^{60}Co irradiation room. The PE/PP-g-PGMA was washed with THF overnight to remove free homopolymers and ungrafted GMA monomer. The PE/PP-g-PGMA was dried to constant mass *in vacuo* at 35 °C. The *Dg* of grafted PE/PP was determined using equation 2.1 while the monomer conversion was determined gravimetrically after vacuum filtration, through a 0.45 μm PTFE membrane filter, of the polymerization mixture that was precipitated in five-fold volumes of methanol, and calculated using equation 2.2. The PGMA homopolymers on the PTFE membrane filter was dried initially in fume hood and then in a vacuum oven. The grafted PGMA on the PE/PP trunk material has contribution to the total conversion and was included in the calculation. The experiments were repeated to

check data precision and the maximum standard error (n=9) calculated was 2%. Gravimetric measurements were performed with a Sartorius CPA 225D balance that has a ±0.01 mg sensitivity.

The theoretical number-average molecular weight, $M_{n,th}$, was determined using the following equation:

$$M_{n,th}[g/mol] = M_{CPPA} + \frac{n_m^0}{n_{CPPA}^0} \times conversion \quad (2.3)$$

where $M_{n,th}$ is the theoretical number average molecular weight of the polymer, n_m^0, the initial quantity (in moles) of the monomer, i.e. GMA, included in the mixture, n_{CPPA}^0, the initial quantity (in moles) of the chain transfer agent (CTA), i.e. RAFT agent, CPPA, included in the mixture and M_{CPPA}, the molecular weight of the CPPA RAFT agent. In order to study the features of γ-ray initiated RAFT-mediated grafting in emulsion state, conventional grafting studies were also performed where PE/PP substrates were grafted with PGMA identically with the exception that no RAFT agent was added to the emulsion.

2.2.4 Characterization of pristine trunk polymer, grafted polymers and free homopolymers

The molecular weights and polydispersity index (PDI) of the free PGMA homopolymers were measured by gel permeation chromatography (GPC) on a Hitachi GPC instrument equipped with a Shodex 9 μm particle size guard column (50 x 7.5 mm) followed by two Shodex GPC columns (300 x 8.0 mm) in series, L-7100 solvent delivery system, L-7490 RI detector and L-7400 UV detector. The guard and GPC columns were kept in a Shimadzu column oven at 40 °C during the analysis. The eluent was THF (1 mL min^{-1} flow rate) and the system was calibrated with polystyrene standards (Polysciences, Inc.) with molecular weights of 150 to 10^6 g mol^{-1}.

The infrared spectra of PGMA homopolymer, pristine PE/PP and PE/PP-g-PGMA were examined by a Perkin Elmer Spectrum One Fourier Transform Infrared (FTIR) spectrophotometer in attenuated total reflectance (ATR) mode. The samples were scanned in the range 650-4000 cm^{-1} with a resolution of 4 cm^{-1}. Peak area calculations were carried out in absorbance mode using the Spectrum software.

Scanning electron microscopy (SEM) images and oxygen elemental maps were taken using a Hitachi SU 3500 (Hitachi, Japan) scanning electron microscope equipped with an energy dispersive x-ray spectrometer (X-Max, Horiba). Pictures of the fibers' surfaces were acquired at low vacuum condition and acceleration voltage of 5 kV while the oxygen elemental maps were taken at an acceleration voltage of 8.5 kV.

Thermal decomposition properties of the pristine PE/PP and PE/PP-g-PGMA were recorded using a TG/DTA 6200 Exstar 6000 (Seiko Instruments Inc., Japan). Thermogravimetric analyses (TGA) were conducted over the temperature range 25 to 500 °C with a programmed temperature increment of 10 °C min^{-1} under dynamic nitrogen atmosphere.

The glass transition temperature, T_g, of the homopolymers and the high *Dg* sample was determined by differential scanning calorimetry (DSC) on a Thermo Plus DSC8230 (Rigaku, Japan). Each sample was packed in a standard aluminum pan that was hermetically sealed. The samples were studied under dynamic nitrogen atmosphere using a cyclic three-stage thermal program. The first stage was a heating at a constant rate (10 °C min^{-1}) from 35 °C to 95 °C. At the end of this stage, the samples were cooled at -2 °C min^{-1} to 35 °C (second stage) and then heated again to 95 °C (third stage) at a constant rate (10 °C min^{-1}). The T_g was determined from the second heating curve using the Thermo Plus 2 software.

X-ray photoelectron spectroscopy (XPS) plots were recorded on a PHI 5000 Versa Probe II Scanning XPS Microprobe with monochromatized Al Kα X-ray source (1486.6 eV photons) at a pass energy of 29 eV for high-resolution scan spectra and 117 eV for survey scan spectra. The anode current was 3.0 mA. The pressure in the analysis chamber was kept at 1 x 10^{-6} Pa or lower during each analysis. The samples were fixed on the sample holder by using indium and carbon adhesive materials. The core level signals were measured at the photoelectron takeoff angle of 45°. All binding energies (BE) were referenced to the C1s hydrocarbon peak at 284.8 eV. Surface elemental stoichiometries were determined from peak-area ratios, after correcting with experimentally determined sensitivity factors as set by the instrument manufacturer.

The proton nuclear magnetic resonance analysis (^{1}H NMR) spectrum of the homopolymer was measured using a Bruker Avance III 300 Nuclear Magnetic Resonance Spectrometer. The sample was dissolved in deuterated chloroform (99% purity, 99.8% deuteration degree, Kanto Chemical Co. Inc, Japan) with tetramethylsilane as internal standard. Peak assignments and integration were performed using Bruker Top Spin 1.3 software.

2.3 RESULTS AND DISCUSSION

2.3.1 Simultaneous grafting

2.3.1.1 RAFT-mediated radiation-induced synthesis of PE/PP-g-PGMA

The group of Pan first reported the controlled radical polymerization under continuous irradiation with γ-rays in the presence of thiocarbonylthio compounds in 2001 [30 – 32]. Since these initial accounts, there has been a substantial effort given to RAFT-mediated radiation-induced homo- and co-polymerizations of several types of monomers [12, 22, 25 – 27, 34]. In their paper, Barner *et al*., proposed a reaction mechanism for RAFT-mediated graft polymerization in solution under a constant source of γ-radiation, wherein the fundamental steps of RAFT mechanism are extended by reaction processes that account grafting from polymeric surfaces [33]. In the simultaneous grafting method applied during the grafting studies, initiating free radicals were formed through application of γ-radiation. Radicals can be generated at PE/PP surfaces and in the monomer emulsion. The radicals formed on the PE/PP surface served as sites of initiation and propagation for the graft chains. Simultaneously, γ-radiation also initiated polymerization of GMA in the emulsion. Both propagating chains, i.e. grafted and free in mixture, then add to the thiocarbonyl group of the CPPA, creating the RAFT radical intermediates. Upon addition of the propagating chains to CPPA molecules, the leaving group radical was released from CPPA and subsequently re-initiated the polymerization steps in the mixture. These reaction steps comprised the pre-equilibrium part of RAFT mechanism. The core steps of the RAFT process is the main equilibrium wherein the free macro radicals that are either covalently bonded to the PE/PP surface or are free in the reaction mixture are adding to the polymeric RAFT agent to form macroRAFT intermediate

radicals which in turn may fragment by releasing the starting materials or the formerly attached polymeric entity. Because RAFT-mediated graft polymerization is not a true living polymerization, termination of propagating chains is still a possibility and this may occur via bimolecular termination reactions between free or surfaced attached macro radicals.

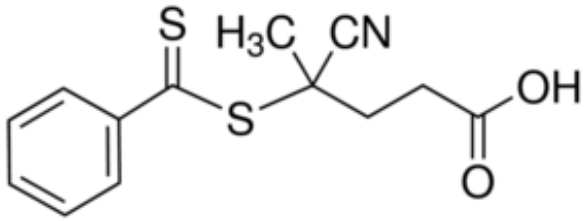

Figure 2.1 4-cyano-4-((phenylcarbonothioyl)thio)pentanoic acid (CPPA) RAFT agent.

In order to study the RAFT-mediated graft polymerization of GMA onto PE/PP, the CPPA RAFT agent was employed in this study (Figure 2.1). CPPA has a carboxylic group which allows good solubility in aqueous solutions and it had been shown to control the polymerization of methacrylate monomers, such as 2-(dimethylamino)ethyl methacrylate and oligo(ethylene glycol) methacrylate, in aqueous media with addition of small amount of organic solvent [24]. Moreover, considering that the application of the resulting graft copolymer is in the field of adsorption, CPPA was found to be the most suitable RAFT agent for this study, as demonstrated in Section 2.3.2, because of its effective RAFT-mediation and more importantly, it yielded graft copolymers with sufficient *Dg* values. Reaction conditions, e.g. monomer concentration, RAFT agent concentration, monomer to RAFT agent ratio and absorbed dose, also affect the RAFT process and determine the observed *Dg* values. The effects of these grafting parameters on the RAFT mediated graft polymerization of GMA onto PE/PP were investigated and the results are summarized in Table 2.1.

Table 2.1. RAFT-mediated graft polymerization of GMA aqueous emulsion (10:1 GMA to Tween 20 weight ratio) from PE/PP at room temperature under γ-irradiation at dose rate of 1 kGy h^{-1}.

Expt.	$C_{GMA,o}$ (wt %)	$C_{CPPA,o}$ (wt %)	n_m^0 / n_{CTA}^0	Dose (kGy)	Dg [a] (%)	Conv. [b] (%)	$M_{n,Th}$ [c] (g mol^{-1})	$M_{n,GPC}$ [d] (g mol^{-1})	PDI [d]	$M_{n,NMR}$ [e] (g mol^{-1})
1	3.0%	0.06%	100	0.5	8.2	38	5,720	4,600	1.43	7,800
2	3.0%	0.06%	100	1	9.5	85	12,386	6,000	1.62	16,600
3	3.0%	0.06%	100	3	10.4	90	13,058	5,900	1.86	N/A [f]
4	3.0%	0.015%	400	0.5	6.6	80	46,150	34,500	4.66	N/A [f]
5	3.0%	0.015%	400	1	6.6	86	49,363	37,500	7.28	N/A [f]
6	5.0%	0.10%	100	0.5	19.2	11	1,886	2,700	1.16	2,000
7	5.0%	0.10%	100	1	23.6	90	13,140	5,900	1.35	15,900
8	5.0%	0.10%	100	3	26.5	91	13,376	5,800	1.47	N/A [f]
9	5.0%	0.025%	400	0.5	14.6	77	43,502	30,000	3.83	43,100
10	5.0%	0.025%	400	1	16.5	89	50,456	31,300	4.35	63,900
11	10.0%	0.20%	100	0.5	26.9	8	1,413	2,500	1.16	2,400
12	10.0%	0.20%	100	1	82.3	53	7,844	4,900	1.16	8,600
13	10.0%	0.20%	100	3	92.7	94	13,613	6,700	1.37	13,300
14	10.0%	0.20%	100	6	93.7	93	13,531	6,500	1.32	15,900
15	10.0%	0.05%	400	0.5	36.0	24	13,643	7,800	1.29	11,100
16	10.0%	0.05%	400	1	43.7	90	51,342	13,600	1.28	51,100
17	10.0%	0.05%	400	3	45.0	92	52,195	13,600	1.38	N/A [f]
18	3.0%	—	—	0.5	1.3	93	—	179,600	7.29	N/A [f]
19	3.0%	—	—	1	2.5	93	—	184,100	7.30	N/A [f]
20	10.0%	—	—	0.5	7.1	95	—	123,000	9.51	N/A [f]
21	10.0%	—	—	1	7.4	96	—	108,000	9.53	N/A [f]

[a] Degree of grafting (Dg) calculated using Eq. (2.1).

[b] Conversion of monomer calculated gravimetrically.

[c] Theoretical number-average molecular weight was calculated from the monomer conversion using Eq. (3.3).

[d] Number average molecular weight, $M_{n,GPC}$, and polydispersity index, PDI, are determined from PGMA homopolymers formed in the polymerization mixture and were obtained from GPC analysis (THF eluent).

[e] Number average molecular weight determined from NMR spectrum of the PGMA homopolymers formed in the polymerization mixture and calculated using Eq. (2.4).

[f] Not available.

In conventional graft polymerization in emulsion state under γ-radiation, the monomer, polymer substrate and water are all exposed to radiation and thereby produce radical species. Irradiation of PE resulted to bond-breaking reactions that lead to production of free radicals, majority of which were allyl, alkyl and polyenyl type [35, 36]. The relative amount of these carbon-centered free radicals depends on the temperature, energy, type of irradiated polymer and type of radiation, and post-irradiation storage time and environment. These radicals served as initiation points for graft polymerization of GMA monomer on the surface of PE/PP while the free polymers in the solution were initiated by the radicals produced upon interaction of GMA and water molecules with γ-radiation. Entries 18-19 and 20-21 show the results after irradiation of PE/PP in 3 and 10% GMA emulsion without the RAFT agent, i.e.

conventional grafting, respectively. These experiments were carried out by γ-irradiation of the samples to 0.5 and 1.0 kGy at a dose rate of 1 kGy h^{-1}. The calculated conversions in these experiments were greater than 90%, indicating a very high rate of polymerization. The combination of the free radical process, provided by the γ-irradiation, and the emulsion technique was known to result in high conversion and high reaction rates of the polymerization process [12]. Due to fast polymerization kinetics, the effect of absorbed dose on *Dg* in these experiments was not obvious. The *Dg* increased with increasing monomer concentration, e.g. at 1 kGy absorbed dose, the calculated *Dg* values were 2.5% and 7.4% for 3% and 10% GMA, respectively. This trend was because of the increase in number of monomer molecules in close proximity to the trunk polymer, which gave higher chance to the monomer to react with the propagating graft chain [22]. Khan and co-workers achieved almost the same Dg values when they grafted 10 % (v/v) methyl methacrylate, which was emulsified with nonionic surfactant octylphenoxy-polyethoxyethanol (Triton X-114), from Jute fibers using conventional simultaneous grafting technique under γ-radiation [37].

The *Dg* values of PE/PP-g-PGMA after γ-irradiation of the polymer substrate in GMA emulsion in presence of the RAFT agent are shown as entries 1-17 in Table 2.1. Comparison of the entries with same monomer concentration and irradiated at the same absorbed dose, with and without RAFT agent (e.g. entries 2 and 5 with entry 19; entries 12 and 16 with entry 21), showed that addition of RAFT agent to the polymerization medium resulted in increased *Dg*. Without RAFT agent, i.e. conventional grafting, the polymerization proceeds via free radical polymerization and irreversible termination of growing polymer chains is a feature intrinsic to this process. Addition of RAFT agent decreased the amount of propagating radicals, both on the PE/PP surface and in the bulk of polymerization medium, by reversible deactivation. This phenomenon reduced the probability of irreversible termination, because the rate of termination is greatly dependent on the number of active radicals in the mixture. The suppression of irreversible termination reactions allowed a pseudo-living system where the graft chains propagated longer [12, 22, 25], resulting in higher *Dg*. Kodama and co-workers also observed a similar trend when they graft polymerized 2-hydroxyethyl methacrylate from PE/PP in the presence of cumyl dithobenzoate RAFT agent under γ-radiation [38]. They attributed the higher *Dg* observed in the presence of RAFT agent to the longer irradiation time of samples with

cumyl dithiobenzoate. In the present study, the irradiation time for both conventional and RAFT-mediated graft polymerization of GMA in emulsion phase were similar, therefore the observed trend can be attributed solely to the presence of RAFT agent and its effects in the graft polymerization system.

The *Dg* of PE/PP-g-PGMA from the RAFT-mediated graft polymerization exhibited dependence on absorbed dose; unlike the results obtained from conventional grafting. The *Dg* rapidly increased after irradiation to 0.5 kGy, then leveled off and the *Dg* did not increase significantly (e.g. entries 11-14 and 15-17). Higher absorbed doses produced more free radicals on the trunk polymer that can initiate more graft chains. As the polymerization proceeded, the monomer conversion increased while the number of monomer molecules available for grafting decreased. The two processes counteracted one another, allowing the *Dg* to reach a stable value and then levels off. In addition, the increase in *Dg* may also be attributed to increase in molecular weight of the graft chains. The RAFT process provided living character to free radical polymerization so the grafted PGMA chains were expected to continue propagating through the polymerization time. It is well known that a reduction in rate of polymerization was often observed in chain transfer polymerization, including RAFT-mediated polymerization, so lower monomer conversion was normally observed at the early portion of the polymerization process [39]. In the case of conventional grafting, the conversion reached a very high value, >90%, at 0.5 kGy; hence further production of free radicals by direct and indirect interaction of γ-radiation with the PE/PP substrate did not result to further increase in *Dg* because of monomer exhaustion.

Increasing the monomer concentration in the RAFT-mediated process increased the *Dg* of the grafted PE/PP (entries 1-3, 6-8, and 11-13). Again, this is simply because of closer proximity with the free radicals generated on the PE/PP substrate and propagating polymer chains. The *Dg* increased with decreasing monomer to RAFT agent ratio (e.g. entries 1-2 and 4-5, 6-7 and 9-10, 12-13 and 16-17). This is contrary to the results found by other researchers wherein the *Dg* increased with increasing monomer to RAFT agent ratio [38, 40]. They attributed the observed trend to higher conversion values of the monomer and increasing molecular weight of grafted polymer chains obtained at the same reaction time when the concentration of RAFT agent was lower. In the present study, the molecular weights

of the graft chains also increased with decreasing RAFT agent concentration, as shown in Table 2.1. The observed trend in this study might be attributed to the indirect suppression of the termination reactions in solutions containing high amounts of the RAFT agent, i.e. low monomer to RAFT agent ratio. The indirect suppression of the termination reactions possibly lead to more propagating grafted chains, resulting in higher *Dg* values for solutions with lower monomer to RAFT agent ratios [12, 22, 25].

The techniques used in this study allowed the synthesis of PE/PP fibers functionalized with epoxide groups from the PGMA chains, grafted in a controlled manner by a one-step method that lead to robust and stable covalent bond between the surface and grafted PGMA at room temperature and without any pre-functionalization step. Table 2.1 shows that the *Dg* can be controlled from 8 to 90%, with graft chains of reasonable dispersity ranging from 1.2 to 1.5, by varying the monomer concentration, absorbed dose, amount of CPPA and monomer to RAFT agent ratio. The optimum *Dg* value depends on the intended application of the final material. For preparation of biocompatible surface, grafting of 2-4% may be sufficient, for fuel cell and battery separator applications grafting of 20-50% would be desired and for adsorption applications even grafting of 100% would be preferred [41]. Further chemical modifications of the PGMA graft chains impart new functional groups to the PE/PP grafted fibers for various applications.

2.3.1.2 Characterization of the homopolymers formed in the polymerization mixture during grafting

In the radiation-grafting experiments performed in this work, formation of coagulum was rarely observed. Moreover, the distinctly colored creamed oils observed floating in the reaction mixtures, as reported in other studies [42, 43], were not observed at any stage during the grafting experiments. Irradiation with γ-rays generated free radicals on the PE/PP trunk polymer and in the monomer emulsion. Subsequently, radicals from monomer and water and radicals generated on the trunk polymer initiated the propagating polymers, which then added to the thiocarbonyl group of the CPPA, creating the RAFT radical intermediates. Because both the grafted chains and free PGMA were controlled by the same CPPA RAFT agent

simultaneously, the molecular weight and molecular weight distribution of the grafted and ungrafted PGMA should be comparable when the grafting occurred from the surface of the trunk polymer [25]. Therefore analyses of the ungrafted/free PGMA in the emulsion not only give us information on the homopolymer part of the grafting mixture but also allow us to estimate the molecular weight and dispersity of the grafted chains. The effects of absorbed dose, GMA concentration, CPPA concentration and monomer-to-RAFT agent ratio on the molecular weight and molecular weight distribution of the free PGMA are shown in Table 2.1. The controlled fashion for the RAFT mediated polymerizations is shown in this table and corresponding figure, Figure 2.2, which depicts the GPC curves of free PGMA at different absorbed doses and monomer-to-RAFT agent ratio.

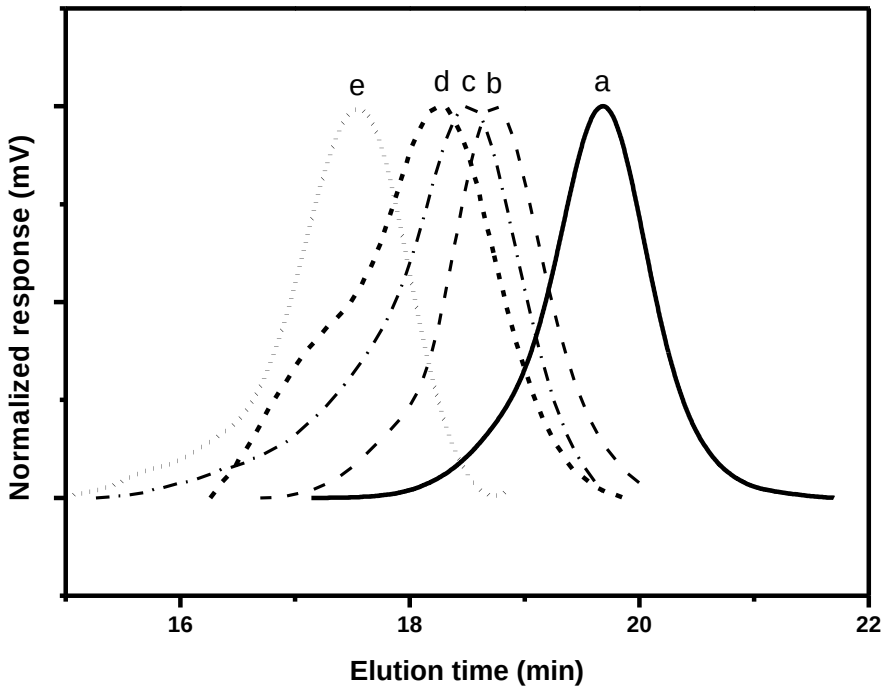

Figure 2.2 GPC plots for free poly(glycidyl methacrylate) formed in the γ-initiated graft polymerization from PE/PP mediated by the RAFT agent 4-cyano-4-((phenylcarbonothioyl)thio) pentanoic acid (CPPA) at 10% (wt/wt) GMA and 1% (wt/wt) Tween20: (a) 0.5 kGy, 100:1 GMA-to-CPPA, $M_{n,GPC}$ = 2500, PDI = 1.16; (b) 1 kGy, 100:1 GMA-to-CPPA, $M_{n,GPC}$ = 4900, PDI = 1.16; (c) 3 kGy, 100:1 GMA-to-CPPA, $M_{n,GPC}$ = 6700, PDI = 1.16; (d) 0.5 kGy, 400:1 GMA-to-CPPA, $M_{n,GPC}$ = 7800, PDI = 1.29; (e) 1 kGy, 400:1 GMA-to-CPPA, $M_{n,GPC}$ = 13600, PDI = 1.28.

Symmetric peaks and narrow molecular weight distributions can be observed from peaks (a) and (b). These peaks were obtained from samples that have low monomer-to-RAFT agent ratio (i.e. high RAFT agent concentration) and irradiated at low absorbed dose. Increasing either the monomer-to-RAFT agent ratio (i.e. low RAFT agent concentration, entries 4-5 and 9-10) or the irradiation time resulted in slight tailing which indicated presence of high molecular weight polymers, which possibly came from the irreversible termination of the propagating chains. Nonetheless, the narrow molecular weight distribution, expressed as PDI, from the GPC trace of samples in Figure 2.2, is an obvious proof that the primary RAFT mechanism was demonstrated during grafting.

In contrast to the RAFT-mediated polymerizations, the conventional polymerizations were characterized by PGMA with very high M_n and broad molecular weight distribution as shown by entries 18-21 in Table 2.1. GMA is a specialty monomer and it is difficult to polymerize via conventional radical polymerization without affecting its epoxide group. During conventional radical polymerization of GMA under γ-radiation, excessive crosslinking via the epoxide group and/or the radicals formed on the polymer chains leads to a gel material for which the application is restricted [40, 44]. However, there was no gel formation observed during the RAFT-mediated polymerization in this study. Rather than the high monomer conversion and high molecular weight polymers at the early portion of the polymerization, which characterize conventional grafting, the polymerization was slower and the resultant polymer had narrow PDI, especially at low targeted M_n values.

At higher targeted M_n, the PDI of the free PGMA were greater than 3, except at 10% monomer concentration (entries 4 and 5, 9 and 10). These data are consistent with the results gathered by other researchers [45, 46]. They suggested that these high PDI values were not due to colloidal instability but were most probably a result of heterogeneous distribution of RAFT agent among the micellar monomer droplets. When higher M_n values were targeted, the lower amount of RAFT agent resulted in a greater number of micellar monomer droplets with different monomer-to-RAFT agent ratios, resulting to different polymerization rates and eventually leading to higher PDIs. At fixed monomer-to-RAFT agent ratio, the concentration of RAFT agent increased with increasing monomer concentration; hence, the PDI of free PGMA

remained reasonably low at 10% monomer concentration even at 400:1 monomer-to-RAFT agent ratio.

The results listed in Table 2.1 show that M_n of PGMA increased with polymerization time and polymers with narrow molecular weight distribution were prepared under ^{60}Co γ-irradiation in the presence of CPPA. Figure 2.3 shows a typical ^1H NMR spectrum of PGMA in $CDCl_3$, with chemical shift assignments, obtained in the RAFT-mediated γ-radiation induced graft polymerization of GMA from PE/PP. The spectra collected in this study agree with those in the literature [47, 48].

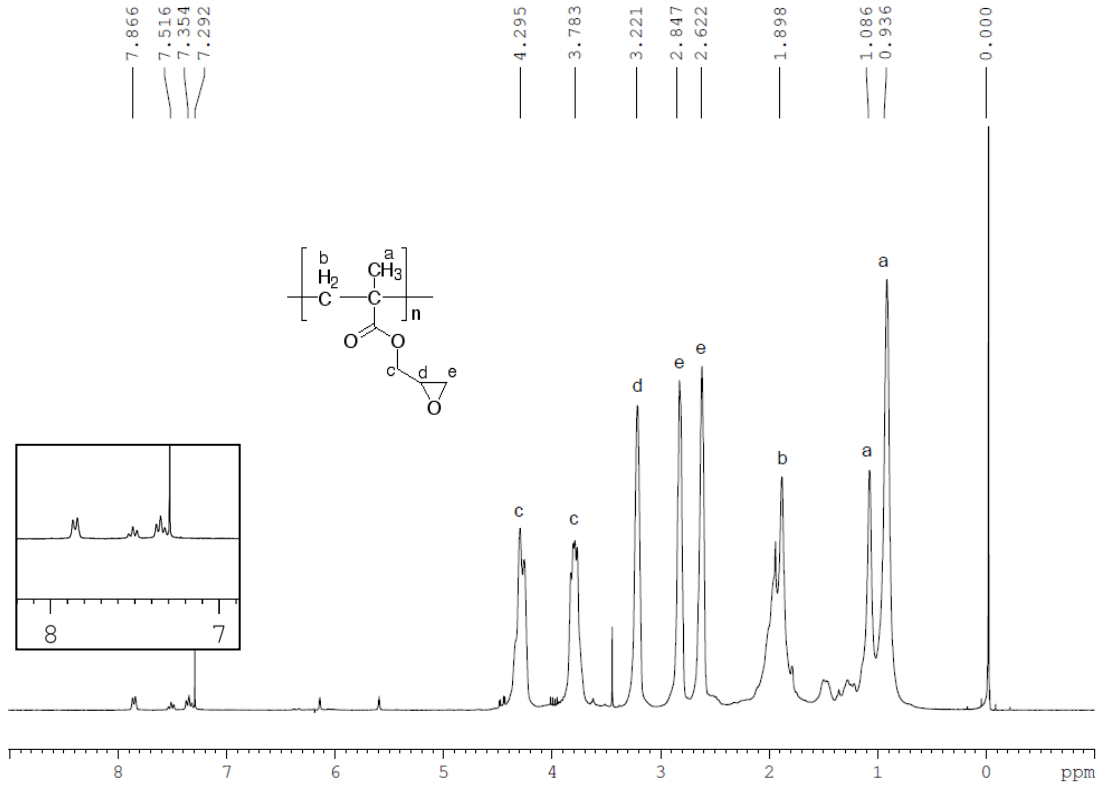

Figure 2.3 ^1H NMR spectrum (300 MHz, $CDCl_3$) of free poly(glycidyl methacrylate) ($M_{n,GPC}$ = 4900, PDI = 1.16) formed in the γ-initiated graft polymerization from PE/PP mediated by the RAFT agent 4-cyano-4-((phenylcarbonothioyl)thio) pentanoic acid (CPPA) at 10% (wt/wt) GMA, 1% (wt/wt) Tween20 and 100:1 GMA-to-CPPA molar ratio. Inset is the plot for peaks between 7.3-8.0 chemical shifts due to dithiobenzoate aromatic protons of CPPA.

The observed ratio of the peak areas of (a), (b) and (d) against (e) is about 3:1; indicating that the oxirane groups in the PGMA remained intact during the γ-radiation induced graft polymerization in the presence of CPPA [49]. The signals at δ = 7.3-8.0 (δ, ppm: 7.90, d, 2H; 7.50, t, 1H; 7.35, t, 2H) correspond to the aromatic protons of dithiobenzoate aromatic hydrogens. Assuming that each macromolecule contains one molecule of dithioenzoate, the $M_{n,NMR}$ of PGMA polymerized with CPPA can be estimated using the following equation:

$$M_{n,NMR} = \frac{I_{a,b}}{I_{7.3-8.0}} \times 142.15 + 279.38 \quad (2.4)$$

where $I_{a,b}$ and $I_{7.3\text{-}8.0}$ are the integral of the peaks at δ = 0.5 – 2.3 (main chain repeating unit, 5H) and δ = 7.3 – 8.0 (dithiobenzoate end-group, 5H), respectively, 142.15 and 279.38 are the molecular weight of GMA and CPPA, respectively. The NMR-based M_n values are tabulated in Table 2.1. The M_n's derived from NMR agreed well with the theoretical molecular weights, $M_{n,th}$, indicating a controlled character of the polymerization in the presence of CPPA under γ-irradiation. Some entries for $M_{n,GPC}$ deviated largely from $M_{n,th}$ and $M_{n,NMR}$, but the observed trends were still similar. The observed discrepancies in M_n were probably due to the different hydrodynamic volumes of PGMA and polystyrene standards in THF solvent.

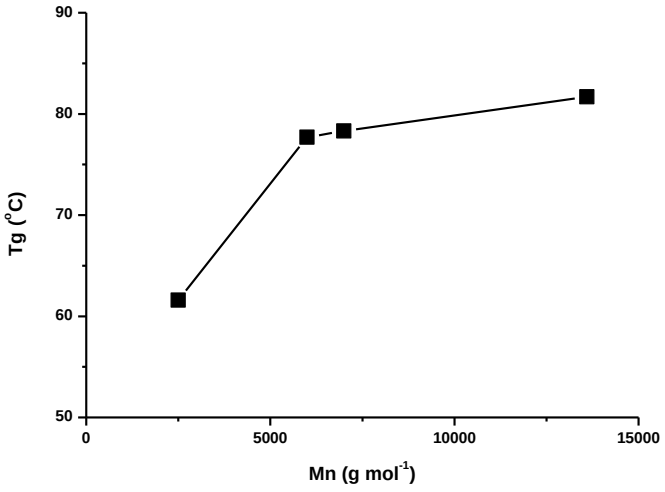

Figure 2.4 Dependence of T_g on molecular weight of free PGMA formed in the γ-initiated graft polymerization from PE/PP mediated by the RAFT agent 4-cyano-4-((phenylcarbonothioyl)thio) pentanoic acid (CPPA).

DSC was utilized to study the thermal transitions during the period of heating under nitrogen atmosphere. The glass transition temperature of free PGMA (PDI $\leq$ 1.38) homopolymers demonstrated dependence towards M_n, wherein the T_g increased with increasing M_n (Figure 2.4). It is well known that the T_g of a given polymer is a function of its chain length [50]. The PE/PP-g-PGMA with 92% *Dg* also exhibited a thermal transition at around 83 °C, higher than its free PGMA counterpart (T_g = 78 °C). The increase in T_g of the grafted sample was ascribed to the constrained mobility of PGMA grafted from PE/PP trunk polymer [25]. This observation confirmed the covalent attachment of PGMA polymers onto the surface of PE/PP, and restriction introduced on the segmental movement of the PGMA polymers as a consequence of grafting. PE/PP-g-PGMA with lower *Dg* values did not produce significant signals during the DSC analysis because of either dilution of the PGMA chains or insufficient amount of analyzed samples due to low bulk density of grafted PE/PP.

2.3.1.3 Characterization of the PE/PP-g-PGMA

The structure of pristine PE/PP and PE/PP-g-PGMA samples were evaluated by FTIR spectroscopy. Figure 2.5 shows the ATR-FTIR spectra of pristine PE/PP and PE/PP-g-PGMA with different *Dg* values. The spectrum of pristine PE/PP trunk polymer has peaks characteristic of its olefinic nature: $–CH_2$ symmetric and asymmetric stretching vibrations at 2848 and 2915 cm^{-1}, respectively, and $–CH_2$ bending vibrations at 1472 cm^{-1}. After grafting with PGMA, new peaks that correspond to the chemical groups present in the grafted polymer chains appear: C=O stretching vibration at 1720 cm^{-1}, C-O stretching vibration at 1120 cm^{-1} and the characteristic oxirane group vibrational modes at around 1250, 900 and 850 cm^{-1}. Similar characteristic peaks were also reported by other researchers [38, 48]. Besides the absorption frequencies of bonds from PGMA, peaks from PE/PP fibers were also observed from the FTIR spectrum of PE/PP-g-PGMA. The functional groups due to the RAFT agent present on the polymer chain ends were not observed because of their low concentration in the sample.

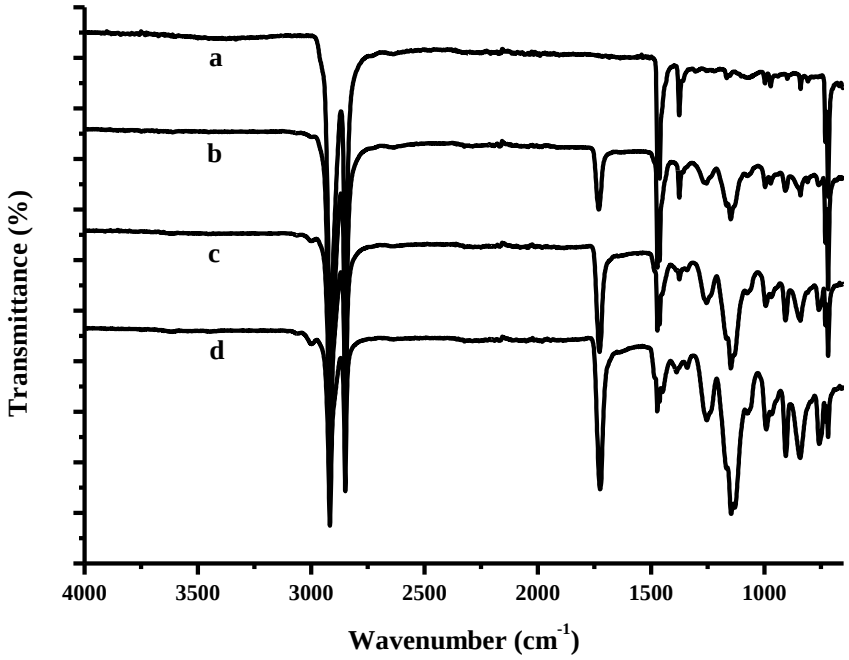

Figure 2.5 ATR-FTIR spectra of (a) pristine PE/PP, (b) PE/PP-g-PGMA, *Dg* = 7%, (c) PE/PP-g-PGMA, *Dg* = 24%, and (d) PE/PP-g-PGMA, *Dg* = 92%.

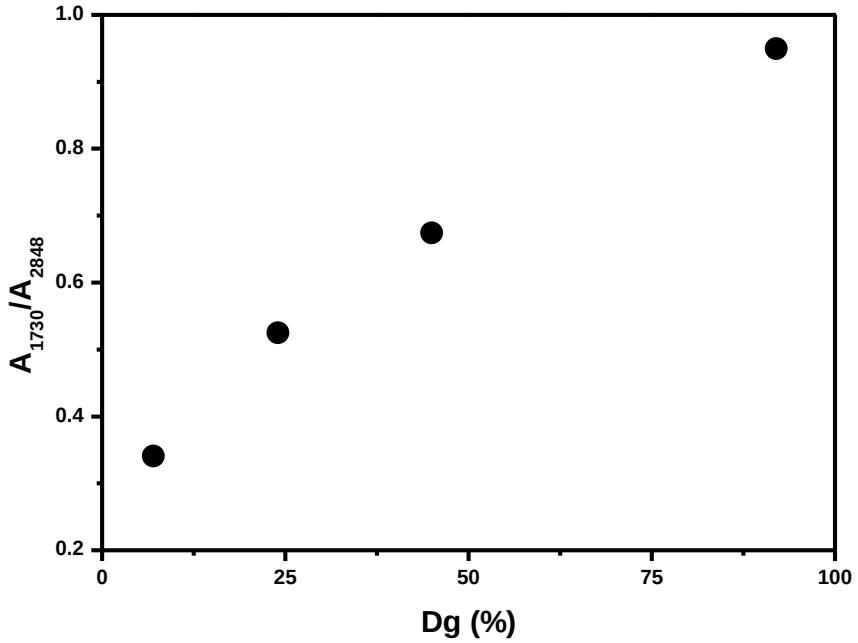

Figure 2.6 Plot of 1730 cm^{-1} and 2848 cm^{-1} peak area ratios at different *Dg*. Peak areas were calculated from FTIR spectrum at absorbance mode.

Further examination of the FTIR spectra of PE/PP-g-PGMA with different *Dg* values showed that the absorption bands due to the C=O, C-O and oxirane group increased with *Dg*, as shown in Figure 2.5b to 2.5d. The observed trend was due to the increase in number of C=O, C-O and oxirane chemical groups at the surface of the grafted material with increment in *Dg* and according to Beer-Lamberts law, the corresponding absorbance of these vibrational transitions must also increase. The peak at 2848 cm^{-1}, which is due to $–CH_2$ symmetric stretch remained almost unaffected by the increase in *Dg*. The plot of the ratio of peak areas (Figure 2.6), calculated in absorbance mode, at 1730 cm^{-1} and 2848 cm^{-1} against different *Dg* of PE/PP-g-PGMA yielded a linear fit with R^2 = 0.98. This plot allows the evaluation of *Dg* of PE/PP-g-PGMA, which is prepared using the same RAFT-mediated graft polymerization technique described in this study, from its ATR-FTIR spectrum.

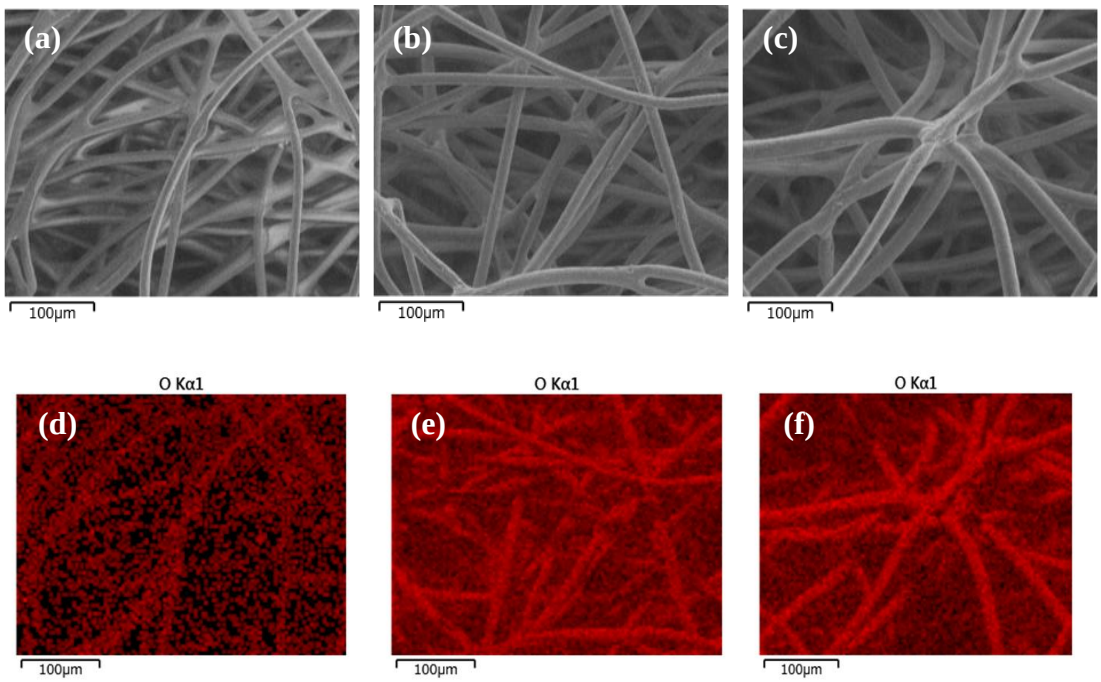

Figure 2.7 SEM images at 300x magnification and elemental oxygen maps of (a), (d) pristine PE/PP; (b), (e) PE/PP-g-PGMA, *Dg* = 24%; and (c), (f) PE/PP-g-PGMA, *Dg* = 92%.

Figures 2.7a to 2.7f show the SEM pictures and corresponding EDX oxygen elemental maps of pristine PE/PP and PE/PP-g-PGMA, with various *Dg*, prepared using RAFT-mediated graft polymerization. The pristine PE/PP was porous and

composed of fibers with homogeneous morphology. The randomly oriented fibers were interconnected and after grafting, no homopolymer aggregation blocking the pores was observed. The oxygen map for the pristine PE/PP fibers shows the presence of oxygen in the material that was supposed to be comprised of carbon and hydrogen only. The detected oxygen atoms might have been incorporated on the fabric during the manufacturing process or due to surface oxidation. After γ-radiation induced RAFT-mediated grafting to 24% and 92% *Dg*, the fiber thickness noticeably increased as illustrated in Figures 2.7b and 2.7c in agreement with other works [22, 38, 40]. Moreover, PE/PP-g-PGMA exhibited higher oxygen density, as shown in Figures 2.7e and 2.7f, compared to the pristine PE/PP. The increase in oxygen density was expected because the grafted PGMA chains contain oxygen atoms in its structure, i.e. from the oxirane and ester groups. These evidences showed that the grafting process was successfully carried out. The sulfur atoms from the RAFT agent ends on the grafted PGMA chains were not detected because of their very low concentration.

Introduction of PGMA chains on PE/PP trunk polymer via RAFT-mediated graft polymerization imparted new chemical bonds that modified the thermal behavior of PE/PP. Figure 2.8 demonstrates the thermal decomposition profile of pristine PE/PP and PP-g-PGMA with various *Dg* values. The PE/PP base material showed a single decomposition profile with maximum weight loss at around 450 °C, in close agreement with previous reports [38, 51]. In PE/PP-g-PGMA, a three-step decomposition profile was observed, with the last step coinciding with the decomposition profile of the PE/PP trunk polymer. The grafted material did not show significant mass loss before 180 °C. The initial decomposition stage was ascribed to the depolymerization from the unsaturated chain terminals and the weight loss above 300 °C was associated with decomposition by random chain scission [52]. The fractional mass loss before 400 °C increased with increasing *Dg*, a clear indication that the thermal decomposition and observed weight losses at lower temperatures were due to the PGMA graft chains.

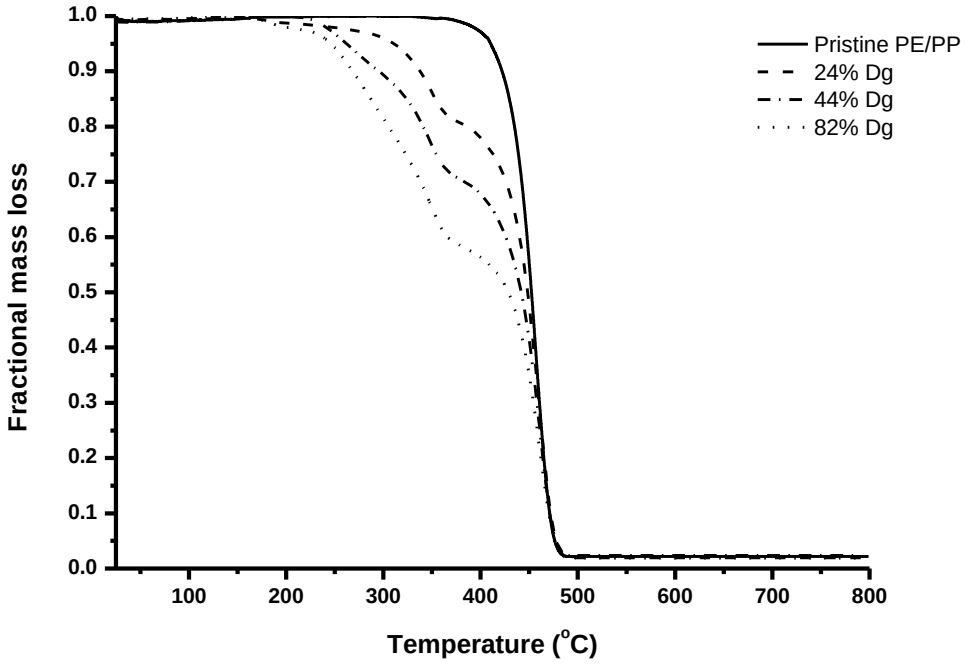

Figure 2.8 Thermogravimetric curves of pristine PE/PP and PE/PP-g-PGMA with different *Dg*.

Survey wide scan and C1s high resolution x-ray photoelectron spectra of pristine and grafted PE/PP and the PGMA homopolymer are shown in Figure 2.9. The surface elemental compositions, which were determined from peak areas of the XPS spectra, are given as insets in the survey scans. The wide survey scan spectra of pristine PE/PP indicated that it was composed of carbon and oxygen atoms. The oxygen atoms in the PE/PP trunk material, which is olefinic in nature, might have been produced from surface oxidation reactions which took place during processing and storage of the material. This observation corroborated with the SEM-EDX oxygen map data of pristine PE/PP presented in Figure 2.7d. Nonetheless, the high resolution C1s spectrum of pristine PE/PP (Figure 2.9b) revealed that the C-C bonds were dominant in its structure, as expected from the olefinic nature of PE/PP. The oxygen content increased from 6% to 13% after grafting, as shown in Figure 2.9c. Moreover, the deconvoluted high resolution C1s spectrum of PE/PP-g-PGMA (Figure 2.9d) showed the presence of other peaks besides the C-C peak. These peaks were attributed to the C-O and C=O bonds that were present in the PGMA graft chains. The presence

of these new peaks and the PDI data from GPC analysis confirmed the successful RAFT-mediated graft polymerization of emulsified GMA from PE/PP under gamma-ray irradiation.

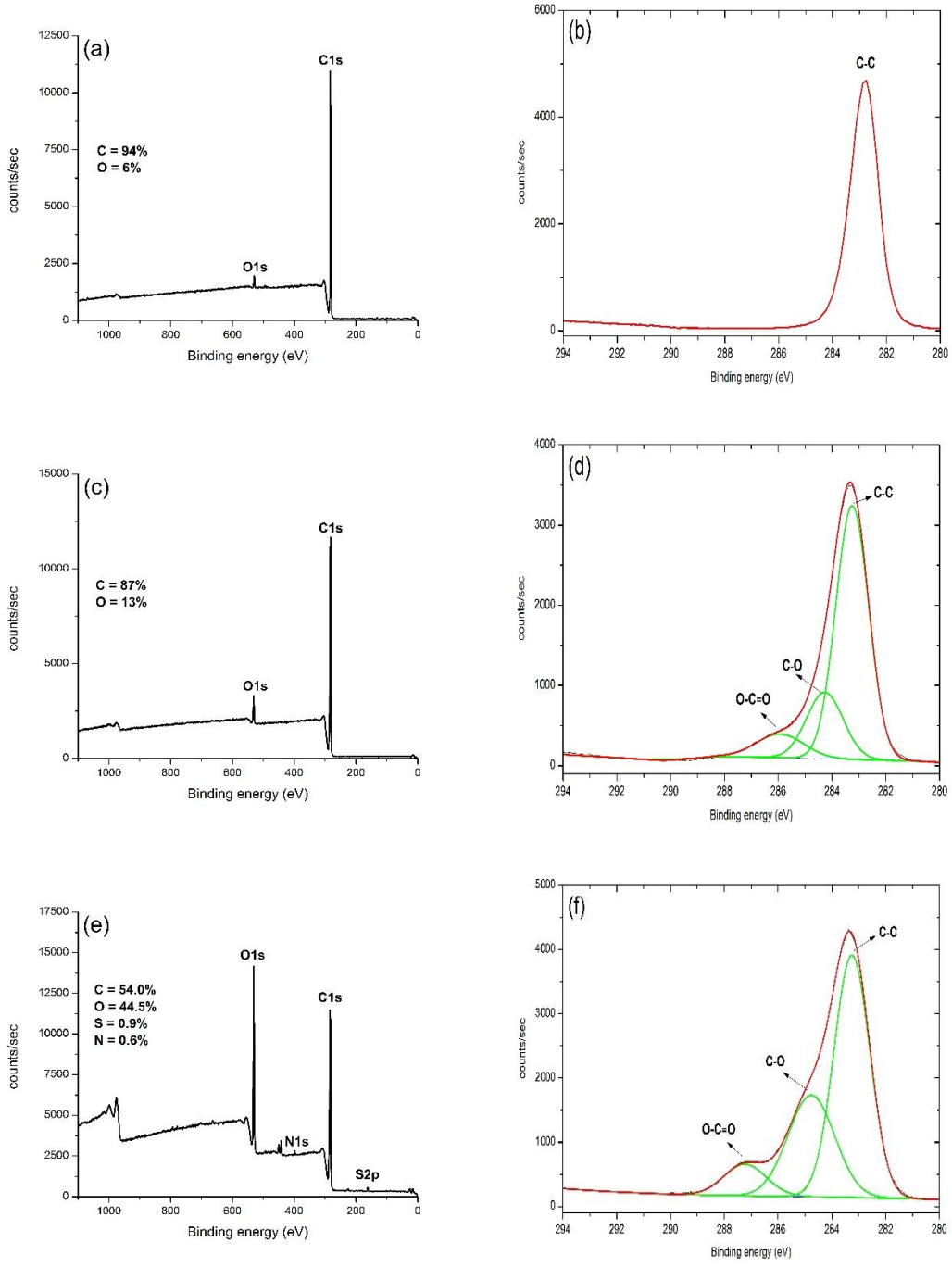

Figure 2.9 XPS survey wide scan and C1s high-resolution spectra of (a) and (b) pristine PE/PP, (c) and (d) PE/PP-g-PGMA, RAFT-mediated grafting *Dg* = 90%, (e) and (f) PGMA homopolymer, RAFT-mediated, $M_{n,GPC}$ = 2500 g mol^{-1}, PDI = 1.16.

Analysis of the PGMA homopolymer (i.e. free PGMA) signified that some of the chains were capped by either the sulfur- or nitrogen-containing portion of the CPPA RAFT agent, as indicated by the presence of S2p and N1s peaks in the XPS survey scan in Figure 2.9e. The S2p peak was not observed from the wide scan spectrum of PE/PP-g-PGMA because of its low concentration on the surface. Furthermore, the atomic C/O ratio calculated after grafting, which was about 6.7, was higher than the theoretically calculated value from the PGMA structure where C/O should be equal to 2.3. This data suggests that the PE/PP trunk polymer substantially contributed to the top 10 nm surface layer, i.e. the top surface layers were not solely constituted by PGMA graft chains. It is possible that some of the RAFT-mediated graft polymerization proceeded inside the surface layers by creating PGMA grafted zones that proceeded inwards by the front mechanism [38, 40, 51].

2.3.2 Pre-irradiation grafting

2.3.2.1 Effects of RAFT agent on pre-irradiation grafting in emulsion phase

In an ideal RAFT-mediated radical polymerization, the RAFT agents reversibly deactivate the propagating radicals so that there is equilibrium between the active and dormant chains [14]. This process indirectly suppresses irreversible termination processes and imparts living characteristics to an otherwise uncontrolled free radical polymerization. Hence, RAFT-mediated radical polymerization belongs to a group of techniques collectively known as controlled radical polymerization (CRP). Graft copolymers of PGMA on PE/PP were synthesized using RAFT mediated graft polymerization in emulsion phase using the pre-irradiation technique. The free radicals produced after electron beam irradiation served as initiation sites for polymerization of GMA molecules from the emulsion. The addition of RAFT agent to the propagating polymer chain is accompanied by the formation of another radical species which also initiate polymerization in the bulk of the monomer solution. Both kind of propagating chains, i.e. grafted and free in the mixture, then add to the thiocarbonyl group of the RAFT agent, creating the RAFT radical intermediates (Figure 2.10). These processes should yield grafted materials with *Dg* values increasing with time. As CRP is not a true living polymerization process, irreversible terminations occurred, mostly in the latter part of the polymerization process. In this

study, no chemical initiators were added to the system, hence the only source of initiating species were the free radicals on the trunk polymer and the expelled free radical from the RAFT agent.

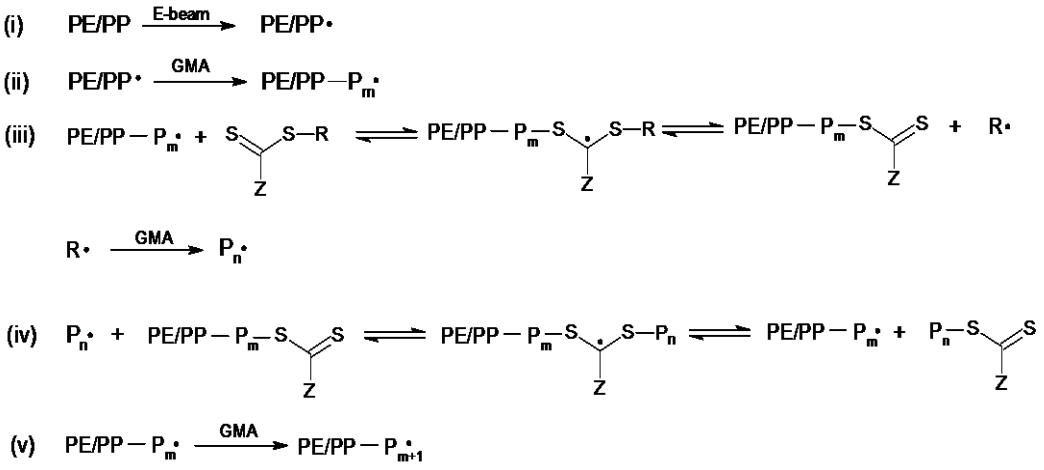

Figure 2.10 Possible reactions for GMA polymerization from irradiated PE/PP surface in presence of CPPA.

The effect of the type of RAFT agent on the *Dg* of the resulting copolymers was evaluated and the results are plotted in Figure 2.11. The data indicate that the use of CPPA in the RAFT-mediated graft polymerization yielded the highest *Dg* among the studied RAFT agents. The high *Dg* values obtained from the use of CPPA is probably due to the presence of the carboxylic acid group in the expelled R moiety from this molecule, which gives it better solubility in the monomer aqueous emulsion. This carboxylic-bearing R-group reinitiates the polymerization in the monomer aqueous emulsion and this process allows the RAFT-mediated reactions to proceed. Otherwise, without reinitiation and noting that no new radical initiators were introduced to the reaction mixture, the propagating chains would have remained reversibly deactivated for a longer period, leading to lower *Dg* values as observed in the use of other RAFT agents. Moreover, the target application for the resulting copolymer is in the field of adsorption so copolymers with *Dg* values around 100% are required. Hence, the succeeding RAFT-mediated graft polymerizations were performed using CPPA as RAFT agent.

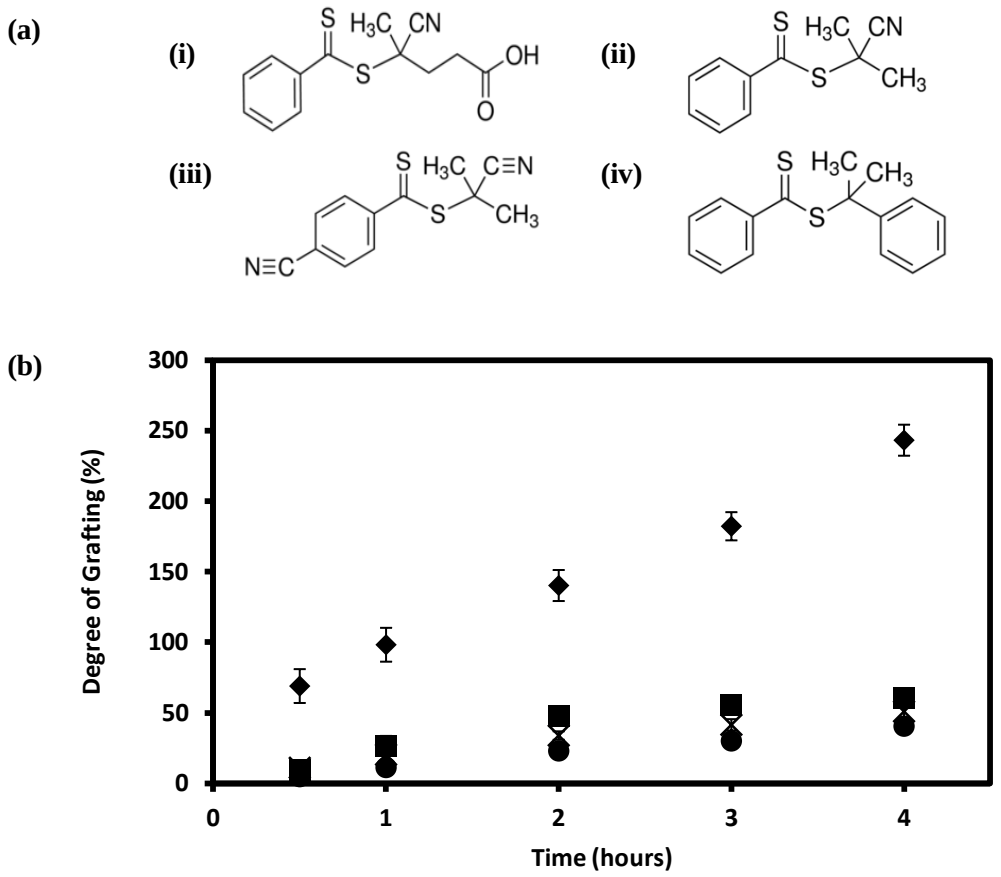

Figure 2.11 (a) RAFT agents evaluated in this study: (i) 4-cyano-4-((phenylcarbonothioyl)thio) pentanoic acid (CPPA), (ii) 2-cyano-2-propyl benzodithioate (CPDB), (iii) 2-cyano-2-propyl 4-cyanobenzodithioate (CPCB), (iv) 2-phenyl-2-propylbenzodithioate (PPB); (b) Variation of *Dg* with reaction time using different RAFT agents: CPPA (♦), CPDB (■), CPCB (x), PPB (●); 3 trials.

Figure 2.10 suggests that the homopolymer molecules produced during the RAFT-mediated graft polymerization of GMA from pre-irradiated PE/PP must contain at least one dithiobenzoate end. The presence of this type of PGMA homopolymer in the reaction medium was verified by ^{1}H NMR spectroscopy. A typical ^{1}H NMR spectrum is given in Figure 2.12. In addition to the characteristic chemical shifts of GMA repeating units, the characteristic signals at 7.3 – 8.0 chemical shift (δ, ppm: 7.90, d, 2H; 7.50, t, 1H; 7.35, t, 2H) assigned to aromatic protons originating from CPPA were also observed. This indicates the existence of dithiobenzoate group from CPPA at one end of the polymer chain. The presence of dithiobenzoate capped PGMA homopolymers in the reaction medium as suggested by

the ^{1}H NMR results supports the proposed reactions for the RAFT-mediated graft polymerization of GMA from pre-irradiated PE/PP backbone polymer shown in Figure 2.10. The spectrum collected in this study agrees well with those obtained by other researchers [47, 48].

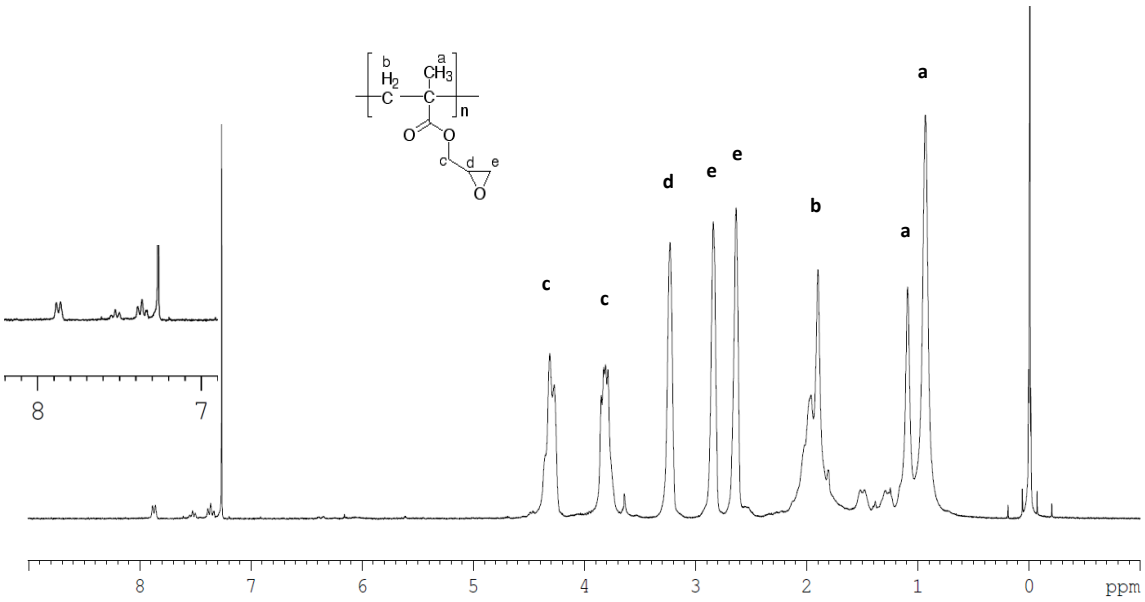

Figure 2.12 ^{1}H NMR spectrum of poly(glycidyl methacrylate) in $CDCl_3$. Inset is the plot for peaks between 7.3-8.0 chemical shift due to aromatic ring protons of the RAFT agent.

(i) Comparison between RAFT-mediated and conventional grafting

Compared to graft polymerization via conventional method, i.e. without chain transfer agents, addition of CPPA in the graft polymerization of emulsified GMA resulted to a decrease in the amount of grafted PGMA, as shown in Figure 2.13. It is known that in chain transfer polymerizations and RAFT-mediated polymerizations, a reduction in rate of polymerization is often observed [39] and the electron beam-induced graft polymerization of GMA on PE/PP in the presence of CPPA is not an exception. The reduction in *Dg* after adding CPPA can be explained by the decrease in the effective amount of propagating chain radicals through chain transfer reactions to CPPA. No chemical initiators were added to the system hence most of the CPPA RAFT agent existing in the solution should have added to the propagating grafted chains, and in the process expelled another radical (R• in Figure 2.10) that reinitiates propagation in the solution. After 30 minutes of reaction with 10% GMA at 400:1 GMA to CPPA molar ratio, the *Dg* increased to 105% and 145% for PE/PP polymers

that were irradiated at 50 and 100 kGy absorbed dose, respectively. The irradiation of PE/PP resulted to bond-breaking reactions which lead to production of free radicals, majority of which are allyl, alkyl and polyenyl type [36, 53]. The relative amount of these free radicals depends on the type of irradiated polymer, temperature, energy and type of radiation, and post-irradiation storage time and environment. These radicals served as initiation points in the graft polymerization of GMA from the PE/PP nonwoven fabric. The higher the amount of energy imparted to PE/PP, i.e. absorbed dose, the greater the number of initiation points formed for graft polymerization which in turn leads to higher *Dg*. The *Dg* continued to increase up to 2 hours reaction time, after which the *Dg* remained almost constant despite the low monomer conversion (< 7%). This observation indicated that most of the grafted chains were irreversibly terminated after 2 hours of reaction. Possible termination reactions for the grafted polymer chains include coupling of two propagating chains [25], disproportionation and reaction between growing polymer chains, grafted or in the bulk, with RAFT radical intermediate [54].

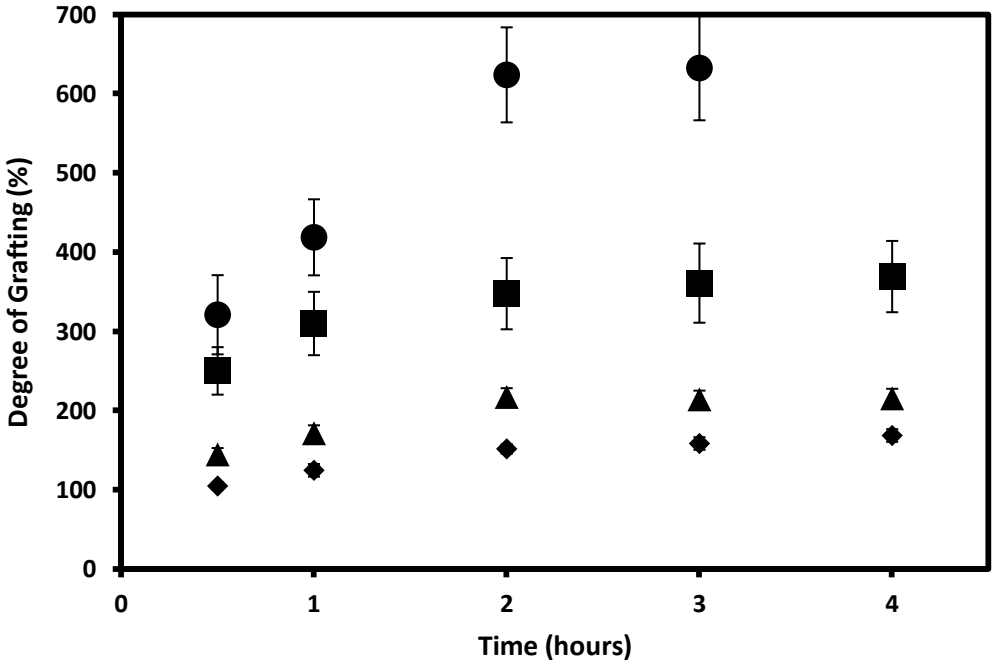

Figure 2.13 Variation of *Dg* with reaction time for the graft polymerization of GMA from PE/PP in presence of RAFT agent (▲-100 kGy, ♦ - 50 kGy) and without RAFT agent (● - 100 kGy, ■ - 50 kGy). GMA concentration, 10% (wt/wt); monomer to surfactant weight ratio, 10:1; monomer to RAFT agent molar ratio, 400:1; reaction temperature, 40 °C, 3 trials.

(a) Reaction with a dormant chain on another fiber

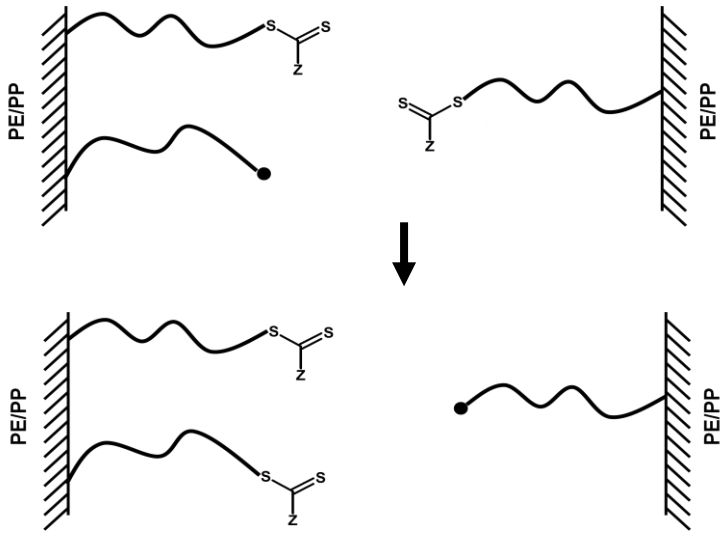

(b) Reaction with a free RAFT agent in the solution

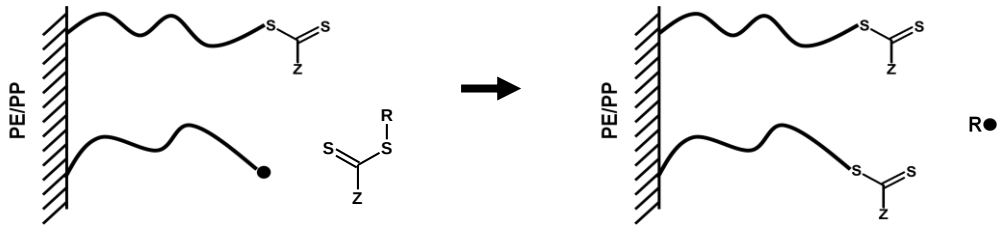

(c) Reaction with a dormant free polymer

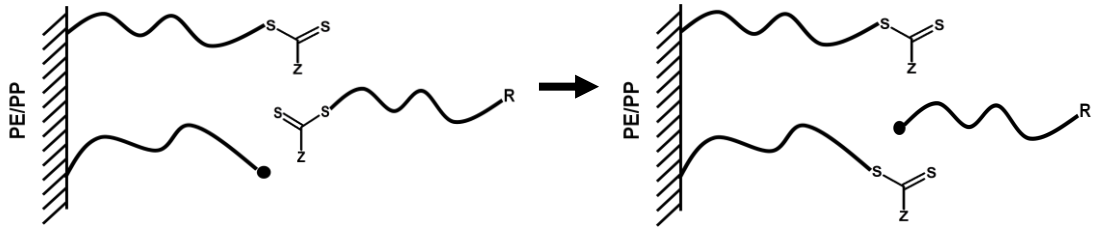

(d) Reaction with a dormant chain on the same fiber

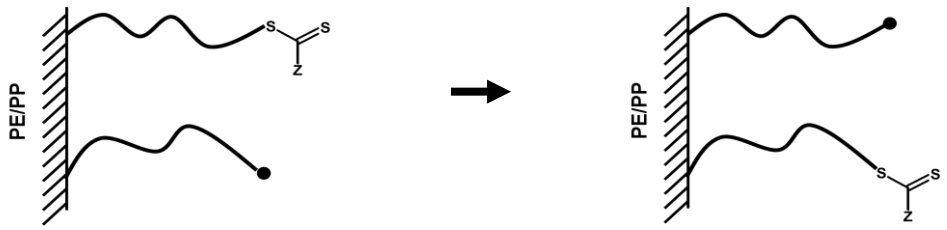

Figure 2.14 Possible chain transfer reactions of the propagating chains and dormant chains.

As shown in Figure 2.10, the propagating grafted polymer chains may add to the RAFT agent resulting to a dormant grafted chain. At this stage, there are two types of grafted chains on the PE/PP surface: propagating grafted polymers with an active radical terminal and dormant grafted polymers with RAFT agent-capped end. The possible chain transfer reactions for the polymerization mediated with surface anchored RAFT agents can be summarized in four modes (Figure 2.14). The propagating grafted chain could react with a RAFT agent-capped dormant chain on another fiber, a free RAFT agent in the solution, a dormant polymer chain in the solution produced during the reinitiation by the expelled radical and its subsequent reaction with another RAFT agent, or a neighboring RAFT agent-capped dormant chain on the same fiber surface. The first mode could have a very slow rate because it requires interpenetration of the grafted polymer layers on the two fibers. The second mode was expected to be negligible after the initial portion of graft polymerization as most of the RAFT agents near the fiber surface have reacted with the propagating grafted chains. This means that the predominant chain transfer modes of the radical on the surface were to react with the dormant chains in the solution capped with RAFT agent or with the neighboring anchored RAFT agents on the dormant grafted polymer chains. The reaction of the propagating grafted polymer chain with the neighboring RAFT agent-capped grafted polymer chains also produced the intermediate RAFT radical. The slow fragmentation of the intermediate RAFT radical was believed to be strongly associated with the retardation commonly observed for RAFT-mediated polymerization as compared to the polymerization without RAFT agents [23, 39]. This slow fragmentation might have also contributed to the lower *Dg* obtained in RAFT mediated graft polymerization as compared to conventional graft polymerization shown in Figure 2.13.

(ii) Effects of monomer concentration

Experimental data showed that generally, *Dg* decreased with increment in GMA concentration (Figure 2.15) at fixed GMA to CPPA ratio. Moreover, all plots were almost linear and the change in *Dg* per unit time, i.e. rate of graft polymerization, increased with decreasing monomer concentration. The effect was more pronounced after an hour of grafting and for polymers that were pre-irradiated at

20 kGy. The trend observed in this study was opposite to what the other researchers have found wherein the *Dg* increased with increasing monomer concentration because of the enhanced availability of the monomer in close proximity to the initiation sites and propagating chains [9 – 11, 13, 55]. The same trend of decreasing *Dg* with increasing monomer concentration was observed by Ueki *et al*., (2007) when they grafted polylactic acid with PGMA via conventional pre-irradiation grafting in emulsion state [56]. They explained the observed relationship between *Dg* and monomer concentration in terms of micelle size, noting that emulsions with lower monomer concentration tend to have micelles with smaller diameter. According to them, smaller micelles have higher surface area that resulted in more contact points between the monomer in the micelles and the irradiated trunk polymer, leading to improved reaction efficiency of graft polymerization. Hence to clarify our observation, we repeated the grafting experiment without adding CPPA. In the absence of RAFT agent, the calculated *Dg* increased with increment in monomer concentration (data not shown), in concurrence with the generally observed trend. Moreover, the initial micelle sizes of the emulsions prepared with or without CPPA were almost similar, e.g. ~ 200 nm for 3% GMA and ~450 nm for 10% GMA. These results indicated that the observed trend was primarily because of the chain transfer reactions induced by the RAFT agent and not from the effects of micelle size. Because the GMA to CPPA ratio was maintained in all the experimental runs, increasing the monomer concentration also increased the CPPA concentration in the emulsion. Higher amount of RAFT agent in the reaction medium enhanced the probability of chain transfer processes of the growing chains. The enhancement of chain transfer events decreased the effective amount of propagating grafted chains per unit time, resulting to lower *Dg* despite the increased GMA concentration.

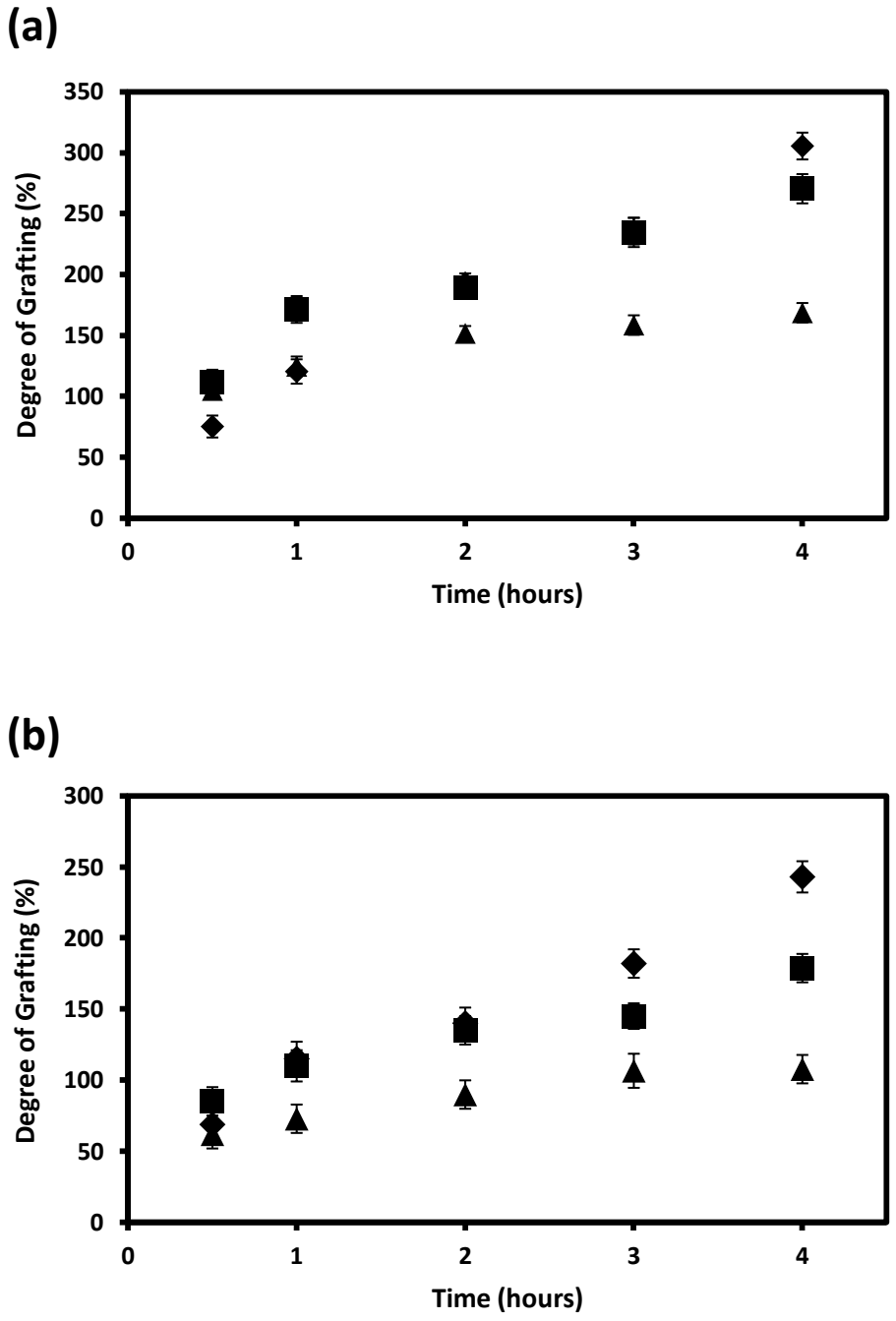

Figure 2.15 Effect of monomer concentration on *Dg* at different reaction times for PE/PP irradiated at (a) 50 kGy and (b) 20 kGy absorbed dose. 10% (▲), 5% (■) and 3% (♦) (wt/wt) GMA concentration; monomer to surfactant weight ratio, 10:1; monomer to RAFT agent molar ratio, 400:1; reaction temperature, 40 °C, 3 trials.

(iii) Effects of monomer-to-RAFT agent ratio

At fixed monomer concentration, the *Dg* increased with increasing GMA to CPPA ratio, i.e. decreasing RAFT agent concentration (Figure 2.16). This observation corroborated our previous explanation on the observed increase in *Dg* with decreasing monomer concentration at fixed GMA to CPPA ratio. Fixing the GMA concentration removes monomer diffusion related effects; hence the observed trend may be attributed only to chain transfer processes. The same trend was observed in previous studies wherein both monomer and RAFT agent were dissolved in organic solvent [38, 40]. Comparison of the *Dg* plots for grafting reactions in the presence and absence of CPPA, shown in Figure 2.17, further highlights the effect of CPPA in the graft polymerization process. Without CPPA, the *Dg* reached an almost constant value after 2 hours reaction time. In the RAFT-mediated graft polymerization, the *Dg* increased almost linearly up to 6 hours reaction time (plot only shows data up to 4 hours) after which the calculated *Dg* values were almost similar. The monomer conversion after 4 hours of reaction was less than 35%. Therefore the almost constant *Dg* value observed after 2 hours of reaction in the absence of CPPA was not due to monomer exhaustion but may be attributed to dominance of irreversible termination reactions. Clearly, this was not the case for the graft polymerization in the presence of CPPA. The *Dg* increased over a longer range of reaction time because of the reversible deactivation of propagating chains that indirectly suppressed the irreversible terminations in the studied system.

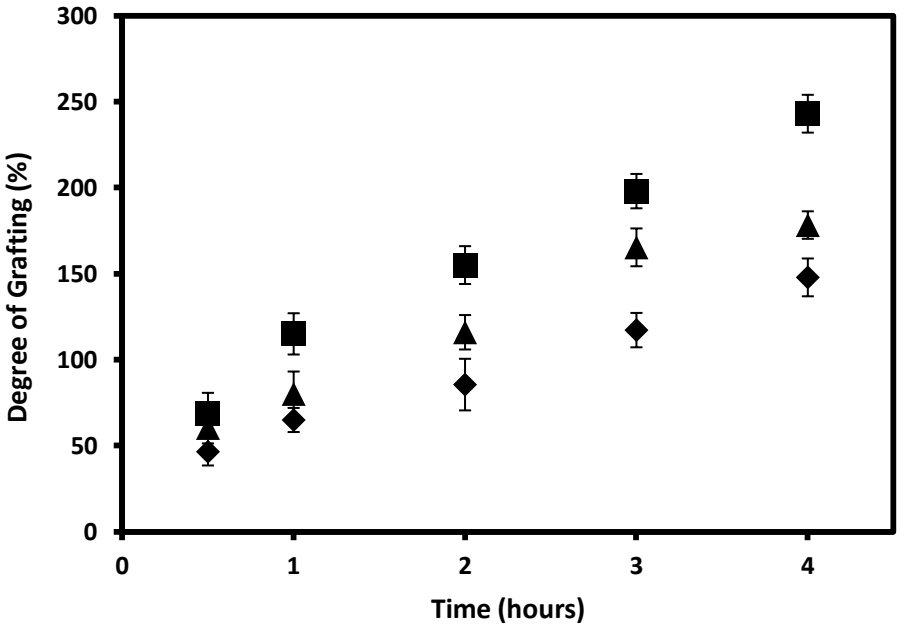

Figure 2.16 Variation of *Dg* with reaction time for the graft polymerization of GMA from PE/PP in presence of RAFT agent at different GMA to RAFT agent molar ratio: ■ - 400:1, ▲- 200:1, ♦ - 100:1. GMA concentration, 3% (wt/wt); monomer to surfactant weight ratio, 10:1; reaction temperature, 40 °C, 3 trials.

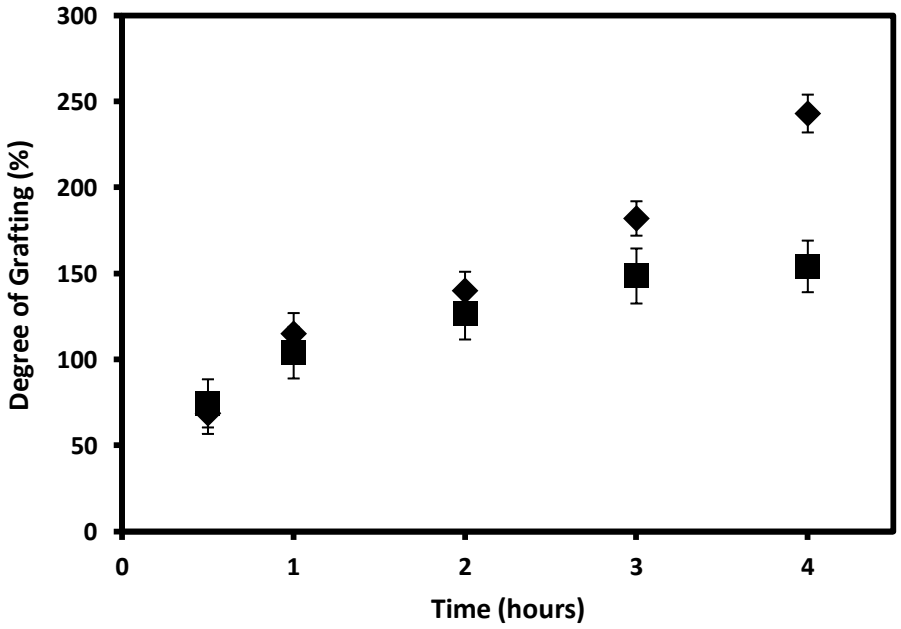

Figure 2.17 Variation of *Dg* with reaction time for the graft polymerization of GMA from PE/PP in presence of RAFT agent (♦) and without RAFT agent (■). Absorbed dose, 20 kGy; GMA concentration, 3% (wt/wt); monomer to surfactant weight ratio, 10:1; monomer to RAFT agent molar ratio, 400:1; reaction temperature, 40 °C, 3 trials.

Some of the synthesized PE/PP-g-PGMA in the current study have more than 150% *Dg*. Very high *Dg* materials (e.g. *Dg* > 200%) were not commonly used because of their undesirable properties, such as brittleness and masking of the trunk polymer's unique properties. Nevertheless, the results of this study indicated that the use of RAFT agent in emulsion state graft polymerization can lead to synthesis of materials with controlled *Dg* over a longer range of reaction time, as compared to conventional grafting in emulsion phase, and controlled graft chain lengths, as discussed below. Moreover, the pseudo-first order kinetic plots were linear over the achieved conversion values in this study and an apparent first-order dependence on monomer concentration was observed. As illustrated in Figure 2.10 and as observed from the experiments, pre-irradiation grafting in the presence of RAFT agents yielded free homopolymers in the bulk of the mixture. These homopolymers were found to approximate the molecular weight and dispersity of the grafted chains [25]. Table 2.2 summarizes the properties of the PGMA homopolymers obtained from the polymerization mixture after 1 and 3 hours of grafting reaction. After an hour of grafting, the PGMA homopolymer had a PDI of 1.53 and this value increased to 1.80 after 3 hours of reaction. No homopolymers were obtained from the reaction mixture for grafting conducted without RAFT agent, so comparison of PGMA produced by conventional grafting cannot be performed. However, the PDI values obtained in this study were significantly lower than the PDI of PGMA homopolymers produced from the gamma radiation-induced graft polymerization of GMA on cellulose which yielded homopolymers with PDI values up to 15 when performed without RAFT agents [40]. The GPC data, together with the *Dg* plots and the discussion above, indicate that control over the graft polymerization of emulsified GMA on irradiated PE/PP was established using CPPA RAFT agent. However, full control over molecular weight and PDI was limited as indicated by the >1.5 values for PDI.

Table 2.2 GPC data for free poly(glycidyl methacrylate) obtained from grafting of GMA from PE/PP. Absorbed dose, 20 kGy; GMA concentration, 3%; GMA to RAFT molar ratio, 400:1; GMA to surfactant weight ratio, 10:1.

Reaction time, h	Dg, %	Conversion, %	$M_{n,GPC}$	PDI
1	98	9.8	6000	1.53
3	182	24.6	11900	1.80

The technique used in the current work allowed the synthesis of PE/PP fibers functionalized with oxirane groups from the PGMA graft chains that had reasonable dispersity. The *Dg* can be controlled from 40% to values greater than 150% by modifying the monomer concentration, absorbed dose and amount of CPPA. Although these *Dg* values were lower than what other authors have obtained after they grafted backbone polymers similar to PE/PP [9, 57, 58], the synthesized grafted materials in the current study have high potential to be used in different applications. The optimum *Dg* value depends on the intended application of the final material. For preparation of biocompatible surface, grafting of 2-4% may be sufficient, for fuel cell and battery separator applications grafting of 20-50% would be desired and for adsorption applications even grafting of 100-150% would be preferred [41]. Further chemical modifications of the PGMA graft chains impart new functional groups to the PE/PP grafted fibers for various applications. Moreover, the use of water, an environment friendly and cheap solvent, as primary component of the grafting mixture was another merit of the process.

2.3.2.2 Surface and thermal properties of grafted materials

The new chemical groups introduced to the nonwoven fabric base material after grafting were detected in the FTIR spectrum shown in Figure 2.18. The spectrum of pristine PE/PP trunk polymer has peaks at 2800-2900 cm^{-1} and 1400-1500 cm^{-1} that correspond to C-H stretching and CH_2 bending modes, respectively. After grafting with PGMA, new peaks appeared that corresponded to the chemical groups present in the grafted polymer chains appear: C=O stretch at 1720 cm^{-1}, C-O stretch at 1120 cm^{-1} and the characteristic oxirane group vibrational modes at around 1250, 900 and 850 cm^{-1}. Similar characteristic peaks were observed from other studies [11, 55, 59]. Besides the absorption frequencies of bonds from PGMA, peaks from PE/PP fibers were also observed from the FTIR spectrum of PE/PP-g-PGMA. The functional groups from the RAFT agent that was present on the polymer chain ends were not observed because of their low concentration in the sample.

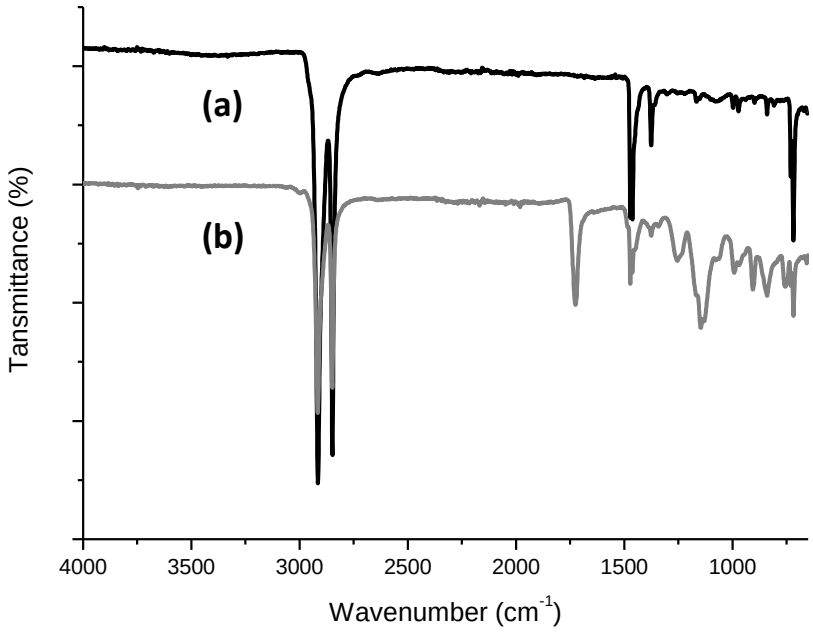

Figure 2.18 FTIR-ATR spectra of (a) pristine PE/PP and (b) PE/PP-g-PGMA synthesized in emulsion state in presence of RAFT agent CPPA.

Figures 2.19a and 2.19b show the fibers' surface images and corresponding EDX oxygen elemental maps of the pristine PE/PP and PE/PP-g-PGMA prepared using RAFT-mediated graft polymerization, respectively. The pristine PE/PP was porous and composed of fibers with homogeneous morphology. The oxygen map of the fibers showed the presence of oxygen in the material that was supposed to be composed of carbon and hydrogen only. The detected oxygen atoms might have been incorporated to the fabric during the manufacturing process or surface oxidation. After grafting to a *Dg* of 150%, the fiber thickness increased noticeably, as illustrated in Figure 2.19b. The density of red dots in the oxygen elemental map of PE/PP-g-PGMA was higher compared to the pristine PE/PP. The increase in oxygen density was expected because the grafted PGMA chains have oxygen atoms in its structure, i.e. from the oxirane and ester groups. These evidences (i.e. FTIR, SEM and EDX data) showed that grafting in the presence of CPPA was successfully carried out. The sulfur atoms from the RAFT agent ends of the grafted PGMA chains were not detected by EDX probably because of their very low concentration.

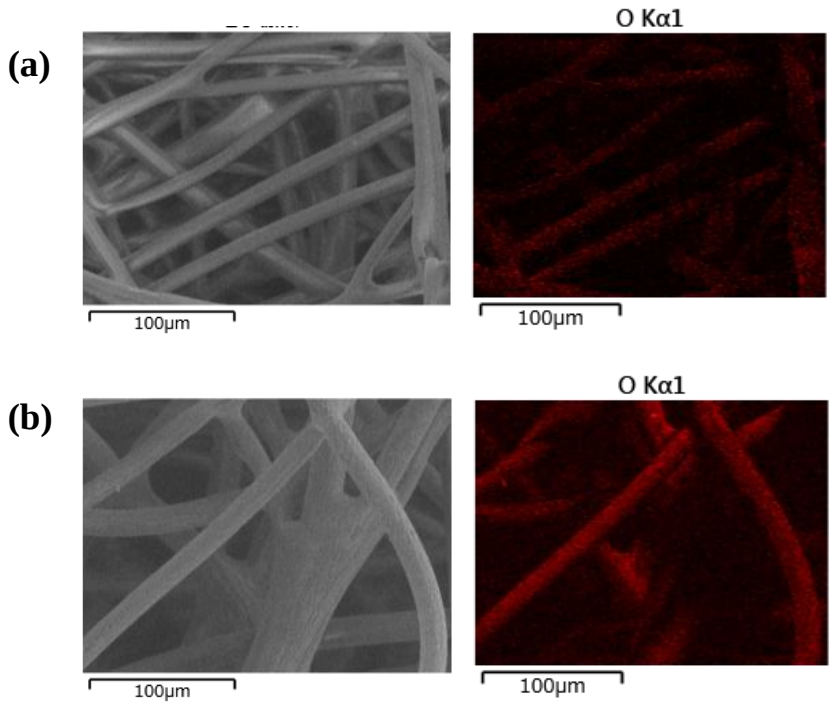

Figure 2.19 SEM images for the fiber surface with corresponding EDX oxygen elemental maps for (a) pristine PE/PP and (b) PE/PP-g-PGMA.

Graft polymerization of GMA on irradiated PE/PP polymer in the presence or absence of RAFT agent imparted new chemical bonds so the thermal behavior of the grafted material was expected to differ from the pristine PE/PP trunk polymer. The thermographs on Figure 2.20 demonstrate the thermal decomposition behavior of pristine PE/PP and grafted PE/PP polymers with almost similar *Dg* and were synthesized with and without CPPA. The PE/PP polymer showed a one-step decomposition profile with maximum weight loss at 458 °C. The derivative thermogravimetric (DTG) curves of the grafted polymers showed two-step decomposition profiles: the first decomposition stage at lower temperature corresponds to the thermal decomposition of grafted PGMA chains and the second one coincides with the thermal decomposition of the PE/PP base material. From the thermogravimetric (TG) and DTG curves, the T_{onset} and T_{max} of the first decomposition stage were 234 °C and 250 °C, respectively, for the CPPA-mediated grafted PE/PP, and 215 °C and 250 °C, respectively, for the grafted PE/PP prepared without CPPA. Because the test conditions, size and packing of samples were

maintained during analysis, the observed differences in the thermal decomposition profiles may be attributed to the properties of the grafted PGMA chains from the two materials. The sharp DTG peak at lower temperature of the CPPA-mediated grafted PE/PP was due to degradation by random chain scission of the grafted PGMA chains [52] onto which degradation of polymer chains from possible branching or crosslinking became superimposed after grafting without CPPA, resulting to peak broadening and appearance of shoulder peak. A similar trend was observed in the thermal degradation of poly(ether ketone)s [60]. The addition of chain transfer agents, such as CPPA, introduces control in *Dg* and also in the molecular weight and dispersity of the graft chains. The GPC data in Table 2.2 indicates reasonable dispersity of the free PGMA and this also reflects the properties of the grafted PGMA [25, 38, 40]. Therefore, the thermal decomposition of graft chains prepared via RAFT-mediated process should have minimum branching and crosslinking due to the controlled nature of the polymerization, resulting to the relatively sharper DTG peak as shown in Figure 2.20. Without CPPA, the process proceeded via the usual free radical polymerization, wherein the grafted chains have more random molecular weights and architecture, leading to broadening of the DTG peak.

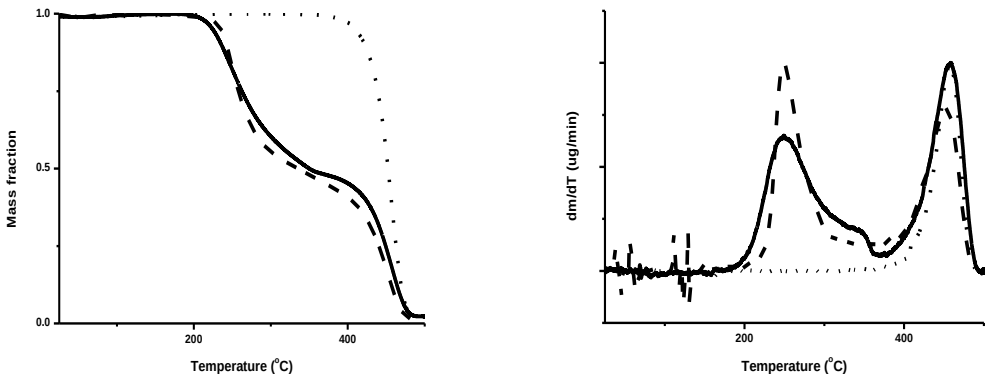

Figure 2.20 Thermogravimetric and derivative thermogravimetric curves for pristine PE/PP (•••), PE/PP-g-PGMA synthesized in presence of CPPA, 100% Dg (- -), PE/PP-g-PGMA conventional synthesis, 120% Dg (–).

2.4 CONCLUSIONS

GMA in emulsion phase was successfully graft polymerized from PE/PP by the combination of the RAFT technique and radiation (electron beam and γ-radiation) - induced initiation, leading to the oxirane group functionalization of the olefinic fibers. The RAFT agent 4-cyano-4-((phenylcarbonothioyl)thio) pentanoic acid was used and the graft polymerization was carried out in a mixture that contained more than 90% water. The combination of CPPA-mediated process and grafting in emulsion state allowed the synthesis of PE/PP grafted polymers with tunable *Dg* over time. The GPC data showed that the PGMA homopolymers, which approximates the properties of the grafted chains, had reasonable distribution of molecular weights. The dependences of *Dg* on the different reaction parameters of the RAFT-mediated process were systematically studied and discussed: for pre-irradiation grafting, the calculated *Dg* increased with increasing absorbed dose and grafting time, but tended to decrease with increment in monomer and CPPA concentrations; for simultaneous grafting, the *Dg* increased with increasing monomer concentration and absorbed dose and decreased with increasing monomer to RAFT agent ratio. Finally, the spectroscopic, thermal and microscopy techniques all support the successful graft polymerization of PGMA from PE/PP. The reactive pendant oxirane group of GMA provides versatility to the PE/PP-g-PGMA which can be useful for different specialty applications.

2.5 REFERENCES

1) Aliev, R. *Polym. Bull.* **2001,** *47*, 99-104.
2) Tsuneda, S.; Saito, K.; Furusaki, S.; Sugo, T.; Okamoto, J. *J. Membr. Sci.* **1991,** *58,* 221-234.
3) Seko, N.; Katakai, A.; Hasegawa, S.; Tamada, M.; Kasai, N.; Takeda, H.; Sugo, T.; Saito, K. *Nucl. Technol.* **2003,** *37,* 535-554.
4) Awual, M.; Urata, S.; Jyo, A.; Tamada, M.; Katakai, A. *Water. Res.* **2008,** *42*, 689-696.
5) Ramirez-Jimenez, A.; Alvarez-Lorenzo, C.; Concheiro, A.; Bucio, E. *Radiat. Phys. Chem.* **2014,** *99,* 53-61.
6) Nasef, M.; Saidi, H. *J. Polym. Res.* **2005,** *12,* 305-312.
7) Nasef, M.; Hagazy, E. *Prog. Polym. Sci.* **2004,** *28,* 499-561.
8) Franks, F. *Water A Comprehensive Treatise: Volume 4: Aqueous solutions of amphiphiles and macromolecules* **1975**, Plenum Press, New York, USA, 585-586.
9) Seko, N.; Bang, L.; Tamada, M. *Nucl. Instrum. Meth. B* **2007,** *265,* 146-149.
10) Seko, N.; Ninh, N.; Tamada, M. *Radiat. Phys. Chem.* **2010,** *79*, 22-26.
11) Madrid, J.; Ueki, Y.; Seko, N. *Radiat. Phys. Chem.* **2013,** *90*, 104-110.
12) Vosloo, J.J.; De Wet-Ross, D.; Tonge, M.P.; Sanderson, R.D. *Macromolecules* **2002,** *35,* 4894-4902.
13) Grasselli, M.; Betz, N. *Nucl. Instrum. Meth. B* **2005,** *236*, 201-207.
14) Matyjaszewski, K. and Spanswick, J. *Mater. Today* **2005,** *8*, 26-33.
15) Rizzardo, E.; Chong, Y.K.; Evans, R.; Moad, G. and Thang, S.H. *Macromol. Symp.* **1996,** *111,* 1-11.
16) Boutevin, B. *Adv. Polym. Sci.* **1990**, *94*, 69.
17) Davis, T.P.; Kukulj, D.; Haddleton, D.M.; Maloney, D.R. *Trends Polym. Sci.* **1995,** *3,* 365-373.
18) Gaynor, S.C.; Wang, J.S.; Matyjaszewski, K. *Macromolecules* **1995,** *28,* 8051-8056.
19) Yu, W.; Kang, E. and Neoh, K. *Langmuir* **2005,** *21,* 450-456.
20) Yoshikawa, C.; Goto, A.; Tsujii, Y.; Fukuda, T.; Yamamoto, K. and Kishida, A. *Macromolecules* **2005,** *38,* 4604-4610.

21) Wang, W.; Neoh, K.; Kang, E. *Macromol. Rapid. Comm.* **2006,** *27*, 1665-1669.

22) Barsbay, M.; Güven, O. *Polymer* **2013,** *54*, 4838-4848.

23) Moad, G.; Chiefari, J.; Chong, Y.K.; Krstina, J.; Mayadunne, R.T.A.; Postma, A.; Rizzardo, E.; Thang, S.H. *Polym. Int.* **2000,** *49*, 993-1001.

24) Millard, P-E.; Barner, L.; Reindhardt, J.; Buchmeiser, M.; Barner-Kowollik, C.; Muller, A. *Polymer* **2010,** *51*, 4319-4328.

25) Barsbay, M.; Güven, O.; Stenzel, M.H.; Davis, T.P; Barner-Kowollik, C.; Barner, L. *Macromolecules* **2007,** *40*, 7140–7147.

26) Khani, M.M.; Woo, D.; Mumpower, E.L.; Benicewicz, B.C. *Polymer* **2017,** *109*, 339-348.

27) Barsbay, M.; Güven, O. *Radiat. Phys. Chem.* **2009,** *78*, 1054–1059.

28) Kavakli, P.A.; Kavakli, C.; Seko, N.; Tamada, M.; Güven, O. *Radiat. Phys. Chem.* **2016,** *127*, 13-20.

29) Moawia, R.M.; Nasef, M.M.; Mohammed, N.H.; Ripin, A. *Radiat. Phys. Chem.* **2016,** *122*, 35-42.

30) Bai, R.K.; You, Y.Z.; Pan, C.Y. *Macromol. Rapid Commun.* **2001,** *22*, 315-319.

31) Bai, R.K.; You, Y.Z.; Zhong, P.; Pan, C.Y. *Macromol. Chem. Phys.* **2001,** *202*, 1970-1973.

32) Hong, C.Y.; You, Y.Z.; Ban, R.K.; Pan, C.Y.; Borjihan, G. *J. Polym. Sci. Part A: Polym. Chem.* **2001,** *39*, 3934-3939.

33) Barner, L.; Quinn, J.F.; Barner-Kowollik, C.; Vana, P.; Davis, T.P. *Eur. Polym. J.* **2003,** *39*, 449-459.

34) Kiani, K.; Hill, D.J.T.; Rasoul, F.; Whittaker, M.; Rintoul, L. *J. Polym. Sci. Part A: Polym. Chem.* **2007,** *45*, 1074–1083.

35) Chiu, K-P.; Liaw, H-H.; Tsay, R-Y. *J. Taiwan Inst. Chem. E.* **2016,** *61*, 1-11.

36) Zhao, Y.; Wang, M.; Tang, Z.; Wu, G. *Radiat. Phys. Chem.* **2010,** *79*, 429-433.

37) Khan, E.; Ahmad, S.R.; Kronfli, E. *Adv. Polym. Tech.* **2002,** *21*, 132-140.

38) Kodama, Y.; Barsbay, M.; Güven, O. *Radiat. Phys. Chem.* **2014,** *105*, 31-38.

39) Prescott, S.; Ballard, M.; Rizzardo E.; Gilbert, R. *Macromolecules* **2005,** *38*, 4901-4912.

40) Barsbay, M.; Kodama, Y.; Güven, O. *Cellulose* **2014,** *21*, 4067-4079.

41) Bhardwaj, Y.; Tamada, M.; Nho, Y-C.; Nasef, M.; Güven, O. *Harmonized Protocol for Radiation-Induced Grafting* **2014**, IAEA, Vienna.

42) Uzulina, I.; Kanagasabapathy S.; Claverie, J. *Macromol. Symp.* **2000,** *150,* 33-38.

43) Monteiro, M.J.; Hodgson M.; De Brouwer, H. *J. Polym. Sci., Part A: Polym. Chem.* **2000,** *38*, 3864-3874.

44) Haloi, D.J.; Mandal P.; Singha, N.K. *J. Macromol. Sci. Part A Pure Appl. Chem.* **2013,** *50*, 121-127.

45) Urbani, C.N.; Nguyen H.N.; Monteiro, M.J. *Aust. J. Chem.* **2006,** *59*, 728-732.

46) Luo, Y.; Cui, X. *J. Polym. Sci. Part A Polym. Chem.* **2006,** *44*, 2837-2847.

47) Hayek, A.; Xu, Y.; Okada, T.; Barlow, S.; Zhu, X.; Moon, J.H.; Marder, S.R.; Yang, S. *J. Mater. Chem.* **2008,** *18*, 3316-3318.

48) Benaglia, M.; Alberti, A.; Giorgini, L.; Magnoni, F.; Tozi, S. *Polym. Chem.* **2013,** *4,* 124-132.

49) Li, G.; Zhu, X.; Zhu, J.; Cheng, Z.; Zhang, W. *Polymer* **2005,** *46,* 12716-12721.

50) O'Driscoll, K.; Amin Sanayei, R. *Macromolecules* **1991,** *24*, 4479-4480.

51) Madrid, J.F.; Barsbay, M.; Abad, L.; Güven. O. *Radiat. Phys. Chem.* **2016,** *124*, 145-154.

52) Zulfiqar, S.; Zulfiqar, M.; Nawaz, M. *Polym. Deg. Stab.* **1990,** *30*, 195-203.

53) Ali, Z.I. *J. Appl. Polym. Sci.* **2006,** *103*, 3461-3469.

54) Monteiro, M.J. and de Brouwer, H. *Macromolecules* **2001,** *34*, 349–352.

55) Wojnarovits, L.; Foldvary, Cs.M.; Takacs, E. *Radiat. Phys. Chem.* **2010,** *79,* 848–862.

56) Ueki, Y.; Seko, N.; Hoshina, H. and Tamada, M. *J. Ion. Exch.* **2007,** *18,* 214-219.

57) Nasef, M.M.; Güven, O. *Prog. Polym. Sci.* **2012,** *37*, 1597–1656.

58) Ma, H.; Morita, K.; Hoshina, H.; Seko, N. *Mat. Sci. App.* **2011,** *2*, 777-785.

59) Sokker, H.; Badawy, S.; Zayed, E.; Eldien, F.; Farag, A. *J. Hazard. Mater.* **2009,** *168,* 137–144.

60) Pielichowski, K.; Nijuguna, J. *Thermal Degradation of Polymeric Materials* **2005,** Rapra Technology Limited, United Kingdom, 126.

CHAPTER 3

TOWARDS ENHANCED REACTIVITY AND ADSORPTION PERFORMANCE THROUGH RAFT-MEDIATED GRAFTING

3.1 INTRODUCTION

Rare earth elements (REEs) are group of metals that have received considerable attention because of their increasing requirements in many advanced applications, especially in clean energy production. Stable supply of REEs is important to answer the increasing demand and to continue further developments [1]. Consequently, the development of practical recovery methods with high efficiency is important to ensure stable supply of these elements.

The recovery processes for REEs usually involve precipitation, extraction and adsorption methods [2 – 5]. More recently, innovation leads to the modification of *E.coli* to produce an REE biosorbent that has increased effectiveness of adsorption [6]. Precipitation and solvent extraction are useful for large-scale operations involving solutions with high concentrations of metal ions. Adsorption, on the other hand, is a simple process that can be utilized in metal ion recovery even from dilute sources. In actual practice, the dissolved REEs are present in solutions that contain other metal ions, such as iron and copper, which also compete for the adsorption sites. Therefore, the adsorbent must have high selectivity for the REEs, in conjunction with other desirable properties such as robustness for repeated use, cost-effective, simple and environment-friendly preparation, and straightforward application.

Several metal ion adsorbents have been prepared through radiation-induced grafting [7 – 13]. The radiation-induced preparation pathway has the advantages such as low cost, simplicity, control over process, and the possibility of grafting monomers that are difficult to polymerize by conventional methods without residues of initiators or catalysts [14]. Radiation-induced graft polymerization in combination with reversible addition-fragmentation chain transfer (RAFT) process have been shown to be an effective approach for synthesizing polymeric materials with tailored and well-defined properties [7, 15 – 17]. Controlled graft copolymerization using radiation for initiation is typically a one-step method that allows the formation of stable bond

between the base polymer surface and grafted polymer under relatively mild conditions [18] and even with the use of monomer emulsion [19, 20]. RAFT polymerization is the only controlled free radical polymerization method that have been successfully applicable in conjunction with radiation-initiation [18]. Controlling the characteristics of radiation grafted polymer chains by RAFT-mediation is important in terms of efficiency and reproducibility [16], hence making it an important topic in preparation of functional materials, such as proton exchange membrane [16], functionalized membrane electrode [21, 22] and metal ion adsorbent [7].

In this chapter, we investigated the beneficial outcomes of adsorbent preparation in a controlled manner by RAFT-mediated grafting. Most processes for rare earth element extraction are generally performed in acidic solutions. The diglycol amic (DA) acid ligand was chosen because it has higher affinity for rare earth metal ions over base metal ions from dilute acidic solutions. We synthesized diglycol amic (DA) acid-modified adsorbents via RAFT-mediated γ-radiation induced grafting (as described in Chapter 3) and subsequent two-step post-grafting functionalization. The effects of RAFT-mediation in adsorbent preparation and in the adsorption of europium (Eu) and samarium (Sm) metal ions were discussed.

3.2 EXPERIMENTAL

3.2.1 Materials

The RAFT agent used in this study, 4-cyano-4-((phenylcarbonothioyl)thio) pentanoic acid (CPPA, > 97%), was purchased from STREM Chemicals, USA. Glycidyl methacrylate (GMA, >95.0%, TCI) was deinhibited by percolation through a column of activated basic alumina (Ecochrom) and then stored at 4 °C. The surfactant, polyoxyethylene sorbitan monolaurate (Tween 20), ethylenediamine (EDA, >99.0%), isopropanol (IPA, >99.7%), tetrahydrofuran (THF, HPLC grade, > 99.8%), dichloromethane (DCM, >95.0%), ethanol (> 99.5%), methanol (HPLC grade, > 99.8%), europium (Eu) and samarium (Sm) standard solutions (1000 ppm), sodium hydroxide (1M, NaOH) and hydrochloric acid acid (1M, HCl) were supplied by Kanto Chemical Co., Japan. The solvents dimethylsulfoxide (DMSO, >99.0%) and N,N'-dimethylformamide (DMF, >99.5%) were obtained from Wako Pure Chemical

Industries, Ltd., Japan while the diglycolic anhydride (DGA, >95.0%) was supplied by Tokyo Chemical Industry Co., Ltd., Japan. All reagents were used as received. Nonwoven fabrics with fibers made of polypropylene coated with polyethylene (PE/PP) were provided by Kurashiki Sen-I Kako Co. Okayama, Japan and were used as trunk polymers for the grafting experiments.

3.2.2 Irradiation and Graft Polymerization

In a conventional RAFT-mediated graft polymerization, PE/PP with 1 cm x 3 cm dimensions and a mass of approximately 0.02 g was mixed into each grafting mixture (~8 g) produced by homogenizing GMA, CPPA and Tween 20 in water at 6000 rpm. The polymerization mixture in glass vial capped with self sealing septum was connected to N_2 bubbling at room temperature for 10 minutes, and then placed in γ-irradiator chamber. After the graft polymerization was carried out at room temperature for the prescribed time, the polymerization was stopped by removing it from the ^{60}Co irradiation room. The PE/PP-g-PGMA was washed with THF overnight to remove free homopolymers and ungrafted GMA monomer. The PE/PP-g-PGMA was then dried to constant weight under vacuum at 35 °C. The degrees of grafting (*Dg*) of grafted PE/PP was calculated from the weight increase relative to the initial weight (equation 3.1), while the monomer conversion was determined gravimetrically (equation 3.2) after vacuum filtration, through a 0.45 μm PTFE membrane filter, of the polymerization mixture that was precipitated in five-fold volumes of methanol. The PGMA homopolymers on the PTFE membrane filter was dried initially in fume hood and then in a vacuum oven. The grafted PGMA on the PE/PP trunk material also added to the total conversion and was considered in the calculation. The experiments were repeated to check data precision and the maximum standard error (n=9) calculated was 2%. Gravimetric measurements were performed with a Sartorius CPA 225D model balance with a $\pm$0.01 mg sensitivity. Samples with 80 – 90% degrees of grafting were used in the preparation of the adsorbents.

$$Dg\,[\%] = \frac{w_g - w_o}{w_o} \times 100 \tag{3.1}$$

$$overall\ conversion\ [\%] = \frac{(w_g - w_o) + w_{free\ PGMA}}{w_{monomer}} \times 100 \tag{3.2}$$

In order to study the distinct features of PE/PP-g-PGMA prepared using γ-ray initiated RAFT-mediated grafting in emulsion state, the reactivity of the grafted samples was compared with those prepared using conventional grafting (i.e. without RAFT agent). Direct γ-irradiation of PE/PP in monomer emulsion that was prepared without the RAFT agent resulted in samples with very low *Dg* [19]. Hence, an alternative grafting procedure was used to produce PE/PP-g-PGMA polymers that have similar *Dg* values with the samples prepared using RAFT mediation. The PE/PP substrates were grafted with PGMA through the conventional electron beam-induced graft polymerization in emulsion and the details were discussed in Chapter 2.

3.2.3 EDA and DA Functionalization Reactions

The functionalization reactions that lead to the immobilization of diglycol amic acid ligands on PE/PP are summarized in Figure 3.1. The effects of temperature and RAFT-mediation in the amount of introduced EDA groups, and the effects of solvents and reaction time in the amount of imparted diglycol amic acid ligands were systematically studied. At least three samples were subjected to each reaction condition and the average of each set was reported.

The precursor amino functional groups were introduced to the PE/PP-g-PGMA by ring-opening reaction of the epoxide groups with EDA. PE/PP-g-PGMA samples were added in a glass reactor vessel that contains 50 g of EDA in aqueous isopropanol (50% wt/wt). The amination reaction was carried out for 30 minutes in a thermostatic water bath at 60 °C. The EDA functionalized PE/PP-g-PGMA was washed extensively with methanol and then dried overnight in a vacuum oven at 35 °C. The EDA group density was calculated using equation 3.3:

$$EDA\ group\ density\ [mmol/gram-adsorbent] = \left(\frac{w_f - w_g}{w_f}\right) \times \frac{1000}{MW} \qquad (3.3)$$

where w_g and w_f are the weights of PE/PP-g-PGMA before and after functionalization, respectively, and *MW* is the molar mass of EDA.

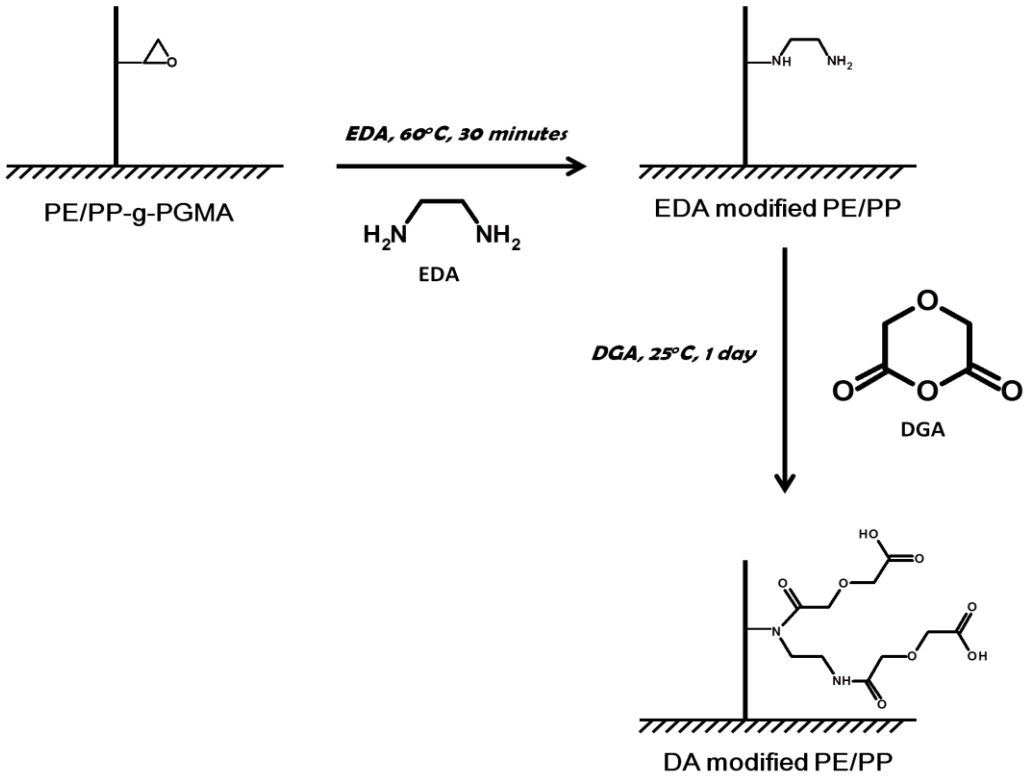

Figure 3.1 Preparation of DA modified PE/PP

The ligand diglycol amic acid (DA) was imparted to the EDA functionalized PE/PP-g-PGMA using modified reaction conditions that were adopted from Ogata *et al*., (2014) [23]. Approximately 0.5 g of diglycolic anhydride was added into 6 mL dichloromethane and the mixture was mixed for an hour. Afterwards, a 1 x 1 cm^2 EDA functionalized PE/PP-g-PGMA was added into the DA mixture. After stirring the reaction mixture at room temperature for a day, the DA functionalized PE/PP-g-PGMA was removed, then washed repeatedly with DCM and ethanol to remove the unreacted diglycolic anhydride and DCM, and finally washed in water with stirring for 4 hours. The DA functional group density on the modified PE/PP was calculated using equation 3.4:

$$diglycol\ amic\ acid\ \ group\ density\ [mmol/gram-adsorbent] = \left(\frac{w_d - w_f}{w_d}\right) \times \frac{1000}{MW} \qquad (3.4)$$

where w_f and w_d are the weights of EDA functionalized PE/PP-g-PGMA before and after reaction with DGA, respectively, and *MW* is the molar mass of DGA.

3.2.4 Characterization of grafted and functionalized polymers

The infrared spectra of PE/PP-g-PGMA, EDA and DA-modified PE/PP-g-PGMA were examined by a Perkin Elmer Spectrum One Fourier Transform Infrared (FTIR) spectrophotometer in attenuated total reflectance (ATR) mode. The samples were scanned in the range 650-4000 cm^{-1} with a resolution of 4 cm^{-1}.

Scanning electron microscopy (SEM) images and oxygen elemental maps were taken using a Hitachi SU 3500 (Hitachi, Japan) scanning electron microscope equipped with an energy dispersive x-ray spectrometer (X-Max, Horiba). Pictures of the fibers' surfaces were acquired at low vacuum condition and acceleration voltage of 5 kV while the oxygen and nitrogen elemental maps were taken at 8.5 kV.

X-ray photoelectron spectra (XPS) were recorded on a PHI 5000 Versa Probe II Scanning XPS Microprobe with monochromatic Al Kα X-ray source (1486.6 eV photons) at pass energy of 29 eV for high-resolution scan spectra and 117 eV for survey scan spectra. An anode current of 3.0 mA was applied. The pressure in the analysis chamber was established at 1 x 10^{-6} Pa or lower during each analysis. The samples were fixed on the sample holder by means of indium and carbon adhesive tapes. The core level signals were measured at the photoelectron takeoff angle of 45°. All binding energies (BE) were referenced to the C1s hydrocarbon peak at 284.8 eV. Surface elemental stoichiometries were determined from peak-area ratios, after correcting with experimentally determined sensitivity factors as set by the instrument manufacturer.

4.2.5 Batch adsorption

Eu and Sm solutions were prepared by diluting the metal ion standards in deionized water. The DA functionalized PE/PP-g-PGMA adsorbent was added to each 25-mL metal ion solution. The batch adsorption studies were conducted in a continuously stirring batch process at room temperature. After 24 hours, the DA functionalized adsorbent was removed and the solution was filtered through a 0.45 μm syringe filter. The metal ion concentration was measured before and after adsorption using inductively-coupled plasma optical emission spectrometry (ICP-OES) (Perkin Elmer Optima 8300, Japan). The amount of adsorbed metal ion was calculated according to equation 3.5:

$$q_e[mg/g] = \frac{(C_o - C_e) \times V}{M} \quad (3.5)$$

where q_e (mg/g) is the amount of metal ion adsorbed per unit mass of adsorbent, C_o and C_e are the initial and final concentration (ppm) of Eu in aqueous phase, respectively, V (L) is the volume of solution and M (g) is the mass of DA functionalized PE/PP-g-PGMA. The adsorption experiments were performed at least twice.

The distribution coefficient (D), which is a useful indication on the degree of affinity of an adsorbent, was defined and calculated using equation 3.6:

$$\mathrm{D} = \frac{(mg\ M^{n+}/g\ of\ dry\ adsorbent)}{(mg\ M^{n+}/mL\ of\ solution)} \quad (3.6)$$

3.2.6 Column adsorption

The adsorbent for column adsorption study was prepared by cutting the DA-modified PE/PP-g-PGMA into 7-mm circular discs. The discs were then packed into a laboratory scale column (7 mm internal diameter). Polyethylene fibers and pristine PE/PP polymers were used to hold the packed adsorbent in place. Metal ion feed solutions were prepared by diluting Eu and Fe standard solutions. The initial pH of the feed solutions was adjusted to 2.50 using a 1M HCl solution. The feed solution was supplied to the column using a peristaltic pump (PSM071AA, Advantec, Japan) and the column effluent solutions were collected by a fraction collector (CHF122SB, Advantec, Japan). The metal ion concentration of the collected fractions was measured using inductively-coupled plasma optical emission spectrometry (ICP-OES, Perkin Elmer Optima 8300, Japan). The relative concentrations (C/C_o) of the effluent solutions were plotted against the column effluent volume, expressed in bed volumes (BV).

3.3 RESULTS AND DISCUSSION

3.3.1 Influence of temperature and reaction time in the amination reaction

The RAFT-mediated radiation-induced graft polymerization of emulsified GMA from PE/PP resulted in grafted polymers with tunable *Dg* and controllable molecular weight [19, 20]. In the present study, we showed experimentally the differences in reactivity and adsorption behavior of functionalized PE/PP-g-PGMA that were prepared with RAFT-mediation from those synthesized using conventional radiation-induced grafting.

Figure 3.2 shows the conversion data at different reaction times and temperatures for the amination reaction between the epoxide groups of graft PGMA and ethylenediamine. As expected, longer reaction time resulted in higher epoxide group conversion because more EDA molecules were able to diffuse into the graft polymer chains and react with the epoxide groups. At 40 °C the calculated conversion values for the amination reaction of PGMA chains from the two samples were distinctly different: PE/PP-g-PGMA samples prepared with RAFT-mediation have higher conversion values than the conventionally synthesized PE/PP-g-PGMA, regardless of EDA concentration and reaction time. The RAFT-mediated and conventionally prepared samples have similar Dg values, hence both samples contain the same amount of PGMA graft chains. It has been established that the PGMA graft chains that were prepared using RAFT-mediation have better molecular weight dispersity than those prepared via the conventional method [14, 17, 19]. Because both grafted polymer substrates have similar Dg, the higher conversion values obtained from the reaction of EDA molecules with the graft PGMA chains that were prepared with RAFT mediation may be attributed to the properties of its graft chains, e.g. better dispersity.

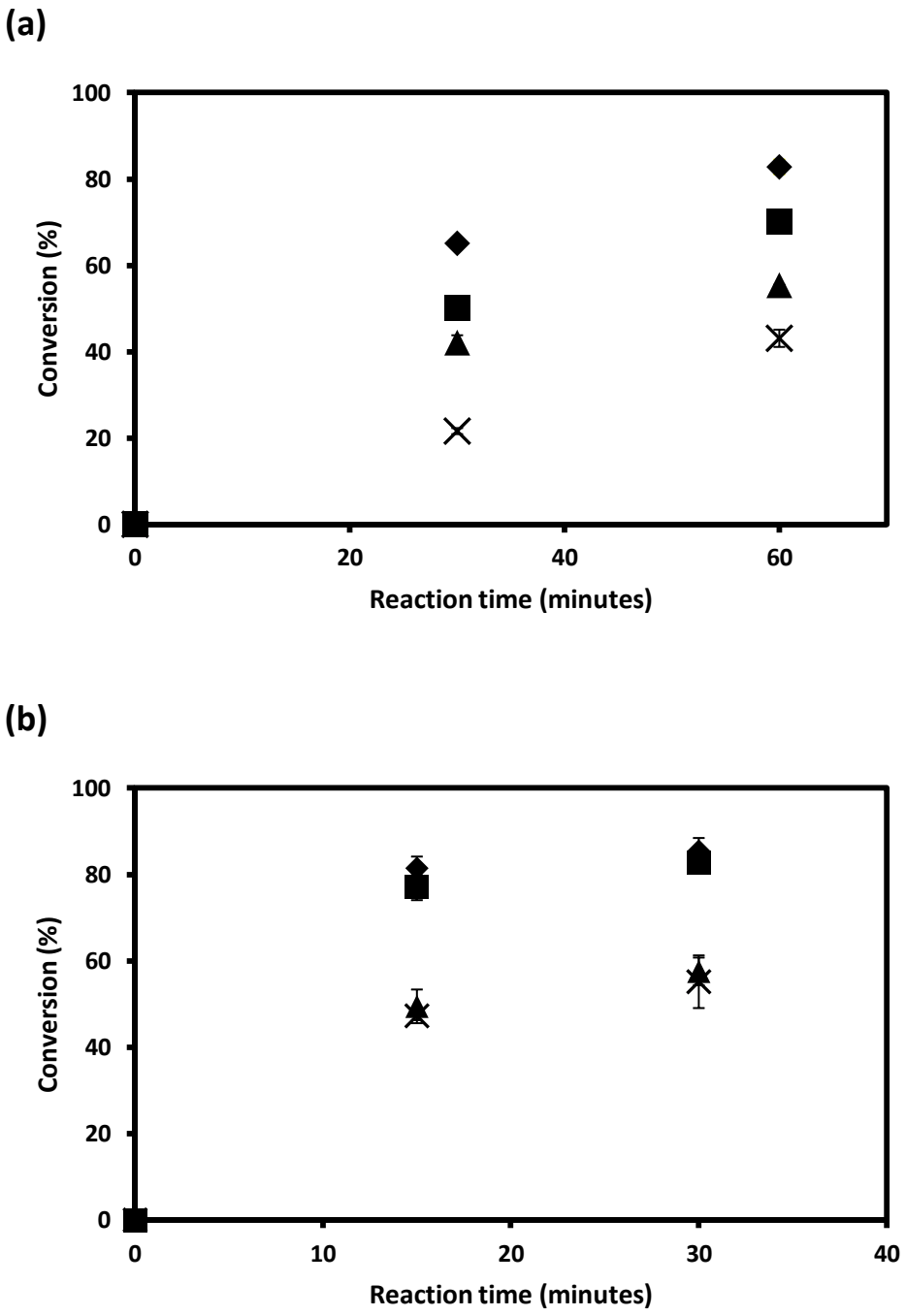

Figure 3.2 Conversion plots for the ring-opening reaction of the epoxide groups from graft PGMA with ethylenediamine at (a) 40 °C and (b) 60 °C: 50% EDA reaction with PE/PP-g-PGMA prepared with RAFT agent (♦), without RAFT agent (■), and 25% EDA reaction with PE/PP-g-PGMA prepared with RAFT agent (▲), without RAFT agent (**x**), 3 trials.

Post-grafting modification of narrowly dispersed PGMA graft chains, which were prepared via atom transfer radical polymerization (ATRP), with small molecules have been shown to result in homogeneous distribution of the small molecules throughout the graft chains, with the observed enrichment of the top layer, due to the better contact between the epoxide group in the top layer and the modifying solution [24]. Their data suggest that top layer has higher degree of interaction with the molecules in the solution compared with the lower portion of the graft chains. RAFT-mediated graft polymerization produces graft chains with narrow dispersity, similar to ATRP polymerization, hence their contact with the EDA molecules in the solution may be assumed to be uniform across the whole grafted fiber surface. On the contrary, modification of graft chains that have wide molecular weight distribution by reaction with EDA solution might have resulted in non-homogeneous interaction of the EDA molecules with the epoxide groups of the different graft chains because of the uneven lengths of the PGMA graft chains, especially at temperatures below the glass transition temperature of PGMA, resulting in an overall lower conversion observed in Figure 3.2a. The top layer of the longer PGMA chains have higher probability of being modified by the EDA solution compared to the shorter PGMA chains, analogous to the enrichment of the topmost layer of graft chains with narrow molecular weight distribution.

At 60 °C, almost similar conversion values were calculated for both RAFT-mediated and conventionally prepared graft polymers, indicating that the PGMA graft chains that were synthesized using the two different methods have similar reactivity towards EDA at this temperature. The glass transition temperature of the graft PGMA depends on its molecular weight and was found to have values between 60 – 80 °C [19, 25]. Hence at 60 °C, the PGMA chains have more mobility and can react more readily with the EDA molecules in the solution. This property, together with the increased kinetic energy of the EDA molecules resulted in similar conversion values, regardless of the mode of synthesis and initial dispersity of the graft PGMA chains. Considering the shorter contact time required for the achieving the same conversion of epoxide to amino groups, the following conditions were employed in the succeeding amination reactions of PE/PP-g-PGMA synthesized with RAFT mediation: 50% EDA concentration, 60 °C reaction temperature and 30 minutes reaction time. These conditions yielded EDA modified RAFT mediated PE/PP-g-

PGMA with ethylenediamine functional group density of approximately 2.0 mmol $gram^{-1}$.

3.3.2 Influence of solvent in the reaction of aminated PE/PP with diglycolic anhydride

The subsequent reaction of EDA modified PE/PP-g-PGMA and diglycolic anhydride in DCM yielded diglycol amic acid modified PE/PP-g-PGMA with approximately 1.8 mmol $gram^{-1}$ diglycol amic acid (DA) functional group density after 1 day reaction time, as shown in Figure 3.3. This ligand group density is 80% higher and achievable in a third of the reaction time compared with the values reported by Ogata *et al*. (2014), wherein they prepared diglycol amic acid modified silica gels from the reaction of aminated silica gel particles and diglycolic anhydride for 3 days [23]. The faster reaction kinetics and higher group density may be attributed to the fibrous nature of the PE/PP-g-PGMA, which has fiber diameter less than 20 μm. This value is typically lower than most functionalized silica gels and resins, making the diffusion rate of diglycolic anhydride into the fiber surface higher than its spherical silica gel counterpart.

Dichloromethane yielded the highest DA group density among the solvents studied (Figure 3.3). All three solvents are classified as polar aprotic, with DCM being less polar than DMSO and DMF [26]. Use of the less polar DCM as solvent lead to a more favorable interaction of diglycolic anhydride with the grafted polymer, because both the PE/PP trunk polymer and PGMA graft chains are non-polar in nature. This resulted in better contact between the dissolved digylcolic anhydride and immobilized EDA groups to give the diglycol amic acid ligands. For the succeeding experiments, the DA modified PE/PP-g-PGMA were prepared in DCM for 1 day.

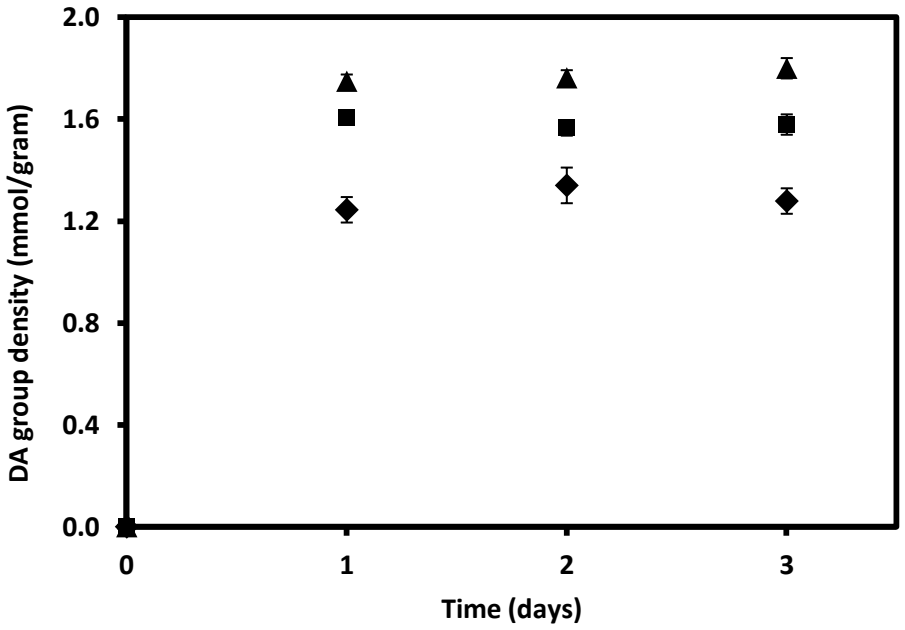

Figure 3.3 Diglycol amic acid (DA) group density resulting from the reaction of the EDA modified PE/PP-g-PGMA with diglycolic anhydride in different solvents as function of reaction time. EDA group density: 2.0 mmol gram^{-1}, room temperature, solvents: dichloromethane (▲), dimethylsulfoxide (■), dimethylformamide (♦), 3 trials.

3.3.3 Characterization of grafted and functionalized polymers

3.3.3.1 FTIR Analysis

Figure 3.4 shows the FTIR spectra of the grafted and functionalized polymeric materials. The PE/PP-g-PGMA exhibited the typical peaks characteristic of both the trunk polymer (CH_2 symmetric and asymmetric stretching vibrations at 2848 and 2915 cm^{-1}, respectively, and CH_2 bending vibrations at 1470 cm^{-1}) and PGMA graft chains (C=O stretching vibration at 1720 cm^{-1}, C-O stretching vibration at 1100 cm^{-1}, and the oxirane/epoxide group vibrational modes at around 1250, 900 and 850 cm^{-1}). Post-grafting modification with EDA resulted in the ring opening reaction of the epoxide groups and introduction of EDA groups. The FTIR spectrum of EDA modified PE/PP-g-PGMA supports this statement. The epoxide ring opening reaction lead to the disappearance of the epoxide group vibrations, and the introduction of the EDA groups resulted in the appearance of new peaks at 3300 cm^{-1} and 1550 cm^{-1}, corresponding to the NH_2 stretching and bending vibrations, respectively. The EDA modified PE/PP-g-PGMA was further reacted with diglycolic anhydride to produce

the adsorbent bearing the diglycol amic acid ligands (Figure 3.1). The DA-modified PE/PP-g-PGMA exhibited broadening of the peak located at around 3100 cm^{-1}, corresponding to the introduced carboxylic acid functional group from diglycol amic acid. Moreover, a new broad peak appeared at around 1600 cm^{-1}, which is attributed to the amide vibrational mode. These features indicate that the diglycol amic acid ligands were successfully imparted to the PE/PP-g-PGMA.

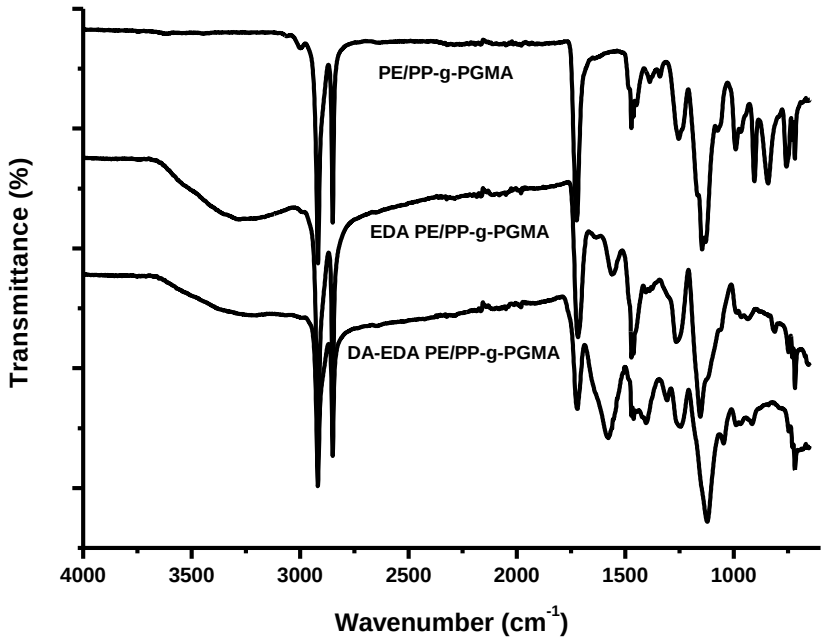

Figure 3.4 FTIR-ATR spectra of PE/PP-g-PGMA, ethylenediamine modified PE/PP-g-PGMA and diglycolic anhydride modified PE/PP-g-PGMA.

3.3.3.2 XPS Analysis

Survey wide scans of the ethylenediamine and diglycolic anhydride modified PE/PP-g-PGMA polymers are shown in Figure 3.5. The surface elemental compositions, which were determined from peak areas of the XPS spectra, are given as insets in the survey scans. Both pristine and grafted PE/PP did not show nitrogen peak in their XPS survey scans [19]. The N1s peak at around 399 eV appeared after the amination reaction of PE/PP-g-PGMA with EDA. This peak was retained, though its intensity was decreased, after the reaction of the EDA modified PE/PP-g-PGMA with diglycolic anhydride. This observation was expected from the structure of the

immobilized diglycol amic acid ligand, which was tethered to the PE/PP through the EDA groups as shown in Figure 3.1. The %N decreased from 6% to 3% after the reaction with diglycolic anhydride because the added diglycol amic acid ligand comprises of carbon, hydrogen and oxygen, resulting in the dilution of nitrogen on the surface of the fibers.

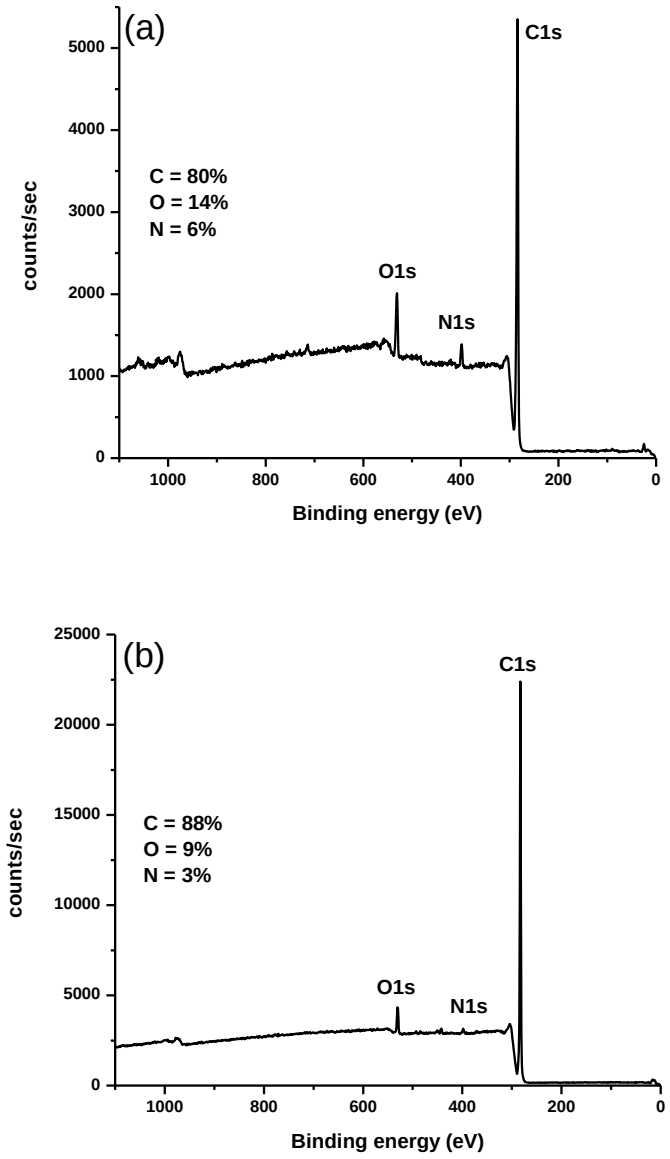

Figure 3.5 Surface elemental composition based from XPS survey wide scan spectra of (a) ethylenediamine modified PE/PP-g-PGMA and (b) diglycolic anhydride modified PE/PP-g-PGMA.

3.3.3.3 SEM-EDX Analysis

The surface morphologies of the pristine PE/PP and PE/PP-g-PGMA, which was prepared through RAFT-mediated γ-radiation induced graft polymerization, are shown in Chapter 2. In summary, the grafted fibers were noticeably thicker and have higher oxygen density than the pristine trunk polymer. Figure 3.6 shows the SEM pictures and EDX oxygen and nitrogen elemental maps of the grafted and functionalized polymeric materials.

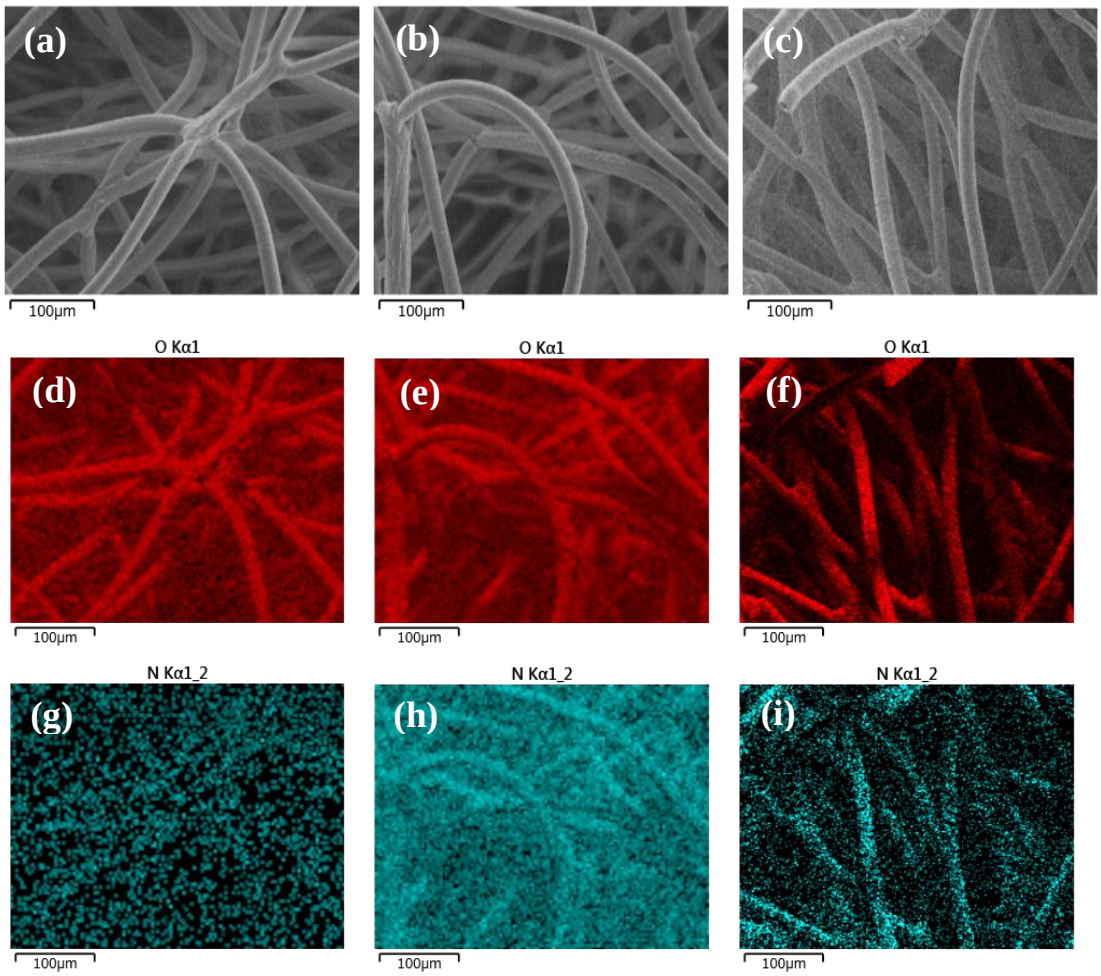

Figure 3.6 SEM images, oxygen and nitrogen elemental maps of PE/PP-g-PGMA (a, d, g), ethylenediamine modified PE/PP-g-PGMA (b, e, h) and diglycolic anhydride modified PE/PP-g-PGMA (c, f, i).

The PE/PP-g-PGMA did not degrade after the amination and diglycolic anhydride reactions, as demonstrated in Figures 3.6b and 3.6c, which shows the modified polymer fibers. Figure 3.6g shows that the pristine PE/PP has almost no nitrogen atoms on its surface, which is consistent with its olefinic nature. The reaction of EDA with the epoxide groups in the PGMA chains of PE/PP-g-PGMA resulted in the attachment of amino functional groups. The nitrogen atoms from the imparted EDA groups are evidently visible in the nitrogen elemental map of the EDA modified PE/PP-g-PGMA (Figure 3.6h). Moreover, the EDA groups that served as attachment points for the diglycol amic acid ligands were preserved after the diglycolic anhydride treatment of the EDA modified PE/PP-g-PGMA, as shown in Figure 3.6i. These images and elemental maps, together with infrared and x-ray photoelectron survey scan spectra discussed above, showed that the functionalization reactions were successfully carried out.

3.3.4 Adsorption experiments

In order to investigate the rare earth adsorption behavior of RAFT-mediated and conventionally prepared DA-modified adsorbents, batch adsorption experiments were carried out using acidic solutions of 5 ppm Eu or Sm at room temperature. The adsorption experiments were performed in acidic solutions because the hydrometallurgical processing of rare earth metals from ores is normally carried out in acidic conditions. Both RAFT-mediated and conventionally prepared adsorbents were prepared from grafted polymers with similar degree of grafting values (around 80%) and DA functional group density (1.8 mmol $gram^{-1}$). The relative amounts of rare earth metal ion removed by the adsorbents at different pH values are plotted in Figure 3.7. A striking feature of the plot is the higher Eu and Sm percentage adsorption exhibited by the adsorbent prepared with RAFT-mediation from solutions with initial pH values of 4 and 5. At these pH values, the relative amount of Eu and Sm removed by the adsorbent prepared with RAFT mediation exceeded the conventionally prepared adsorbent by more than 20%. This remarkable characteristic corroborates with the earlier observation made above in the discussion of the amination of grafted polymers. The adsorption data suggests that the better molecular weight distribution imparted by grafting in the presence of the RAFT agent lead to a more efficient

contact between the diglycol amic acid ligands in the adsorbent and the rare earth metal ions in the solution, resulting in higher amount of rare earth metal ion adsorbed.

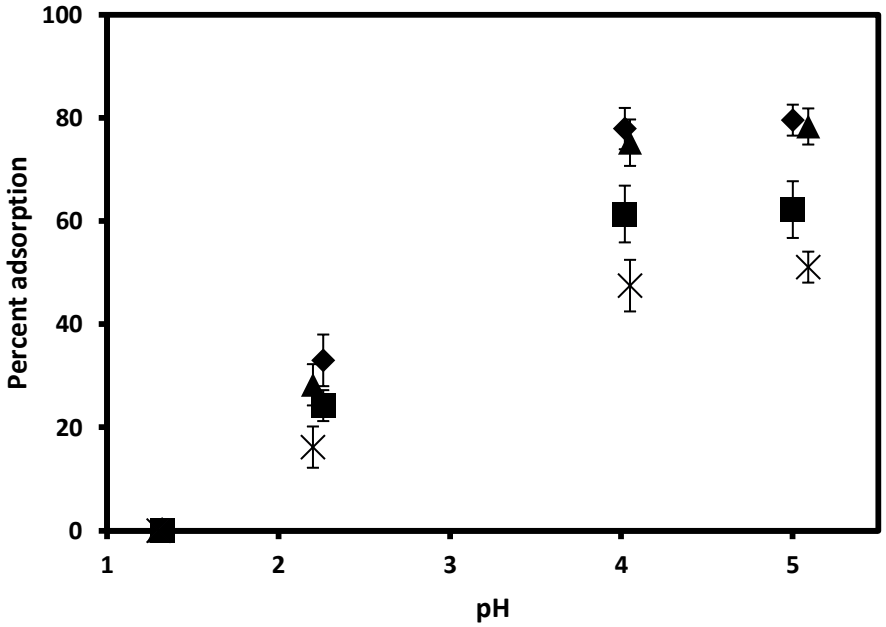

Figure 3.7 pH dependence of Eu and Sm adsorption on the diglycolic anhydride modified PE/PP-g-PGMA. Mass of adsorbent: 15 mg; volume of Eu/Sm solution: 25 mL; initial concentration of metal ions: 5 ppm; Eu adsorption using adsorbent prepared with RAFT-mediation (◆) and without RAFT-mediation (■); Sm adsorption using adsorbent prepared with RAFT-mediation (▲) and without RAFT-mediation (**x**); 2 trials.

Even at pH 2.20, the enhancement in adsorption performance brought by RAFT-mediation can be clearly observed, although not as high as the 20% improvement seen at pH 4 and 5. However, at pH less than 1.50, all of the prepared adsorbent showed almost no metal ion uptake. This observation is contrary to the data reported by Ogata *et al*. (2014) wherein they obtained appreciable adsorption from solutions with pH 1.0 [23]. Nonetheless, all the obtained results confirm the beneficial effects of RAFT-mediation in adsorbent preparation, in addition to the environmental gain from the radiation-induced graft polymerization in emulsion phase. It must be noted that Eu and Sm batch adsorption experiments were also performed using RAFT-mediated PE/PP-g-PGMA and aminated PE/PP-g-PGMA. The results indicate

that the grafted PE/PP did not adsorb quantifiable amounts of Eu or Sm, while the aminated PE/PP-g-PGMA only removed less than 15% of the Eu and Sm from the 5 ppm solutions at pH 5.

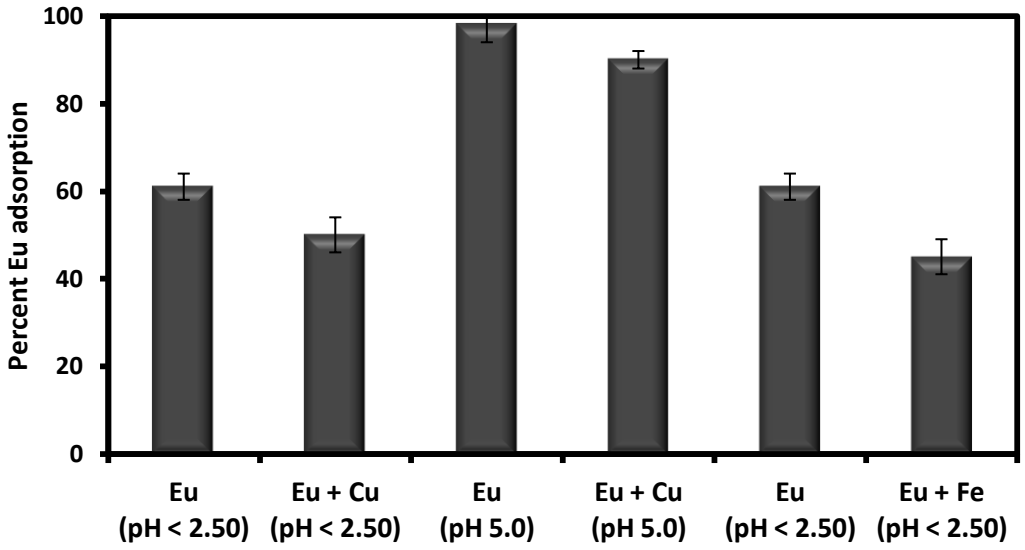

Figure 3.8 Effect of competing Cu and Fe ions on Eu adsorption by the DA modified PE/PP-g-PGMA prepared with RAFT-mediation. Mass adsorbent: 15 mg; volume of metal ion solution: 25 mL; initial concentration of metal ions: 1 ppm; 2 trials.

Table 3.1 Distribution coefficients (D) for the indicated metal ions.

Metal ions	**Eu/Cu, pH 2.20**		**Eu/Cu, pH 5**		**Eu/Fe, pH 2.20**	
	Eu	**Cu**	**Eu**	**Cu**	**Eu**	**Fe**
D	1.5×10^3	0	1.1×10^4	3.0×10^3	1.1×10^3	1.3×10^2

In an actual recovery process of rare earth metals, the target element normally exists with other metals, such as copper or iron. Hence, a practical adsorbent must be able to selectively remove the target metal. Moreover, its performance must not be significantly affected by the presence of other metal ions. Figure 3.8 shows the dependence of Eu adsorption on the presence of Cu and Fe ions at two pH values. The Eu adsorption of the adsorbent did not decrease appreciably in the presence of Cu and Fe ions in solutions with 2.20 and 5.0 pH values. Moreover, at pH 2.20, only Eu was selectively adsorbed (50% adsorption) from the solution and almost no Cu was removed. The adsorbent, however, adsorbed Cu ions at pH 5.0 but it maintained its

selectivity for Eu over Cu even at higher pH, removing 90% Eu and 69% Cu from the 1 ppm solution. In the presence of Fe at pH 2.20, the adsorbent selectively removed Eu, at almost 50% adsorption, while the Fe concentration in the solution was only decreased by 9%. Fe precipitates at pH higher than 3.5 so the adsorption experiment with Fe as competing ion was only performed at pH 2.20. The selectivity of the synthesized adsorbent for Eu over Cu and Fe in solutions with different pH values is also evident from the calculated distribution coefficients (Table 3.1). The calculated D for Eu was >3 times higher than Cu at pH 5 and almost 10 times higher than Fe at pH less than 2.5. The higher selectivity for Eu is believed to be because of the tridentate nature of the diglycol amic acid ligand [23, 27].

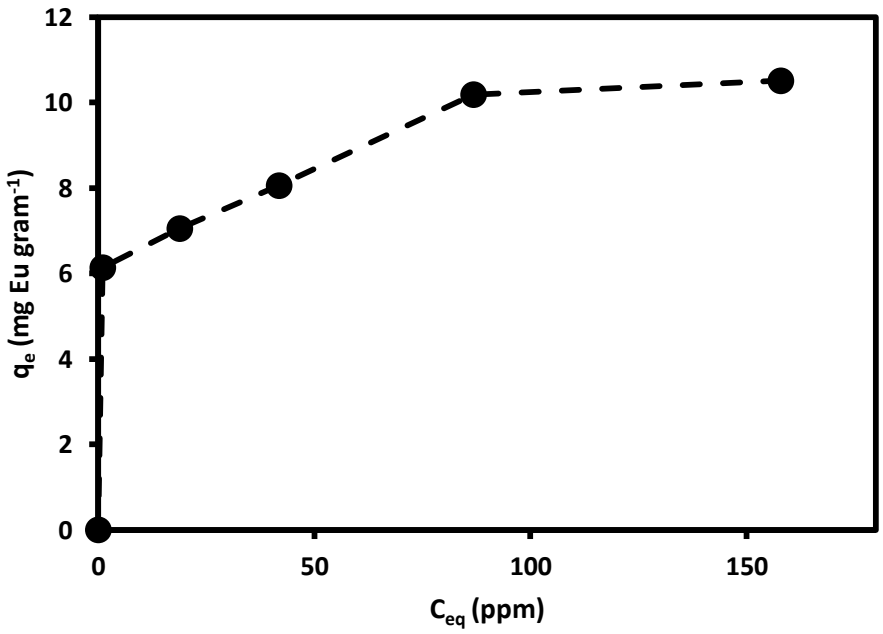

Figure 3.9 Adsorption isotherm of Eu on DA modified PE/PP-g-PGMA at 25 °C. Mass adsorbent: 15 mg; initial pH: 2.20, volume of Eu solution: 25 mL; time: 24 hours.

The adsorption isotherm of Eu on the DA modified PE/PP-g-PGMA, which was prepared with RAFT mediation, at 25 °C is shown in Figure 3.9. An experimental adsorption capacity of 10 mg Eu per gram adsorbent was observed from the adsorption isotherm plot. The data from Figure 3.9 were fitted into Langmuir and Freundlich models, two of the most commonly used models to describe adsorption

isotherms and predict equilibrium distribution of the adsorbate. The data were fitted into Langmuir and Freundlich models, and the results of least squares fitting yielded coefficient of determination (R^2) values of 0.993 and 0.852, respectively. The results indicate that the adsorption of Eu on the DA-modified PE/PP-g-PGMA follows the Langmuir model and a theoretical adsorption capacity of 10.9 mg Eu per gram adsorbent, based from the Langmuir model, was calculated. The calculated theoretical adsorption capacity is almost similar to the experimentally determined adsorption capacity.

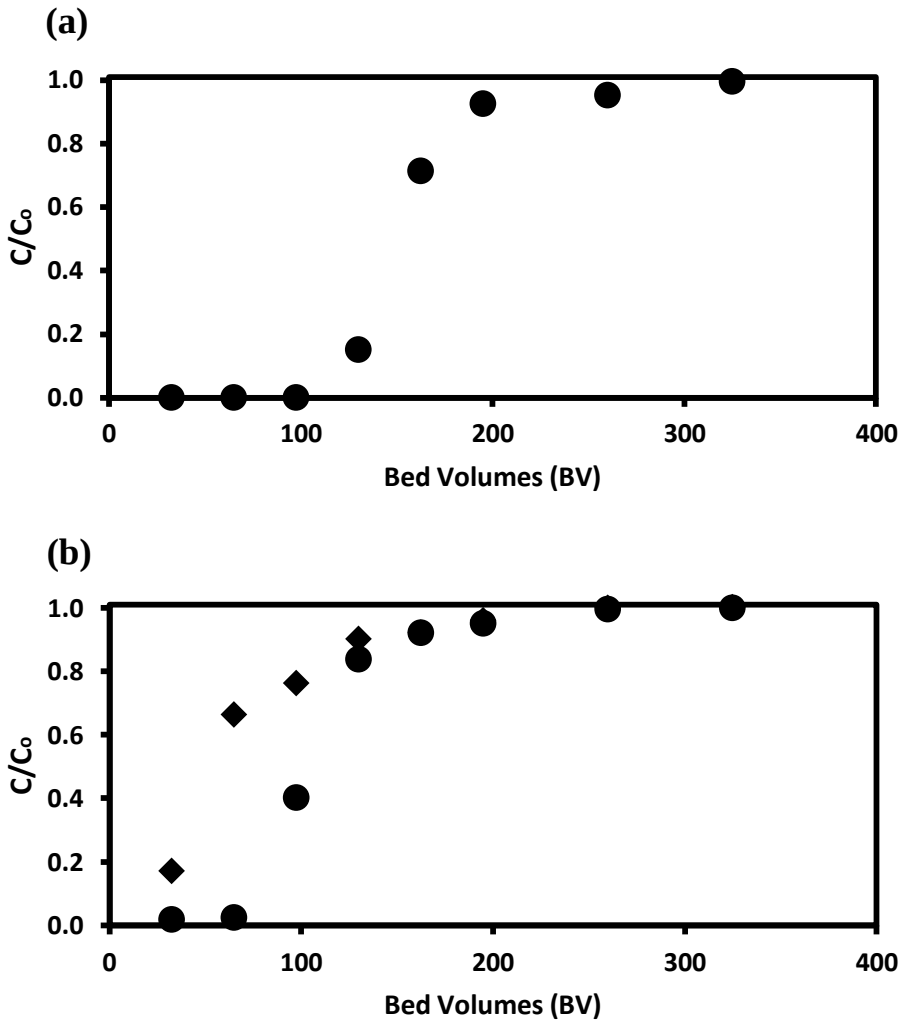

Figure 3.10 Plot of effluent relative concentration against effluent volume, in BV, for the column mode adsorption of (a) Eu, and (b) Eu (●) and Fe (◆) using DA modified PE/PP-g-PGMA. Adsorbent: 26.9 mg, 4 mm height, 7 mm diameter; space velocity 250 $hour^{-1}$; Eu and Fe initial concentration: 1 ppm.

The performance of the DA-modified PE/PP-g-PGMA adsorbent in removing Eu via column mode adsorption is demonstrated in Figure 3.10. A 26.9 mg packed adsorbent was able to treat more than 100 BV of 1 ppm Eu (Figure 3.10a) before reaching $C/C_o = 0.1$. Afterwards, the effluent concentration increased until it reached $C/C_o = 1.0$, i.e. saturated adsorbent, at more than 325 BV. The DA-modified adsorbent exhibited selectivity for Eu over Fe in the column adsorption test, as shown in Figure 3.10b. After 65 BV, the relative concentrations of Eu and Fe in the effluent solution were 0.03 and 0.66 respectively, indicating that the adsorbent has higher affinity for Eu than Fe. The high selectivity of the adsorbent for the rare earth element Eu over the Fe ion based from the column experiments agree with the batch adsorption data presented above, and with other studies which also utilized the diglycol amic acid ligand [23, 27].

3.4 CONCLUSIONS

A graft copolymer with improved reactivity and adsorption performance was synthesized using radiation-induced graft polymerization and subsequent post-grafting reactions. The PGMA graft chains from the PE/PP-g-PGMA that was prepared in emulsion phase through radiation-induced RAFT-mediated graft polymerization showed higher reactivity towards amination reaction at 40 °C compared to the conventionally prepared grafted PE/PP. At 60 °C, the grafted polymer prepared using the two methods exhibited similar reactivity. The fibrous nature of aminated PE/PP-g-PGMA lead to the faster kinetics in the diglycolic anhydride reaction, resulting in diglycol amic acid ligands immobilized on PE/PP with 1.8 mmol $gram^{-1}$ functional group density. The DA modified PE/PP-g-PGMA prepared with RAFT mediation showed higher Eu and Sm adsorption percentage than the DA adsorbent prepared using conventional grafting. The DA modified PE/PP-g-PGMA exhibited selectivity for Eu over Cu and Fe in acidic solutions. The introduction of RAFT polymerization in the DA-modified adsorbent preparation process enhanced the reactivity and performance in terms of Eu and Sm adsorption. The synthesized adsorbent shows high potential for rare earth recovery applications.

3.5 REFERENCES

1) Fernandez, V. *Resources Policy* **2017,** *53*, 26-45.
2) Kubota, F.; Goto, M.; Nakashio, F. *Solvent Extr. Ion Exch.* **1993,** *11*, 437–453.
3) Lee, G.S.; Uchikoshi, M.; Mimura, K.; Isshiki, M. *Sep. Purif. Technol.* **2010,** *71*, 186–191.
4) Innocenzi, V.; Vegliò, F. *J. Power Sources* **2012,** *211*, 184–191.
5) Baba, Y.; Fukami, A.; Kubota, F.; Kamiya, N.; Goto, M. *RSC Adv.* **2014,** *4*, 50726–50730.
6) Hosomomi, Y.; Wakabayashi, R.; Kubota, F.; Kamiya, N.; Goto, M. *Biochemical Engineering Journal* **2016,** *113*, 102-106.
7) Barsbay, M.; Kavakli, P.A.; Tilki, S.; Kavakli, C.; Guven, O. *Radiation Physics and Chemistry* **2017**, DOI: 10.1016/j.radphyschem.2017.03.037.
8) Madrid, J.F.; Lopez, G.E.P, Abad, L.V. *Radiat. Phys. Chem.* **2017c,** *136,* 54-63.
9) Kavakli, P.A.; Kavakli, C.; Seko, N.; Tamada, M.; Güven, O. *Radiat. Phys. Chem.* **2016,** *127*, 13-20.
10) Madrid, J.; Ueki, Y.; Seko, N. *Radiat. Phys. Chem.* **2013,** *90*, 104-110.
11) Seko, N.; Ninh, N.; Tamada, M. *Radiat. Phys. Chem.* **2010,** *79*, 22-26.
12) Ueki, Y.; Seko, N.; Hoshina, H,; and Tamada, M. *J. Ion Exch.* **2007,** *18*, 214-219.
13) Seko, N.; Katakai, A.; Tamada, M.; Sugo, T.; and Yoshii, F. *Separation Science and Technology* **2004,** *39*, 3753-3767.
14) Barsbay, M.; Güven, O. *Polymer* **2013,** *54*, 4838-4848.
15) Akbulut, M.; Barsbay, M.; Guven, O. *Radiation Physics and Chemistry* **2017,** DOI: 10.1016/j.radphyschem.2017.01.041.
16) Celik, G.; Barsbay, M.; and Guven, O. *Polymer Chemistry* **2016,** *7*, 701-714.
17) Kodama, Y.; Barsbay, M.; Güven, O. *Radiat. Phys. Chem.* **2014,** *94*, 98-104.
18) Barsbay, M.; Guven, O. *Radiation Physics and Chemistry* **2009,** *78*, 1054-1059.
19) Madrid, J.F.; Ueki, Y.; Abad, L.V.; Yamanobe, T.; Seko, N. *Journal of Applied Polymer Science* **2017a,** *134,* 45270.
20) Madrid, J.F.; Abad, L.V.; Yamanobe, T.; Seko, N. *Colloid and Polymer Science* **2017b,** *295,* 1007-1016.

21) Barsbay, M.; Guven, O.; Bessbousse, H.; Wade, T.L.; Beuneu, F.; Clochard, M.-C. *Journal of Membrane Science* **2013,** *445,* 135-145.

22) Barsbay, M.; Guven, O. *Radiation Physics and Chemistry* **2014,** *105,* 26-30.

23) Ogata, T.; Narita, H.; and Tanaka, M. *Chem. Lett.* **2014,** *43,* 1414-1416.

24) Barbey, R.; Laporte, V.; Alnabulsi, S.; and Klok, H.A. *Macromolecules* **2013,** *46,* 6151-6158.

25) Celik, S.U., Bozkurt, A. *European Polymer Science* **2008,** *44,* 213-218.

26) Solangi, I.B.; Bhatti, A.A.; Qazi, M.A.; Memon, S.; and Bhanger, M.I. *Pak. J. Anal. Environ. Chem.* **2012,** *13,* 129-136.

27) Ogata, T.; Narita, H.; Tanaka, M.; Hoshino, M.; Kon, Y.; Watanabe, Y. *Separation and Purification Technology* **2016,** *159,* 157-160.

CHAPTER 4

CONCLUSIONS AND PERSPECTIVES

The works included in this thesis provided results on the radiation-mediated synthesis, characterization and application of graft copolymers. The knowledge founded from the radiation grafting on cellulosic and lignocellulosic polymers were further built on and developed by introducing RAFT-mediation to impart control in the polymerization process. The union of radiation-induced graft polymerization in emulsion phase and RAFT-mediation allows the synthesis of graft copolymers with fine tuned properties in a reaction mixture that is primarily composed of water as solvent. This thesis maximized the possibilities provided by radiation-induced graft polymerization to synthesize grafted polymers in both conventional and controlled-fashion, and to offer new perspective for the development of enhanced materials that might serve as platforms for future applications. The conclusions from our investigations are categorized according to the respective chapters.

4.1 Radiation-induced graft polymerization in solution and emulsion phases: modification of cellulosic and lignocellulosic polymeric materials

Chapter 1 considered the facile process of radiation-induced grafting of dissolved and emulsified GMA monomer from cellulosic and lignocellulosic materials. The graft copolymerization processes were carried out using simultaneous and pre-irradiation grafting techniques under controlled reaction parameters. The studies and results presented in this chapter are the first reports on the modification of abaca/polyester (APNWF), water hyacinth fibers (WHF) and microcrystalline cellulose (MCC) polymers through radiation grafting. The pre-irradiation grafting of APNWF was initiated using electron beams while γ-irradiation was employed in the simultaneous irradiation grafting of WHF and MCC in glycidyl methacrylate (GMA) solution. The grafted poly(glycidyl methacrylate) (PGMA) chains from WHF-g-PGMA and APNWF-g-PGMA were further reacted with ethylenediamine in a one-step process. The optimum conditions for the synthesis and subsequent functionalization of the cellulosic and lignocellulosic backbone polymers were given in the main text. The FTIR-ATR spectra, TGA thermographs, SEM images and EDX plots and maps of the pristine, grafted and functionalized WHF, APNWF and MCC

confirmed the successful graft polymerization and functionalization of GMA on the polymer backbones.

The aminated forms of WHF-g-PGMA and APNWF-g-PGMA were applied as adsorbents for heavy metal ions. It was established that the adsorption process using the synthesized amino-type adsorbents were dependent on contact time, initial pH and concentration of the solution. The results of adsorption experiments, coupled with kinetics and comparison with control resins experiments, indicate the very high potential of applying the functionalized polymers for removing heavy metals (Cu^{2+}, Cr^{3+}, Pb^{2+} and Ni^{2+}) from aqueous solutions. The wettability test showed that the grafted MCC was more hydrophobic than the pristine MCC, making it more compatible with a non-polar solvent. The hydrophobic character that was imparted to the otherwise strongly hydrophilic MCC may be useful in its application as compatibilizer or reinforcing agent in composites. This study particularly offers interesting perspectives involving the possibility to exploit the epoxide group functionality present in the grafted polymer chains for coupling a broad range of ligands, including diamines. Moreover, such functionalities can facilitate the development of new platforms for metal adsorption based from lignocellulosic materials which a lot of agricultural and industrial sectors already consider as waste. Further studies can focus on the design of more selective adsorbents synthesized through radiation-induced graft polymerization. Also, further studies about the introduction of grafted polymer chains other than PGMA with the intention of modifying the wettability of a surface may prove to be useful in different advanced applications that rely on surface performance.

4.2 RAFT-mediated graft polymerization in emulsion phase: electron beam and γ-radiation initiation

Chapter 1 provides the basic background on radiation grafting in emulsion phase. **Chapter 2** discussed the first attempt studies to perform emulsion phase RAFT-mediated radiation-induced graft polymerization in an endeavor to combine their own individual merits. In **Chapter 2**, GMA in emulsion phase was successfully graft polymerized from PE/PP by the combination of the RAFT technique and radiation (electron beam and γ-radiation) - induced initiation, leading to the oxirane group functionalization of the PE/PP fibers. The RAFT agent 4-cyano-4-

((phenylcarbonothioyl)thio) pentanoic acid (CPPA) was used and the graft polymerization was carried out in water-based emulsions. The combination of RAFT-mediated process and radiation grafting in emulsion state allowed the synthesis of graft copolymers with tunable *Dg* over time. The GPC data showed that the PGMA homopolymers, which approximates the properties of the grafted chains, have reasonable narrow distribution of molecular weights. In pre-irradiation grafting, the calculated *Dg* increased with increasing absorbed dose and grafting time, but tended to decrease with increment in monomer and CPPA concentrations while in simultaneous grafting, the *Dg* increased with increasing monomer concentration and absorbed dose and decreased with increasing monomer to RAFT agent ratio. The NMR data indicate that the epoxide group was retained after the irradiation process. The graft PGMA chains exhibited higher glass transition temperature than the free PGMA, primarily because of its limited mobility when grafted on the trunk polymer surface. Finally, the spectroscopic, thermal and microscopy techniques all support the successful graft polymerization of PGMA from PE/PP. The different observations and characterizations used in this study all point to the involvement of RAFT-mediation in the emulsion-based radiation grafting process. This is an important finding because most of the industrial polymerizations are performed in emulsion. Further studies may focus on the evaluation of the effects of using other RAFT agents, and also in the up-scaling and automation of the process. Although it have been established by other researchers that the molecular weight and molecular weight distribution of the graft chains are almost similar with the free homopolymers, further experiments to evaluate its validity in different systems, including the one presented in this thesis, would be interesting, provided that techniques for the efficient cleavage of the PGMA chains from the PE/PP surface will become available.

4.3 Towards enhanced reactivity and adsorption performance through RAFT-mediated grafting

The main goal of **Chapter 3** was to study the selected properties that were imparted to the graft copolymer prepared with RAFT-mediation, and to compare it with the conventionally synthesized graft copolymers. A graft copolymer with improved reactivity and adsorption performance was prepared using radiation-induced RAFT-mediated graft polymerization in emulsion phase, followed by post-grafting reactions. The PGMA graft chains from the PE/PP-g-PGMA that was prepared in

emulsion phase through radiation-induced RAFT-mediated graft polymerization showed higher reactivity towards amination reaction at 40 °C compared to the conventionally prepared grafted PE/PP. The versatility of the epoxide group functionalization was demonstrated in this study, wherein it served as a precursor group that was further modified by subsequent reactions with ethylenediamine and diglycolic anhydride. The fibrous nature of aminated PE/PP-g-PGMA lead to the faster kinetics in the diglycolic anhydride reaction, resulting in diglycol amic acid ligands immobilized on PE/PP. The DA modified PE/PP-g-PGMA prepared with RAFT mediation showed higher Eu and Sm adsorption percentage than the DA adsorbent prepared using conventional grafting. The DA modified PE/PP-g-PGMA exhibited selectivity for Eu over Cu and Fe in acidic solutions. The introduction of RAFT polymerization in the DA-modified adsorbent preparation process enhanced the reactivity and performance in terms of Eu and Sm adsorption. The synthesized adsorbent shows high potential for rare earth recovery applications. Supplementary studies on its performance against other rare earth elements, including the effect of other important adsorption factors, could lead to a more efficient adsorbent system. The results of this study clearly show the benefits that were derived from the inclusion of RAFT-mediation in the adsorbent synthesis. More studies can elucidate the mechanisms of different graft copolymer chains analyzing the influence of side chains and molecular weight distribution on the adsorption activity.

Overall this thesis successfully highlighted the possibility of combining the beneficial characteristics of radiation grafting in emulsion phase and RAFT-mediation to produce graft copolymers with tunable and enhanced properties. It has been shown that the graft copolymer with either natural or synthetic base polymers could be used as platform for different applications, and addition of RAFT-mediation in the synthesis process leads to materials with enhanced characteristics. All these properties could be utilized and combined for future designs of more specialized applications that could contribute for the improvement of human life and the society.

APPENDIX I: Publications and presentations arising from this thesis

Publications:

Jordan F. Madrid, Yuji Ueki, Lucille V. Abad, Takeshi Yamanobe, Noriaki Seko (2017), *RAFT-mediated graft polymerization of glycidyl methacrylate in emulsion from polyethylene/polypropylene initiated with γ-radiation*, Journal of Applied Polymer Science 134, 45270. DOI: 10.1002/app.45270.

Jordan F. Madrid, Lucille V. Abad, Takeshi Yamanobe, Noriaki Seko (2017), *Effects of chain transfer agent on the electron beam-induced graft polymerization of glycidyl methacrylate in emulsion phase*, Colloid and Polymer Science 295, 1007-1016.

Jordan F. Madrid, Lucille V. Abad (2015). *Modification of microcrystalline cellulose by gamma radiation-induced grafting*, Radiation Physics and Chemistry 115, 143-147.

Jordan F. Madrid, Guillermo M. Nuesca, Lucille V. Abad (2014), *Amine functionalized radiation-induced grafted water hyacinth fibers for Pb^{2+}, Cu^{2+} and Cr^{3+} uptake*, Radiation Physics and Chemistry 97, 246-252.

Jordan F. Madrid, Yuji Ueki, Noriaki Seko (2013), *Abaca/polyester nonwoven fabric functionalization for metal ion adsorbent synthesis via electron beam-induced emulsion grafting*, Radiation Physics and Chemistry 90, 104-110.

Madrid, J.F., Nuesca, G.M., Abad, L.V. (2013), *Gamma radiation-induced grafting of glycidyl methacrylate (GMA) onto water hyacinth fibers*, Radiation Physics and Chemistry 85, 182-188.

Presentations:

Jordan F. Madrid, Yuji Ueki, Lucille V. Abad, Takeshi Yamanobe, Noriaki Seko (2017). *RAFT-mediated polymerization in emulsion phase: γ- and electron beam initiated grafting (Poster Presentation)*, Polymer Preprints, Japan Vol. 66. 66th Macromolecular Symposia**.** Ehime University, Matsuyama-shi, Ehime Prefecture, Japan (20 – 22 September 2017).

Jordan F. Madrid, Yuji Ueki, Lucille V. Abad, Takeshi Yamanobe, Noriaki Seko (2017), *Functionalization of PE/PP with Oxirane Groups via RAFT-Mediated γ-radiation induced graft polymerization of emulsified glycidyl methacrylate (Oral Presentation)*, 32nd Philippine Chemistry Congress "Chemistry Changes Choices". Puerto Princesa City, Palawan, Philippines (31 May – 2 June, 2017).

Jordan F. Madrid, Lucille V. Abad, Takeshi Yamanobe, Noriaki Seko (2016), *RAFT-mediated grafting of poly(glycidyl methacrylate) in emulsion state from polyethylene/polypropylene nonwoven fabric via electron beam pre-irradiation (Oral Presentation)*, 31st Philippine Chemistry Congress "Chemistry Beyond Borders: Blurring Traditional Boundaries". Iloilo City, Philippines (13 – 15 April, 2016).

Jordan F. Madrid, Yuji Ueki, Noriaki Seko (2013), *Development of an amine-type adsorbent by electron beam-induced grafting of glycidyl methacrylate onto a nonwoven fabric (Oral Presentation)*, 28th Philippine Chemistry Congress "Chemistry in 3D: Discovering Wealth, Defining Problems, Developing Solutions". Siliman University, Dumaguete City, Philippines(April 10 – 12, 2013).

Madrid, J.F., Nuesca, G.M., Abad, L.V. (2013), *Gamma radiation-induced grafting of methacrylate to water hyacinth fibers: Functionalization and metal ion uptake kinetics (Poster Presentation)*, 28th Philippine Chemistry Congress "Chemistry in 3D: Discovering Wealth, Defining Problems, Developing Solutions". Siliman University, Dumaguete City, Philippines (April 10 – 12, 2013).